Universität Hamburg
DER FORSCHUNG | DER LEHRE | DER BILDUNG

Contamination Niches: An Ecological Framework for Understanding PFAS Exposure Patterns in Marine Predators

Dissertation

with the aim of achieving a doctoral degree

at the Faculty of Mathematics, Informatics and Natural Sciences

Department of Earth System Sciences

at University of Hamburg

submitted by

Rui Shen

Hamburg, 2025

Department of Earth Science

Date of Oral Defense: **19th Jan. 2026**

Reviewer:

Prof. Dr. Corinna Schrum, Institute of Oceanography, University of Hamburg

Dr. Thomas Larsen, Institute for Prehistoric and Protohistoric Archaeology, University of Kiel

Members of the examination commission:

Prof. Dr. Corinna Schrum, Institute of Oceanography, University of Hamburg

Prof. Dr. Gerhard Schmiedl, Department of Earth System Sciences, University of Hamburg

Prof. Dr. Flemming Dahlke, Institute of Marine Ecosystem and Fisheries Science, University of Hamburg

Prof. Dr. Stefan Trapp, Department of Environmental and Resource Engineering, Technical University of Denmark

Dr. Thomas Larsen, Institute for Prehistoric and Protohistoric Archaeology, University of Kiel

Chair of the Subject Doctoral Committee

Earth System Sciences: Prof. Dr. Hermann Held

Dean of Faculty MIN: Prof. Dr.-Ing. Norbert Ritter

Table of Contents

Acknowledgement

“路漫漫其修远兮，吾将上下而求索” – ‘The road ahead is long and arduous, yet I shall search high and low in my quest for knowledge.’ This timeless verse from Qu Yuan’s *Li Sao* captures the essence of my doctoral journey, a path of persistent inquiry that has been made possible through the collaborative efforts, institutional support, and personal guidance of many remarkable individuals.

I extend my sincere gratitude to Professor Corinna Schrum for her supervision of this doctoral work and for the confidence she placed in this research. Your willingness to oversee this interdisciplinary project and provide the necessary institutional framework has been essential to completing this thesis.

I am grateful to Dr. Ralf Ebinghaus for bringing me into the LOMVIA project and making this research possible. Your vision for bringing together different scientific disciplines created the foundation that allowed this thesis to develop at the intersection of ecological theory and contamination science.

To Dr. Thomas Larsen, my heartfelt appreciation for your dedicated guidance throughout this PhD journey. Your patient mentorship, creative problem-solving, and unwavering support have shaped not only this research but my development as a scientist. The countless discussions, your enthusiasm for exploring new theoretical frameworks, and your encouragement during challenging moments made this work possible. Your insight to bring ecological perspectives into contamination research provided the foundation for developing innovative analytical approaches. This collaboration has profoundly influenced my perspective on the field and will continue to guide my future research.

I would like to warmly thank Dr. Daniel Vassão for his generous technical assistance and steadfast confidence in this research. Your expertise and collaborative spirit made tackling analytical challenges not only possible but genuinely enjoyable. Your encouragement and enthusiasm for the work have been a constant source of motivation.

A special thanks goes to my dearest friend Bingmeng, whose companionship has illuminated this journey as an act of becoming, a condition invented and shaped moment by moment, day by day, through will, intelligence, and heart. To all my friends who have shared in this experience - Y.M., Deborah, Nikoleta, my flatmates and neighbours, and many others - your presence has made this academic pursuit far more meaningful.

I am grateful to my yoga teachers, Nina & Benjamin, Marina, Sukera, Juliette, Silke and Suse, and ballet teacher Moe for their guidance in developing my inner strength and resilience. Through your teaching, I have gained insights that enriched my understanding beyond the academic realm.

Finally, my deepest gratitude goes to my parents, whose unwavering love, support, and belief in my dreams have been the foundation for this entire journey. Your encouragement made this achievement possible.

'You go far as long as you keep a smile.'

Summary

Per- and polyfluoroalkyl substances (PFAS) accumulate in marine predators at concentrations that can vary by several orders of magnitude even among individuals at similar trophic positions. This degree of individual variation is not adequately explained by traditional bioaccumulation theory, which typically assumes linear, concentration-dependent accumulation along trophic pathways. To address this gap, this thesis introduces the 'contamination niche' framework: an extension of Hutchinson's ecological niche theory that incorporates the exposure to contaminants as an emergent ecological dimension. Marine predators occupy multidimensional ecological niches defined by spatial, temporal, and dietary foraging decisions—namely, where, when, and what they forage. These decisions shape chemical exposure patterns, linking contaminant dynamics to behavioural ecology.

A contamination niche is defined as the characteristic profile of chemical exposure that an organism maintains, defined by three quantifiable properties: exposure magnitude (total PFAS concentration), compositional structure (relative abundance of PFAS classes), and within-group exposure variability (the consistency at temporal or individual levels). If contamination niches reflect ecological structures rather than statistical artefacts, then the PFAS exposure should exhibit a systematic, non-random organisation across these dimensions. Individuals occupying the same contamination niche should, therefore, display distinguishable and internally consistent combinations of concentration, composition, and temporal stability.

This framework is empirically grounded in data from 112 individuals of two sympatric seabird species—the common guillemot (*Uria aalge*) and Brünnich's guillemot (*Uria lomvia*)—breeding at five colonies across Iceland that span an Arctic-to-Atlantic oceanographic gradient (June–July 2018). PFAS concentrations were analysed in plasma, while stable isotope values ($\delta^{13}C$ and $\delta^{15}N$) were measured in both plasma and red blood cells to elucidate foraging patterns across short-term temporal scales.

Chapter 3 demonstrates that the variability in PFAS exposure represents an ecological signal rather than random noise. The variability of PFOS exhibited threshold responses corresponding to the Arctic-Atlantic oceanographic regimes, driven by spatial foraging

differences. In contrast, the variability of long-chain PFCAs showed more gradual variation linked to dietary indicators. These compound-specific patterns suggest that PFAS exposure is structured by foraging strategy, supporting the existence of discrete contamination niches.

Chapter 4 identifies and characterises three distinct contamination niches. The first, High-Exposure Atlantic Foragers, comprises predominantly of *U. aalge*. These individuals exhibited elevated concentrations of PFAS and PFOS-dominated profiles; their high temporal consistency suggests reliable foraging within food webs influenced by Atlantic waters. The second group, Low-Exposure Arctic Foragers, is largely composed of *U. lomvia.* This group displayed lower overall concentrations, profiles dominated by long-chain PFCAs, and greater temporal variability, reflecting a seasonal foraging strategy in Arctic environments. Finally, Intermediate-Exposure Mixed Foragers were characterised by moderate concentrations of PFAS and compositional profiles that approximated matched population averages, coupled with intermediate temporal consistency. These findings indicate that the interaction between foraging behaviour and oceanographic context systematically structures marine predators exposure to contaminants.

This thesis proposes the contamination niche as an extension of niche theory, reframing contaminant exposure as a structured outcome of behavioural and ecological processes. The framework bridges ecology and environmental science, offering a tool for improved biomonitoring, ecological risk assessment, and conservation planning in rapidly changing marine systems. While constrained by single-season sampling and potential temporal mismatches between isotopes and PFAS incorporation, these findings establish a conceptual and empirical foundation for future research linking individual behaviour with contaminant dynamics across ecological scales.

Zusammenfassung

Per- und polyfluorierte Alkylsubstanzen (PFAS) reichern sich in marinen Prädatoren in Konzentrationen an, die selbst bei Individuen auf ähnlichen trophischen Ebenen um mehrere Größenordnungen variieren. Dieses Ausmaß an individueller Variabilität wird durch die traditionelle Bioakkumulationstheorie, die üblicherweise von einer linearen und konzentrationsabhängigen Anreicherung entlang trophischer Pfade ausgeht, nur unzureichend erklärt. Um diese Lücke zu schließen, führt die vorliegende Dissertation das Konzept der „Kontaminationsnische" (*contamination niche*) ein: eine Erweiterung von Hutchinsons ökologischer Nischentheorie, welche die Schadstoffexposition als eine emergente ökologische Dimension integriert.

Marine Prädatoren besetzen multidimensionale ökologische Nischen, die durch räumliche, zeitliche und nahrungsökologische Entscheidungen bei der Nahrungssuche definiert werden. Diese Entscheidungen formen chemische Expositionsmuster und verknüpfen somit die Schadstoffdynamik mit der Verhaltensökologie. Eine Kontaminationsnische wird hier als das charakteristische Profil der chemischen Exposition definiert, das ein Organismus aufrechterhält. Sie wird durch drei quantifizierbare Eigenschaften charakterisiert: das Expositionsniveau (Gesamt-PFAS-Konzentration), die strukturelle Zusammensetzung (relative Häufigkeit der PFAS-Klassen) und die Variabilität der Exposition innerhalb einer Gruppe (Konsistenz auf zeitlicher oder individueller Ebene). Sofern Kontaminationsnischen ökologische Strukturen widerspiegeln und nicht bloß statistische Artefakte sind, sollte die PFAS-Exposition eine systematische, nicht-zufällige Organisation über diese Dimensionen hinweg aufweisen. Folglich sollten Individuen, die dieselbe Kontaminationsnische besetzen, unterscheidbare und in sich konsistente Kombinationen aus Konzentration, Zusammensetzung und zeitlicher Stabilität zeigen.

Dieses Rahmenkonzept ist empirisch in Daten von 112 Individuen zweier sympatrischer Seevogelarten begründet: der Trottellumme (*Uria aalge*) und der Dickschnabellumme (*Uria lomvia*). Die Datenerhebung erfolgte im Juni und Juli 2018 in fünf Kolonien in Island, die einen Gradienten von arktischen bis hin zu atlantischen ozeanographischen Bedingungen abdecken. Dabei wurden die PFAS-Konzentrationen

im Plasma analysiert, während stabile Isotopenwerte $\delta^{13}C$ und $\delta^{15}N$) sowohl im Plasma als auch in den roten Blutkörperchen bestimmt wurden, um Nahrungssuchmuster über kurzfristige zeitliche Skalen zu aufzuklären.

Kapitel 3 belegt, dass die Variabilität der PFAS-Exposition ein ökologisches Signal und kein Zufallsrauschen darstellt. Die Variabilität von PFOS wies Schwellenwertreaktionen auf, die den arktisch-atlantischen ozeanographischen Regimen entsprachen und durch Unterschiede in der räumlichen Nahrungssuche getrieben wurden. Im Gegensatz dazu zeigte die Variabilität langkettiger PFCAs eine graduellere Veränderung, die mit trophischen Indikatoren korrespondierte. Diese verbindungsspezifischen Muster legen nahe, dass die PFAS-Exposition durch die Strategie der Nahrungssuche strukturiert wird, was die Existenz diskreter Kontaminationsnischen untermauert.

Kapitel 4 identifiziert und charakterisiert drei distinkte Kontaminationsnischen. Die erste Gruppe, „Atlantik-Jäger mit hoher Exposition“ (*High-Exposure Atlantic Foragers*), setzt sich überwiegend aus *U. aalge* zusammen. Diese Individuen wiesen erhöhte PFAS-Konzentrationen sowie PFOS-dominierte Profile auf; ihre starke zeitliche Konsistenz deutet auf eine zuverlässige Nahrungssuche in von atlantischen Gewässern beeinflussten Nahrungsnetzen hin. Die zweite Gruppe, „Arktis-Jäger mit geringer Exposition“ (*Low-Exposure Arctic Foragers*), besteht weitgehend aus *U. lomvia*. Diese Gruppe zeigte niedrigere Gesamtkonzentrationen, Profile mit einer Dominanz langkettiger PFCAs sowie eine höhere zeitliche Variabilität, was eine eher saisonal geprägte Nahrungssuche in arktischen Umgebungen widerspiegelt. Schließlich waren „Misch-Jäger mit mittlerer Exposition“ (*Intermediate-Exposure Mixed Foragers*) durch moderate PFAS-Konzentrationen und Zusammensetzungsprofile gekennzeichnet, die dem Populationsdurchschnitt nahe kamen, gepaart mit einer mittleren zeitlichen Konsistenz. Diese Ergebnisse verdeutlichen, dass die Interaktion zwischen dem Verhalten bei der Nahrungssuche und dem ozeanographischen Kontext die Schadstoffexposition bei marinen Prädatoren systematisch strukturiert.

Die vorliegende Arbeit etabliert die Kontaminationsnische als eine Erweiterung der Nischentheorie und definiert die Schadstoffexposition als ein strukturiertes Ergebnis verhaltensbezogener und ökologischer Prozesse neu. Das Konzept schlägt eine Brücke

zwischen Ökologie und Umweltwissenschaften und bietet ein Werkzeug für verbessertes Biomonitoring, ökologische Risikobewertung und Naturschutzplanung in sich schnell verändernden marinen Systemen. Wenngleich durch eine einzelne Probenahmezeitraum und potenzielle zeitliche Diskrepanzen zwischen der Einlagerung von Isotopen und PFAS limitiert, bilden die Ergebnisse eine konzeptionelle und empirische Grundlage für künftige Forschungsarbeiten, die individuelles Verhalten mit der Schadstoffdynamik über ökologische Skalen hinweg verknüpfen.

Chapter 1: General Introduction

1.1 Per- and Polyfluoroalkyl Substances in Marine Ecosystems

Per- and polyfluoroalkyl substances (PFAS) are a diverse class of anthropogenic chemicals that have become widely distributed in global ecosystems since their commercial introduction in the 1940s [1-3]. Characterised by exceptionally stable carbon-fluorine bonds, these compounds resist natural degradation processes and have been incorporated into numerous consumer and industrial products—including non-stick cookware and water-repellent textiles to firefighting foams and food packaging—due to their unique hydrophobicity, lipophobicity, thermal stability, and surfactant properties (Fig. 1-1) [3,4]. PFAS contamination in marine environments now occurs at concentrations comparable to or exceeding those of legacy persistent organic pollutants (POPs) in many regions [5,6].

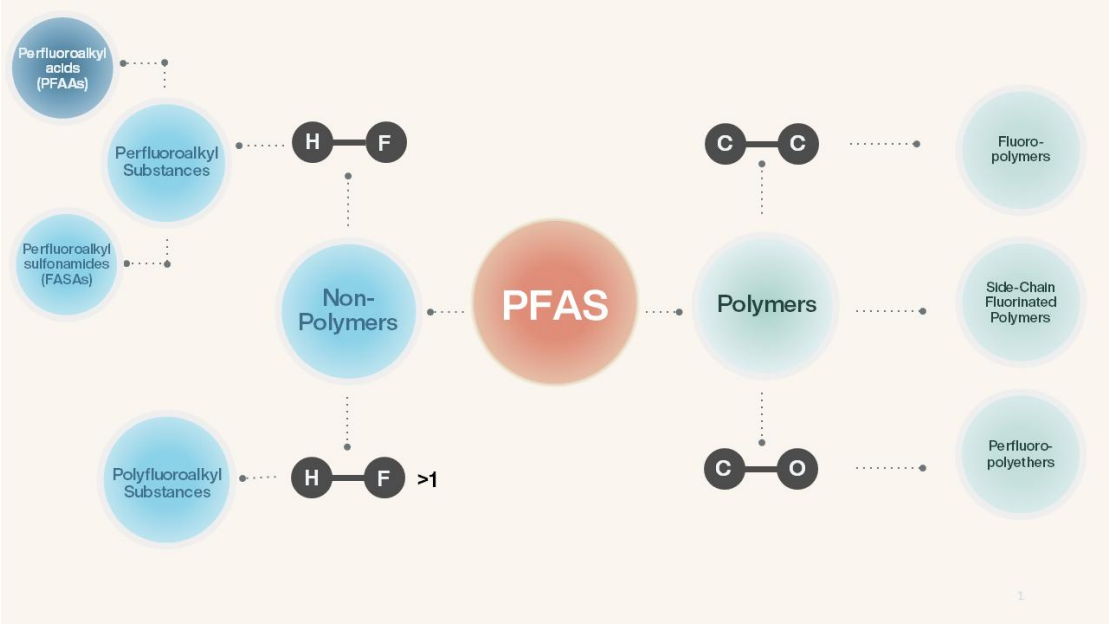

Figure 1-1. Diversity and Classification of Per- and Polyfluoroalkyl Substances (PFAS). Schematic overview of PFAS chemical classes illustrating the complexity of this contaminant group. The PFAS universe encompasses both non-polymeric compounds (left, including perfluoroalkyl acids (PFAAs), perfluoroalkyl sulfonamides (FASAs), and polyfluoroalkyl substances) and polymeric compounds (right, including fluoropolymers, side-chain fluorinated polymers, and perfluoropolyethers). Structural elements show characteristic carbon-fluorine (C-F) and carbon-carbon (C-C) bonds that confer exceptional environmental persistence, while functional groups (C-O bonds) determine bioaccumulation properties.

Unlike legacy POPs such as dichlorodiphenyltrichloroethane (DDT) and polychlorinated biphenyls (PCBs), which are predominantly lipophilic and accumulate in adipose tissues, most PFAS exhibit strong protein-binding affinities [7-9]. This fundamental difference results in distinct exposure patterns; PFAS primarily concentrate in protein-rich tissues such as the blood, liver, and kidneys, rather than adipose tissue [8,10-12]. These unique binding properties have profound implications for PFAS dynamics in marine food webs, where protein content and binding affinities vary substantially across organisms and tissues. For instance, PFOS exhibits approximately ten-fold higher protein affinity than long-chain perfluorocarboxylic acids (PFCAs) [13-15], resulting in divergent accumulation kinetics, elimination rates, and tissue distribution patterns [16,17]. These mechanistic differences suggest that individual PFAS congeners may respond distinctly to biological and environmental factors, allowing for a more sophisticated analysis of contamination patterns beyond rudimentary measurements of total concentration. These compound-specific properties provide the foundation for investigating how PFAS accumulation patterns vary across different exposure scenarios and biological systems.

The global distribution of PFAS is driven by their chemical stability, variable water solubility, atmospheric transport potential, and continued production, despite increasing regulatory scrutiny [18]. Marine ecosystems serve as major repositories for these compounds through riverine inputs, atmospheric deposition, and oceanic circulation patterns [19-22]. This widespread contamination creates spatially heterogeneous exposure landscapes that the marine organisms encounter, with concentrations varying by orders of magnitude across oceanographic regions and water masses [23]. Consequently, understanding how PFAS movement through marine food webs therefore requires integrated approaches that consider both environmental transport mechanisms and the ecological processes mediating exposure and accumulation in marine predators.

1.2 Trophic Transfer and Marine Predators as Contamination Sentinels

While multiple processes influence contaminant dynamics in marine ecosystems, trophic transfer is the primary focus of research regarding how chemicals move from environmental media *via* primary producers to successive consumer levels [24,25]. Traditional bioaccumulation research has focused on trophic magnification, the progressive increase in contaminant concentrations at each trophic step [26,27], quantified through biomagnification factors (BMFs) and trophic magnification factors (TMFs) [9,28]. These metrics have successfully demonstrated vertical contaminant transfer for many persistent organic pollutants [29,30], establishing the theoretical framework that higher trophic level organisms accumulate greater contaminant burdens through dietary uptake [31].

However, traditional approaches to assessing contaminant exposure encounter inherent conceptual constraints when applied to marine food webs [32]. Although trophic magnification models assume linear relationships between trophic position and contaminant concentration, marine food webs exhibit multidimensional characteristics that these reductive frameworks cannot capture [33]. Seasonal variations in prey availability create temporal shifts in trophic pathways [34]; similarly, trophic transfers involve intricate predator-prey networks rather than unidimensional chains [35], and spatial heterogeneity in both the baseline levels of contamination and food web structure generates geographic variation in exposure patterns [36,37]. These multidimensional dynamics mean that organisms at similar trophic positions may experience divergent exposure regimes depending on their specific foraging strategies, habitat utilisation, and temporal activity patterns. Consequently, the variability observed in contaminant concentrations among marine predators may reflect meaningful ecological signals rather than analytical uncertainty. This suggests that higher-trophic-level organisms integrate exposure information across the multidimensional marine food web in ways that cannot be captured through linear biomagnification models alone.

The selection of trophic level for assessing contaminant exposure within an ecosystem involves important trade-offs between measurement precision and ecological

representativeness. Although analytical uncertainty increases at each trophic level due to cumulative variability [31,38], higher-level predators integrate exposure information across broader spatial, temporal, and pathway dimensions than do lower-level organisms [39,40]. Top predators forage across multiple habitats and water masses [41], capture contamination signals over extended time periods through longer tissue turnover rates [42], and integrate exposure from diverse prey sources representing multiple contamination pathways [43]. This integration effect suggests that, despite greater individual variability, marine predators may provide more representative signals of ecosystem-wide contamination patterns and emergent exposure relationships that are undetectable through the analysis of individual environmental compartments alone [44,45]. However, this integration also raises the questions of whether such broad-scale signals obscure important fine-scale contamination patterns or specialised exposure pathways that might be critical for understanding ecosystem health and species-specific vulnerabilities [46].

Marine top predators, particularly seabirds, thus constitute optimal sentinels for understanding ecosystem-level contaminant exposure patterns and testing hypotheses regarding ecological influences on exposure [43-45]. Their position at or near the apex of marine food webs, combined with their long lifespans, high metabolic rates, and capacity for contaminant accumulation, makes them valuable integrators of contamination signals across spatial and temporal scales that exceed the scope of environmental monitoring alone [43,44]. As central-place foragers during breeding seasons, seabirds repeatedly return to fixed colony locations while exploiting specific foraging areas, creating well-defined spatial linkages between contamination sources and biological receptors which facilitate the interpretation of the exposure patterns [47-49].

Seabirds also demonstrate ecological plasticity, with many species exhibiting individual specialisation in foraging strategies despite population-level generalist patterns [50-53]. This combination of site fidelity during breeding and diverse foraging tactics creates natural experimental systems for investigating how ecological strategies influence contaminant exposure. Their diverse foraging behaviours—ranging from surface feeding to deep diving, coastal foraging to pelagic hunting—provide opportunities to examine how different ecological strategies may influence contaminant exposure

patterns across multiple dimensions [54]. Furthermore, their migratory patterns enable them to integrate contaminants across broad spatial scales, though this integration also presents challenges for the interpretation of exposure sources and timing.

Traditional trophic transfer models, while valuable for establishing general patterns, lack the explanatory power required to account for the substantial variability observed in PFAS concentrations among individuals, populations, and species occupying similar trophic positions. PFOS concentrations in seabird tissues range from below detection limits to over 1,500 ng/g wet weight, representing orders of magnitude of variation even among species with comparable trophic ecology [55,56]. These patterns suggest that factors beyond trophic position—such as spatial foraging patterns, prey specialisation, temporal foraging consistency, or physiological differences—may significantly influence PFAS accumulation in marine predators. This variability, rather than representing analytical noise, likely reflects meaningful ecological signals that reveal how organisms partition exposure through their multidimensional foraging strategies.

1.3 Knowledge Gaps in Understanding PFAS Accumulation in Marine Ecosystems

Despite extensive research documenting the presence of PFAS in marine environments and biota [5,57], important knowledge gaps remain regarding the ecological mechanisms governing their accumulation patterns in marine ecosystems. An analytical review of the existing literature reveals three methodological and conceptual constraints that limit current understanding of PFAS dynamics in marine predators.

First, the trophic position framework exhibits inconsistent explanatory utility regarding the substantial variability observed in PFAS concentrations among individuals, populations, and species occupying similar trophic positions [8,31,38,58]. Quantitative analysis reveals that seabird species with similar $\delta^{15}N$ values can differ in PFAS concentrations by an order of magnitude [59-61], suggesting that factors beyond trophic position drive exposure. While this pattern has been documented across multiple species and geographic regions [62,63], other studies have reported strong correlations between isotopic indicators and PFAS concentrations [61], highlighting the need for frameworks capable of accounting for this variability. Furthermore, individuals within

the same population can exhibit a threefold variation in PFAS concentrations despite similar diets [64], indicating that spatial foraging patterns, prey specialisation, or physiological differences may predispose marine predators to varying accumulation rates.

Second, traditional approaches have predominantly focused on mean concentration values rather than examining concentration magnitudes, compositional profiles, and variability patterns as distinct indicators of ecological processes [65,66]. This limitation has become increasingly apparent as analytical capabilities have expanded to detect multiple PFAS simultaneously [67]. Different PFAS exhibit distinct environmental distributions, protein-binding affinities, and elimination rates in biological systems [8]. If these compound-specific properties interact with ecological factors—such as prey selection, habitat utilisation, or foraging consistency—they could theoretically generate accumulation patterns that correspond to specific foraging strategies. However, this potential has received limited empirical investigation. These multidimensional contamination data (magnitude, composition, and variability) may provide complementary information about foraging strategies not captured by concentration measurements alone, yet they have to date received limited integrated analytical attention.

Third, most studies have insufficiently accounted for the multidimensional nature of exposure pathways, particularly how spatial habitat utilisation and temporal foraging consistency interact with dietary preferences to shape contaminant profiles [68,69]. Seabirds forage across marine environments where PFAS exhibit distinct spatial distributions, with concentrations varying by two orders of magnitude across oceanographic regions and water masses [19,70,71]. However, how these spatially structured contamination landscapes interact with seabird foraging strategies remains poorly understood, especially under the constraints of central-place foraging during breeding seasons. This limitation has become particularly relevant as climate change alters oceanographic regimes and associated contamination distributions, with potential consequences for Arctic-Atlantic boundary dynamics that may restructure both food webs and contaminant pathways [18].

1.4 Theoretical Framework: Ecological Niches and Contaminant Exposure

Ecological niche theory provides a robust conceptual foundation for understanding the multidimensional resource partitioning in biological communities. Schoener [72] originally formalised this theory by identifying habitat type, dietary resources, and temporal activity patterns as the primary axes of niche differentiation. Pianka [73] subsequently expanded this framework by demonstrating that the coexistence of species depends fundamentally on differential resource utilisation across multiple dimensions rather than separation along single ecological gradients. Hutchinson's [74] conceptualisation of the ecological niche as an *n*-dimensional hypervolume of environmental conditions remains central to the understanding how organisms partition resources and respond to environmental variability across multidimensional ecological landscapes [75,76]. The number and identity of relevant dimensions can vary among systems and taxa [77].

Central-place foraging theory provides additional theoretical grounding for understanding how breeding constraints may structure the patterns of contamination exposure in colonial seabirds [48,78,79]. During breeding seasons, the requirement to return repeatedly to fixed colony locations creates spatial constraints [47] that may mediate exposure to spatially structured contaminant landscapes, potentially generating predictable relationships between foraging specialisation and contamination patterns. Optimal foraging theory suggests that organisms balance resource predictability against energetic reward, potentially creating a temporal consistency in foraging strategies that could generate characteristic contamination patterns [80].

This multidimensional theoretical framework contrasts with traditional approaches to the bioaccumulation of contaminants, which have predominantly relied on trophic magnification models that reduce sophisticated ecological relationships to linear functions of trophic position [31,46]. While trophic magnification factors (TMFs) and biomagnification factors (BMFs) have successfully demonstrated vertical contaminant transfer through food webs for many persistent organic pollutants, these approaches often cannot explain substantial within-trophic-level variation or inter-specific differences in accumulation patterns among organisms occupying similar positions in

food webs [31]. Furthermore, these one-dimensional models cannot capture spatial and temporal dimensions that influence contaminant exposure in natural systems, particularly for compounds like PFAS that exhibit varied protein-binding affinities and spatially heterogeneous environmental distributions.

Emerging research demonstrates the potential for chemical contaminant profiles to function as ecological tracers, revealing niche partitioning and the patterns of resource use not readily discernible through conventional ecological methods. Lyons *et al.* [81] demonstrated that the patterns of persistent organic pollutants can distinguish among shark species with overlapping geographic ranges, revealing subtle ecological differentiation that traditional dietary analysis could not resolve. Similarly, Tartu *et al.* [82] showed that mercury profiles in seabirds reflected species-specific wintering areas and migratory strategies, establishing contaminant patterns as markers of ecological specialisation. However, other studies have reported weak correlations between indicators of foraging ecology and contaminant patterns [63,69,83], highlighting the need for more comprehensive frameworks that account for ecological factors.

In this thesis, I conceptualise exposure patterns as the chemical signals that reflect the ecological strategies and life histories of marine predators, proposing that these patterns encode information about how organisms interact with their environment across spatial, temporal, and dietary dimensions. From this perspective, I propose extending ecological niche theory to encompass contaminant exposure as an additional dimension of niche space. This framework proposes that, just as organisms partition resources, their ecological behaviours and niches across time and space also lead to differential chemical exposure. If contaminant exposure patterns reflect ecological specialisation rather than stochastic variation, then characteristic exposure profiles could emerge that correspond to distinct ‘contamination niches’, analogous to how species occupy characteristic positions in traditional resource space through their ecological adaptations.

This contamination-niche framework offers several theoretical advantages over traditional bioaccumulation models. First, it reframes variability in contaminant patterns as potentially meaningful ecological information rather than statistical noise to be minimized, transforming how we interpret heterogeneity in exposure data. Second,

it conceptualises chemical exposure as an ecological landscape shaped by the spatial and temporal patterns of organismal movement and foraging, integrating contamination into broader ecological frameworks. Third, it provides a multidimensional alternative to biomagnification models that have shown limited ability to explain the substantial variability observed in field studies.

1.5 Study Area and Methodological Considerations

This thesis was conducted within the framework of the LOMVIA project (Linking Oceanography and Multi-specific, spatially-Variable Interactions of seabirds and their prey in the Arctic), which primarily focused on seabird foraging ecology, food-web structure, and habitat use around Iceland. While LOMVIA provided the logistical and scientific foundation for the collection of seabird samples and ecological data, the analysis of PFAS and the development of a contamination niche framework presented herein represent an independent extension of this research. Iceland offers an exceptional natural setting for developing and testing the contamination niche framework due to its unique oceanographic and ecological gradients. The convergence of Arctic and Atlantic water masses around Iceland creates strong oceanographic gradients in temperature, productivity, and prey communities [84], providing a natural experimental setting to investigate how these environmental variations may influence seabird foraging strategies and, consequently, patterns of PFAS exposure. Moreover, Iceland's sympatric guillemot colonies (*U. aalge* and *U. lomvia*) exhibit overlapping yet distinct foraging strategies, enabling comparative analysis of how species-specific ecological divergencies influence contaminant accumulation patterns across distinct oceanographic regimes (Fig. 1-2).

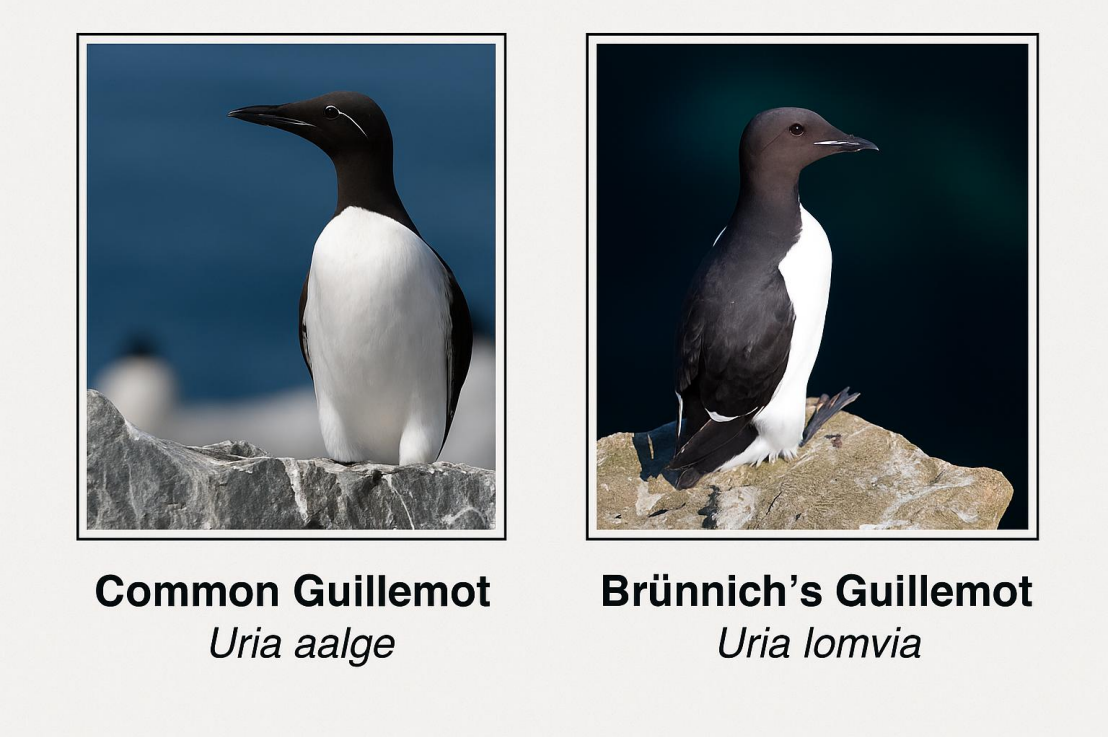

Figure 1-2. Guillemot Species. Left: Common Guillemot (*Uria aalge*) with pointed bill and brownish plumage, typically foraging in Atlantic-influenced waters. Right: Brünnich's Guillemot (*Uria lomvia*) showing thicker bill with pale gape stripe and darker coloration, specialised for Arctic-influenced environments. Photos courtesy of Norwegian Polar Institute.

The Arctic-influenced waters are characterised by seasonal sea ice coverage, prey communities including lipid-rich Arctic cod (*Boreogadus saida*) and ice-associated copepods, and pronounced seasonal productivity cycles limited to 1-4 months during spring and summer [85]. In contrast, Atlantic-influenced waters support year-round productivity, prey communities with greater diversity of forage fish species, and more stable thermal conditions that facilitate extended foraging seasons [86]. These contrasting oceanographic regimes create divergent prey availability patterns and seasonal foraging opportunities that may shape predator contamination patterns.

The presence of the two closely related guillemot species at multiple Icelandic colonies (Fig. 1-3) allows for an examination of how nuanced ecological differences translate into contamination patterns while accounting for phylogenetic and environmental factors. These species exhibit overlapping but distinct foraging strategies, with *U. lomvia* showing a preference for Arctic-influenced waters and ice-associated prey, while *U. aalge* typically forages in warmer Atlantic-influenced waters [87,88]. Both species function as central-place foragers during breeding, constraining their

movements to predictable ranges that can be linked to specific oceanographic conditions and contamination landscapes.

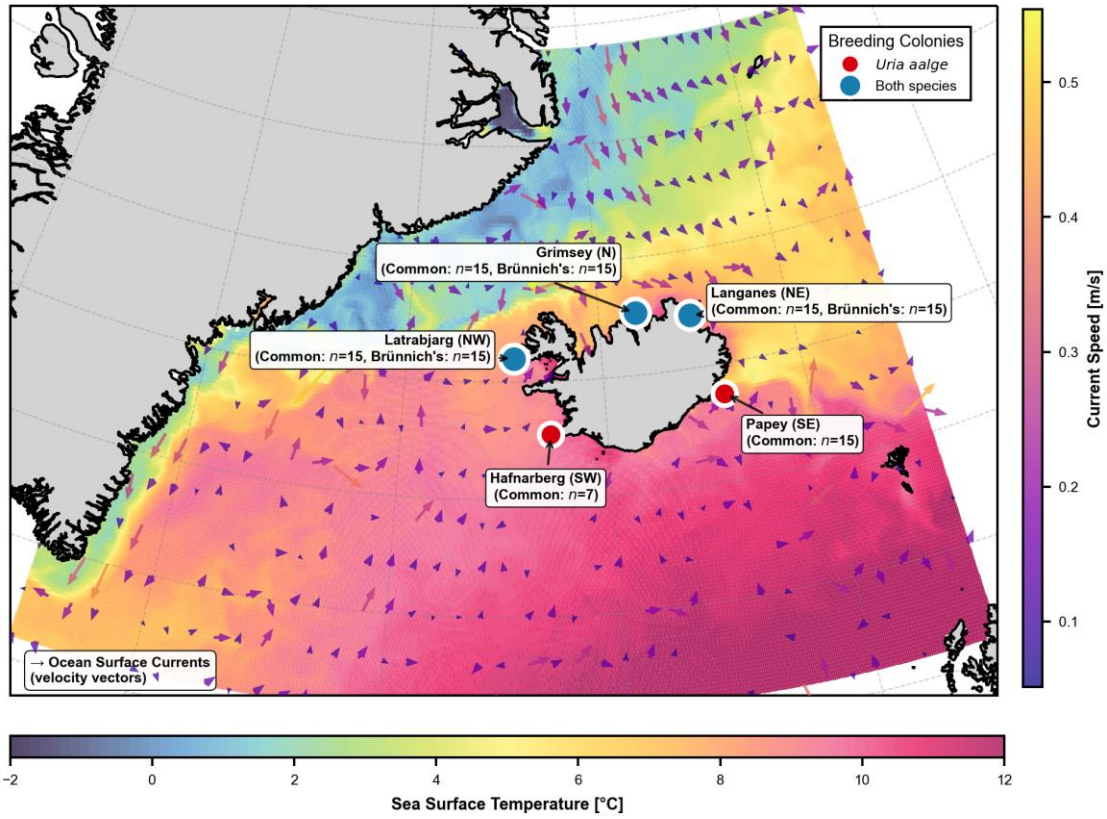

Figure 1-3. Distribution of Common Guillemot (*U. aalge*) and Brünnich's Guillemot (*U. lomvia*) sampling locations across Iceland. Five coastal breeding colonies were sampled: Latrabjarg (NW), Grimsey (N), Langanes (NE), Hafnarberg (SW), and Papey (SE). Both species coexist at three northern and western colonies (Latrabjarg, Grimsey, and Langanes), while only Common Guillemots were sampled at the two southern colonies (Hafnarberg and Papey) in June-July 2018. Reprinted from Chapter 3 (manuscript accepted for publication).

Several methodological considerations are integral to interpreting the results from this system. This study's focus on breeding season exposure limits our understanding of the annual accumulation patterns that occur during migration and winter periods. The temporal mismatch between stable isotope turnover (weeks) and PFAS persistence (months to years) requires a cautious interpretation of observed correlations, as they may reflect a composite of current foraging strategies and historical exposure patterns. Sample size limitations may constrain the ability to detect subtle ecological signals against the background of individual physiological variation, particularly for compound-specific analyses where detection frequencies vary among PFAS classes. Additionally, the breeding season sampling window may not capture the annual patterns of exposure that occur during migration or winter periods.

1.6 Research Focus and Objectives

This dissertation examines how ecological processes structure PFAS exposure patterns in marine predators during the breeding season. By examining variability patterns and exposure clustering in sympatric guillemot species across the Arctic-Atlantic gradient, my aim is to move beyond traditional trophic magnification approaches to investigate the multidimensional ecological influences on contaminant exposure.

Chapter 3 investigates whether PFAS exposure variability functions as an ecological signal, examining potential threshold effects across the Arctic-Atlantic gradient and compound-specific responses to spatial and trophic indicators. Building on evidence for structured variability patterns, Chapter 4 develops and tests a contamination niche framework by analysing discrete clustering in exposure patterns and their associations with foraging ecology indicators. Based on PFAS analysis and dual-tissue stable isotope measurements ($\delta^{13}C$, $\delta^{15}N$) in blood plasma and red blood cells with different turnover rates to assess temporal foraging consistency, samples from the two guillemot species were collected at five Icelandic colonies spanning Arctic and Atlantic oceanographic influences during June-July 2018.

The following main hypotheses were tested in this dissertation:

(1) PFAS exposure variability patterns will exhibit ecological structuring rather than random variation, with compound-specific responses to ecological indicators due to differential compound properties. Given the stronger protein-binding affinity of PFOS compared to PFCAs, compounds will show differential associations with ecological indicators, with threshold effects across the Arctic-Atlantic gradient (Chapter 3).

(2) PFAS exposure patterns will form discrete, non-random clusters corresponding to distinct foraging strategies. These potential contamination niches show significant associations with isotopic niche metrics, species identity, and colony location, with predictive relationships between foraging ecology indicators and exposure patterns (Chapter 4).

(3) The integrated variability and niche clustering analyses reveal that chemical exposure patterns in marine predators emerge from multidimensional foraging strategies, with spatial, temporal, and dietary dimensions resulting in distinct contamination regimes that show significant associations with ecological indicators and non-random clustering patterns (Chapters 3 and 4 combined).

Chapter 2: Methodological Overview

This thesis integrates field-based ecological sampling with laboratory-based chemical and isotopic analyses to investigate how multidimensional foraging strategies structure PFAS exposure in marine predators. The research utilises Iceland's position at the Arctic-Atlantic oceanographic boundary [84,89], where contrasting water masses support distinct prey assemblages and food-web structures [36,37] that provide opportunities to investigate the ecological influences on contamination patterns through differential ecological pathways.

The study focuses on two sympatric guillemot species (*U. aalge* and *U. lomvia*) breeding at five Icelandic colonies spanning this oceanographic gradient. These guillemots provide suitable model organisms for investigating the relationships between contamination and ecology due to their central-place foraging behaviour during breeding [47,48], their overlapping yet distinct ecological niches [87,88], and their position as marine predators that potentially integrate contamination signals across multiple trophic pathways. Blood samples were collected from adult birds during the breeding season (June-July 2018) and separated into plasma and red blood cell fractions to assess temporal patterns in foraging behaviour across different tissue turnover rates.

2.1 PFAS Chemical Analysis

PFAS analyses were conducted at the Helmholtz-Zentrum Hereon in Germany, using high-performance liquid chromatography coupled with tandem mass spectrometry (HPLC-MS/MS) to quantify 14 target PFAS in plasma samples. The targeted analysis included nine perfluoroalkyl carboxylic acids (PFCAs: C5-C13), four perfluoroalkyl sulfonic acids (PFSAs: C4, C6, C8, and C10), and hexafluoropropylene oxide dimer acid (HFPO-DA). This compound selection captured both legacy compounds (particularly PFOS and long-chain PFCAs) known to biomagnify in marine food webs and emerging compounds of regulatory concern. Plasma samples were selected for analysis due to the binding affinity of PFAS to albumin [8,13], a primary blood plasma protein, making plasma a suitable matrix for detecting recent exposure patterns.

2.2 Stable Isotope Analysis and Ecological Interpretation

Stable isotope analyses ($\delta^{13}C$, $\delta^{15}N$) for both plasma and red blood cells were performed at the GEOMAR Stable Isotope Facility (Kiel, Germany), providing integrated dietary and habitat-use information over distinct temporal scales. Blood plasma isotope values reflect foraging patterns integrated over approximately 3-5 days, while red blood cell values represent longer integration periods of 3-4 weeks [42,90]. This dual-tissue approach allows for the assessment of temporal consistency in foraging behaviour during the breeding season, addressing limitations in traditional bioaccumulation studies that typically rely on single-tissue measurements.

The dual-isotope approach provides complementary ecological information for interpreting contamination patterns within the Arctic-Atlantic oceanographic gradient. Carbon isotope ratios ($\delta^{13}C$) serve as indicators of spatial habitat use, with values following latitudinal and water mass gradients around Iceland. More negative $\delta^{13}C$ values are associated with Arctic-influenced waters and their prey communities, while less negative values indicate foraging in warmer, more saline Atlantic-influenced waters. This spatial differentiation is particularly relevant given Iceland's position at the confluence of distinct oceanographic regimes with contrasting productivity cycles and prey assemblages. Nitrogen isotope ratios ($\delta^{15}N$) reflect both trophic position and regional oceanographic conditions, representing the combined influence of prey selection and baseline nitrogen sources. Arctic waters typically exhibit more negative $\delta^{15}N$ baselines compared to Atlantic waters [91,92], while within-system variation reflects trophic level differences among prey types.

The temporal resolution provided by the dual-tissue analysis enables the assessment of foraging consistency, a dimension that has received limited attention in marine bioaccumulation research. Strong correlations between plasma and red blood cell isotope values may indicate consistent foraging strategies maintained over the breeding period, whereas weak correlations suggest temporal shifts in habitat use or prey selection that could influence contaminant exposure pathways.

2.3 Analytical Framework

The resulting chemical and isotopic datasets were combined to examine the spatial, temporal, and dietary dimensions of contamination exposure through an integrated data science approach that extends beyond traditional bioaccumulation frameworks. This methodology addresses a recognised limitation in bridging contamination science and ecology: the treatment of exposure variability as statistical noise rather than potentially informative ecological signals that may reflect specialised foraging strategies [31,38].

Unsupervised machine learning methods were employed to identify patterns in the multidimensional data without the use of predetermined assumptions about exposure groupings. Dimensionality reduction techniques extracted the primary sources of variation in PFAS profiles, whilst unsupervised clustering algorithms detected potential discrete contamination patterns in both exposure magnitudes and compositional profiles. This data-driven approach enabled exploration of natural groupings that may reflect ecological processes rather than imposed taxonomic or geographic categories, representing an application of pattern recognition techniques to the study of contamination ecology.

Supervised learning methods were then applied to test predictive relationships between ecological indicators and contamination patterns, whilst statistical modelling assessed the relative influence of biological and environmental factors on exposure outcomes. Pattern recognition techniques identified potential threshold effects across environmental gradients and quantified the associations between foraging strategies and contaminant profiles, enabling an investigation of possible ecological transitions that may structure chemical exposure in marine systems.

This analytical framework enabled the investigation of contamination patterns across multiple ecological dimensions whilst accounting for the hierarchical structure inherent in ecological data and addressing the temporal mismatch between ecological indicators (weeks) and contaminant persistence (months to years) [60,93] that complicates the interpretation of exposure-ecology relationships.

Chapter 3: Arctic-Atlantic gradient shapes PFAS exposure variability in sympatric guillemot species off Iceland

Note: This chapter is accepted for publication in *Environmental Science & Ecotechnology* following revision

Shen, R., Ebinghaus, R., Vassão, D.G., Ratcliffe, N., & Larsen, T. (2025). Arctic-Atlantic gradient shape PFAS exposure variability in sympatric guillemot species off Iceland. *Environmental Science & Ecotechnology,* (ESE-D-25-00426).

Abstract

Per- and polyfluoroalkyl substances (PFAS) are persistent organic pollutants of growing environmental concern in marine ecosystems. While previous approaches have focused on mean concentrations, we here propose treating PFAS exposure variability as an ecological signal rather than statistical noise. To examine this variability-as-signal hypothesis, we analysed PFAS concentrations in plasma and stable isotopes in plasma and red blood cells from 112 individuals of two sympatric guillemot species (*Uria lomvia*, $n = 45$; *Uria aalge*, $n = 67$) across five Icelandic colonies during the 2018 breeding season. The dual-tissue isotopic approach allowed us to assess foraging consistency across different temporal scales, providing context for interpreting PFAS exposure patterns. PFAS variability was dominated by two compound groups: Long-chain perfluoroalkyl carboxylic acids (PFCAs, 79% of variance) and perfluorooctane sulfonate (PFOS, 13% of variance). We standardised individual variability into *z*-scores to quantify individual expression of these exposure patterns, revealing three distinct variability clusters that corresponded with oceanographic transitions between Arctic and Atlantic waters. Segmented regression analysis showed that significant threshold effects at the Arctic-Atlantic habitats (isotopic breakpoints $\delta^{13}C_{consist} = 0.19$, $\delta^{15}N_{consist} = 0.00$) with contrasting ecological drivers: PFOS variability responded to habitat-driven shifts ($\delta^{13}C$, $p < 0.01$) and PFCA variability to trophic indicators ($\delta^{15}N$). Both species exhibited similar PFAS patterns when foraging in the same water masses, with notable exceptions where niche partitioning occurred at oceanographic boundaries. Our findings demonstrate that water mass characteristics and foraging strategies create structured PFAS variability patterns that reflect local ecological adaptations within broader geographical gradients. This variability-focused framework reveals ecological dimensions of contamination that complement traditional mean-based approaches and may improve understanding of contaminant risks in rapidly changing marine ecosystems.

Keywords: PFAS exposure variability; water mass thresholds; multi-tissue isotopes; sympatric guillemots; marine bioaccumulation

3.1 Introduction

Marine ecosystems, encompassing more than 90% of Earth's habitable biosphere volume [94], are threatened by multiple anthropogenic pressures [95], including the ubiquitous presence of synthetic chemical compounds such as per- and polyfluoroalkyl substances (PFAS) [96]. These persistent organic pollutants, notable for their stable carbon-fluorine bonds, are exceptionally resistant to environmental degradation processes [1] and accumulate in living organisms [5,9]. The toxic effects of PFAS pose measurable risks to both human and ecosystem health, especially within marine environments where biomagnification can be pronounced through efficient trophic transfer from phytoplankton to apex predators [9,28,56,97].

The unique physicochemical properties of PFAS determine their bioaccumulation patterns in marine organisms [8,58]. Marine predator tissues show a predominance of perfluorooctane sulfonate (PFOS) and long-chain perfluoroalkyl carboxylic acids (PFCAs) [55,56,96,98]. PFOS demonstrates enhanced protein-binding affinity and prolonged retention in organisms due to its sulfonate group, which forms stronger bonds with serum proteins than the carboxylate groups of PFCAs [8,13,99,100]. These molecular-level differences create distinct exposure patterns in predators, with PFOS exhibiting greater persistence and integrating exposure over longer time periods compared to PFCAs of similar chain length [58,101]. Such compound-specific dynamics fundamentally shape how PFAS are transferred and magnified across trophic levels in marine food webs [9,28,31,38].

PFAS bioaccumulation research has relied heavily on mean-based metrics like trophic magnification factors (TMFs) and biomagnification factors (BMFs) [31,38,102-105]. These approaches obscure ecological nuances by averaging exposure across temporal and spatial scales [31]. Rather than dismissing variability as statistical noise, we propose recognising it as biologically informative. Variability in PFAS in tissue concentrations within and among populations represents ecological signals that reveal contaminant pathways that mean-based analyses may not capture. This reframing turns individual differences from mere measurement error into ecological insight. For instance, when seabirds display constrained variability, it may indicate specialised foraging within consistent habitats and prey, whereas high variability among

individuals can reflect exposure to seasonal prey communities or spatially heterogeneous habitats [25,106]. Recognising these variability patterns becomes ever more critical as climate change reshapes marine ecosystems, forcing predators to shift their foraging behaviour and, in turn, modifying contaminant exposure pathways.

Spatial patterns of PFAS distribution in marine ecosystems reflect the dynamic integration between ecological and oceanographic processes [18]. Previous research has primarily attributed these patterns to long-range transport and geographic variability [19,20,63,107,108]. However, distribution gradients also stem from differences in food web structures and habitat dynamics [109]. Arctic waters may exhibit relatively homogeneous PFAS exposure among individuals within a species due to strong habitat segregation, low species richness, and greater ecological specialisation such as a reliance on lipid-rich prey. The relatively high homogeneity in both habitat and diet reduces inter-individual differences in contaminant exposure, as most individuals forage within similar ecological niches. These marine systems typically display more modular and less connected food web structures than temperate regions [25,110]. Atlantic waters, in contrast, support more diverse prey assemblages including various forage fish and mesopelagic fauna. This greater connectivity and year-round prey availability may create more integrated trophic networks with higher species interactions and diverse feeding opportunities compared to Arctic systems [36].

Seabirds, as central-place foragers during breeding seasons, provide an ideal model to explore these dynamics [43,47]. The period offers a natural framework for examining PFAS exposure variability, as central-place foraging behaviour confines individuals to localised ranges for chick provisioning [50,111-113]. As a result, central-place foraging itself can promote more homogeneous exposure patterns among individuals, an effect that is independent of whether birds breed in Arctic or temperate environments [114,115]. Case in point, two sympatric seabird species, Brünnich's guillemots (*Uria lomvia*; UL) and common guillemots (*Uria aalge*; UA), have overlapping ecological niches despite UL's preference for more lipid-rich prey and colder foraging habitats [88]. In contrast, outside the breeding season, both species disperse across diverse habitats and prey communities [41,116], potentially leading to greater heterogeneity in contaminant exposure. By focusing on the breeding season of these two species, this

study leverages the ecological consistency of central-place foraging to disentangle how spatial habitat use and trophic interactions shape PFAS exposure patterns.

Iceland's coastal waters, situated at the confluence of cold Arctic and warm Atlantic currents, present a unique natural laboratory for investigating PFAS exposure in marine ecosystems [89,117,118]. This region lies at the boundary between Arctic and temperate waters, creating distinct oceanographic and ecological zones [84]. To the north, cold Arctic waters with seasonal sea ice coverage generally exhibit lower primary productivity than temperate waters, except for localized hotspots such as ice edges and polynyas [37,84]. These Arctic systems experience pronounced seasonal production limited to a one to four month period during spring and summer [85], creating more dynamic trophic relationships [119]. In contrast, the warmer Atlantic-influenced waters to the south without sea ice, generally support higher and more consistent primary productivity [84,86]. Atlantic influenced ecosystems around Iceland have more complex, stable, and highly connected food webs than Arctic systems, because the mixing of Arctic and Atlantic water masses introduces a wider range of prey species and ecological niches [36,120]. This convergence creates abrupt ecological transitions, where isotopic baselines ($\delta^{13}C$, $\delta^{15}N$) and prey communities shift sharply across water masses, which in turn makes it possible to test how oceanographic thresholds structure PFAS variability patterns.

To gain insight into foraging consistency at individual levels, we employ stable isotope analysis across two blood fractions with different turnover rates. Plasma integrates dietary information over short periods (~1 week), and red blood cells reflect longer timeframes (~3-4 weeks) [42]. By integrating isotopic values across these tissues, we assess how temporal consistency in foraging behaviour shapes individual PFAS exposure patterns. This dual-tissue approach provides a more detailed understanding of how individual foraging strategies translate into PFAS variability patterns than is possible with single-tissue analysis.

In this study, we explore contaminant dynamics in marine ecosystems by reconceptualising PFAS exposure variability as an ecological signal rather than statistical noise. By using Iceland's position at the Arctic-Atlantic interface, we hypothesize that PFAS exposure variability contains structured ecological signals

reflecting species-specific foraging strategies and oceanographic influences. We predict that UL and UA will exhibit distinct PFAS exposure variability profiles, with UL showing more constrained variability patterns and UA exhibiting broader patterns.

3.2 Methods and Materials

3.2.1 Study Design

We analysed 112 blood samples from UA ($n = 67$) and UL ($n = 45$) collected at five colonies across Iceland during June and July 2018 (Fig. 3-1) [87]. The sampling locations encompassed diverse oceanographic influences along both north-south and east-west gradients. Three northernmost colonies (NW, N, NE) harboured both UA and UL populations, while two southernmost colonies (SE, SW) harboured UA only. At the three northernmost colonies where both species coexist, we collected 15 samples per species per colony ($n = 45$ UL, $n = 45$ UA from northernmost colonies). At the two southernmost colonies where only UA breeds, we collected 15 samples at SE and 7 samples at SW due to logistical constraints. We separated blood samples into cells and plasma to evaluate guillemot foraging across different temporal scales. We measured PFAS concentrations in plasma, as these compounds exhibit strong binding affinity to albumin, a primary blood plasma protein. Stable isotope patterns in the North Atlantic show distinct spatial trends: $\delta^{13}C$ values follow a latitudinal gradient, with higher values in Atlantic-influenced waters than in Arctic waters, while $\delta^{15}N$ values indicate both trophic position and local oceanographic conditions [92]. The presence of both species at northernmost colonies facilitated direct interspecies comparisons of PFAS exposure. The balanced sampling design at northernmost colonies ($n = 15$ per species) provides adequate statistical power for direct interspecies comparisons of PFAS exposure, while the presence of both species at these northernmost colonies facilitates examination of species-specific responses to shared oceanographic conditions. Migration patterns differ between species: UL undertake extensive migrations from their high-latitude breeding sites to lower-latitude wintering areas, with the NW colony typically wintering in Southwest Greenland, and N and NE colonies wintering off West Greenland and north of Iceland [113]. UA generally winter closer to their breeding colonies, though some individuals migrate to the Mid-Atlantic Ridge or the waters between the Faroe Islands, Scotland, and Shetland Islands [121].

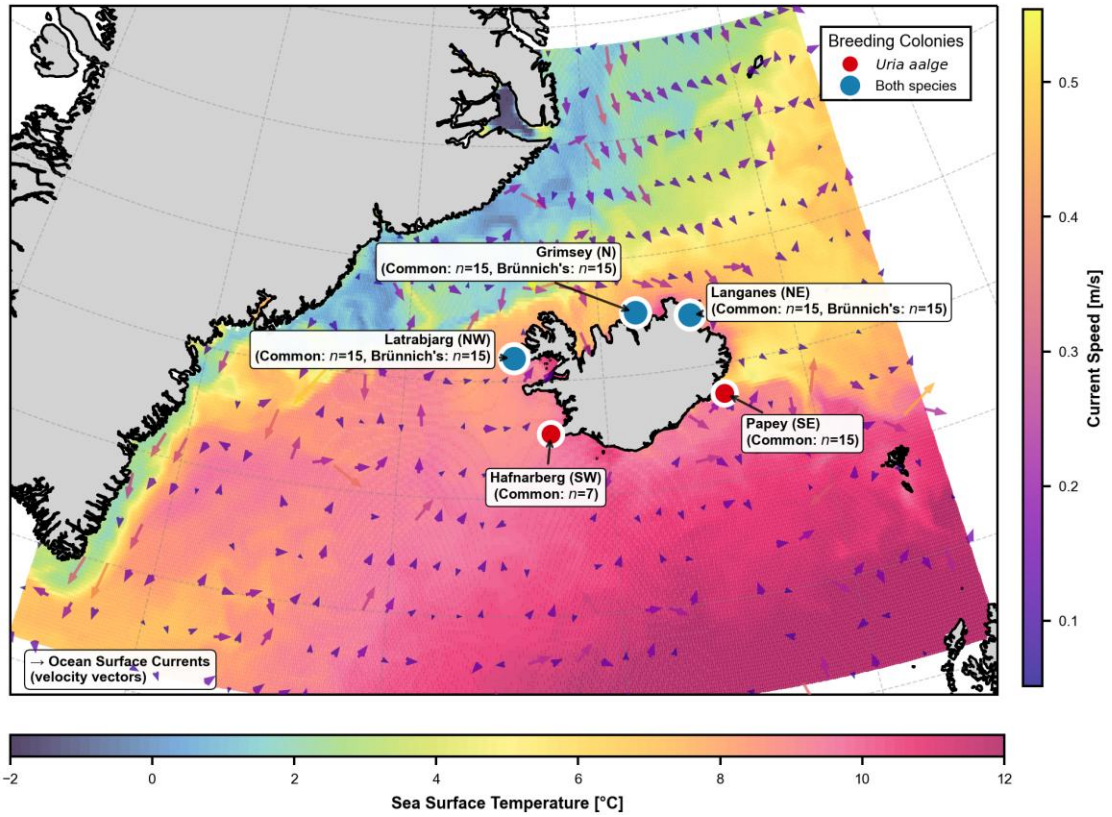

Figure 3-1. Sea-surface temperature and guillemot sampling sites around Iceland (June 2018). Sea surface temperature (SST) is shown alongside the major ocean currents influencing Icelandic waters: the warm Irminger and North Atlantic Currents, and the cold East Greenland and East Icelandic Currents. Guillemots were sampled at five colonies. Látrabjarg (northwest [NW]; 65.50° N, 24.52° W), located at the interface between the warm Irminger Current and the cold East Greenland Current; Grímsey Island (north [N]; 66.57° N, 18.02° W), primarily influenced by the warmer waters of the Irminger Current with some contribution from the cooler East Icelandic Current; Langanes peninsula (northeast [NE]; 66.38° N, 14.54° W), where the Irminger and East Icelandic Currents meet; Papey (southeast [SE]; 64.59° N, 14.18° W), situated in the cool East Icelandic Current, near its convergence with the warm North Atlantic Current; and Hafnaberg (southwest [SW]; 63.75° N, 22.75° W), affected by the warmer waters of the North Atlantic Current. The three northern colonies (NW, N, and NE) host both common guillemots (*Uria aalge*, UA) and Brünnich's guillemots (*Uria lomvia*, UL). The NW colony is the largest colony (343,900 guillemot pairs; UA:UL = 1.9:1.0), and the N colony is the second largest (71,400 pairs; UA:UL = 16.4:1.0) as per a 2008 census [122]. Only UA breeds in the two southern colonies (SE and SW). SST data are from Copernicus Marine Environment Monitoring Service Global Ocean Physics Reanalysis.

3.2.2 Sample Collection

To ensure a representative cross-section of Icelandic seabird populations, all blood samples were collected from selected breeding colonies, as described in Bonnet-Lebrun [87]. Approximately 1 mL of blood was collected from each seabird via venipuncture,

using rapid, minimally invasive sampling techniques to ensure bird welfare. Post-collection, blood samples were centrifuged using a Micro Star 12 centrifuge (VWR, Leuven, Belgium) at 12,300 rpm for 4 minutes to separate plasma and cells. The separated components were transferred to glass petri dishes and dried at ambient temperature in a desiccator for 4 to 6 days.

3.2.3 PFAS Chemical Analysis

PFAS analysis was performed on plasma samples at the Helmholtz-Zentrum Hereon (Geesthacht, Germany). The targeted analysis included 14 PFAS: nine PFCAs (C5-C13), four PFSAs (C4, C6, C8, C10), and HFPO-DA (complete list in Table A1, Appendix A).

PFAS extraction from dried plasma samples was performed using a modified quaternary ammonium salt-based ion-pairing method.[123,124] Prior to extraction, samples were fortified with ^{13}C-labeled PFAS internal standards and buffered with sodium carbonate (1 mL, 0.5 M, pH 10.0). The detailed extraction protocol is provided in the Supporting Information.

Analysis was conducted using HPLC-MS/MS with electrospray ionization in multiple reaction monitoring (MRM) mode. Chromatographic separation was achieved using a Synergi Fusion-RP C18 column with a water-methanol gradient containing ammonium acetate buffer. Method detection limits were 0.05-0.07 ng/mL for all target compounds, with data reported on dry weight basis (ng/g DM) consistent with the dried sample preparation approach. Detailed analytical parameters, as well as Quality Assurance and Quality Control (QA/QC) procedures, are provided in the Appendix A.

3.2.4 Stable Isotope Analysis

The isotope data for blood cells reported in this study have already been published by Bonnet-Lebrun [87]. The plasma isotope data, however, are presented here for the first time. The isotope data are expressed in delta (δ) notation:

$$\delta = \left(\frac{R_{sample}}{R_{standard}} - 1\right) \times 1000$$

Where R_{sample} is the ratio of the heavy to light isotope in the sample, and $R_{standard}$ is the ratio of the heavy to light isotope in the standard. To express the isotopic data as per mil (‰), they are multiplied by 1000. The isotope ratios are expressed relative to Vienna Pee Dee Belemnite (VPDB) for carbon and atmospheric air for nitrogen. Elemental content and bulk isotope values of blood cells were prepared according to Bonnet-Lebrun [87] and determined at the Stable Isotope Facility of the Experimental Ecology Group, GEOMAR, Kiel with a customised, high sensitivity elemental analyser connected to a stable isotope ratio mass spectrometer (DeltaPlus Advantage, Thermo Fisher Scientific, Germany) as described by Hansen and Sommer [125]. The standard deviations for $\delta^{13}C$ and $\delta^{15}N$ and ranged from ± 0.15‰ to ± 0.25‰ (n = 3).

3.2.5 Statistical Analysis

All statistical analyses were conducted using Python 3.9.16 with associated libraries, including Pandas 1.5.3, NumPy 1.24.3, SciPy 1.10.1, Scikit-learn 1.2.2, Statsmodels 0.13.5, Matplotlib 3.7.1, and Seaborn 0.12.2. Our analytical approach consisted of four sequential steps designed to characterise PFAS variability patterns and their relationships with ecological indicators.

First, PFAS concentration data were log-transformed to improve normality. We then conducted Principal Component Analysis (PCA) on these log-transformed concentrations to reduce the dimensionality of the multi-compound dataset and identify the primary patterns of covariation among PFAS across individual birds Based on the patterns revealed by PCA (Appendix A), we then standardised each individual's PC scores into *z*-scores to quantify how much each bird expresses these covariation patterns. A *z*-score of zero represents average variability for that exposure pattern across the population. Negative *z*-scores indicate more constrained (consistent) exposure patterns,

whereas positive *z*-scores indicate more variable (heterogeneous) exposure patterns. Note that in this study, the application and interpretation of *z*-scores is tailored to the specific PCA loading patterns found in this dataset, allowing us to identify individuals with consistently constrained versus heterogeneous exposure patterns that may reflect different foraging strategies. Second, we implemented *k*-means clustering to characterise population-level patterns in PFAS variability. We determined the optimal number of clusters using silhouette analysis, which maximizes within-cluster similarity and between-cluster separation. Silhouette scores (-1 to +1) measure clustering quality, where higher values indicate better cluster assignment, zeros suggest borderline cases, and negative values indicate likely misclassification. This approach allowed us to identify distinct PFAS variability profiles across the study populations. Finally, to detect potential threshold effects in relationships between isotopic consistency and PFAS variability patterns, we employed bivariate segmented regression. We calculated isotopic consistency scores ($\delta^{13}C_{consist}$ and $\delta^{15}N_{consist}$) using PCA to capture the shared consistency between tissues followed by standardisation into z-scores. A consist score of zero represents the overall population mean, with positive and negative scores indicating consistently higher or lower isotopic values across tissues, respectively. The absolute magnitude of these scores reflects how strongly an individual's isotopic pattern deviates from the population mean across both temporal scales. For the bivariate segment analysis, the dataset was split into training (80%) and testing (20%) sets. Optimal breakpoints for segmented regression were identified by minimizing the sum of squared residuals. Models included base effects for both isotopic indicators, segment effects for values above identified breakpoints, and interaction terms. Model performance was evaluated using R^2 and RMSE. Based on the identified breakpoints, individuals were classified into habitat-associated segments to assess how oceanographic regimes influenced PFAS variability patterns. All statistical tests were two-tailed, with significance levels set at $\alpha = 0.05$. 95% confidence intervals were reported where appropriate. Detailed descriptions of these calculations and additional statistical methods are provided in the Appendix A.

3.3 Results

3.3.1 PFAS Variability Patterns

Analysis of PFAS concentrations in plasma samples revealed consistent patterns of exposure across the two seabird species UA and UL. Long-chain PFCAs (C9-C13) and PFOS (linear and branched) were the dominant compounds detected in all samples. PFOS accounted for 62-73% of the total PFAS burden in UA and 70-89% in UL, highlighting its predominance in both species. Among PFCAs, PFUnDA (C11) and PFTrDA (C13) were the most abundant, with median concentrations ranging from 10.0 to 23.3 ng/g DM in UA and 6.6 to 10.0 ng/g in UL. Short-chain PFCAs (e.g. PFPeA, PFHxA) and PFBS as well as HFPO-DA were not detected in any samples. Detection frequencies and concentration ranges are summarized in Table 3-1, while Fig. 3-2 illustrates median PFAS profiles across species and colonies.

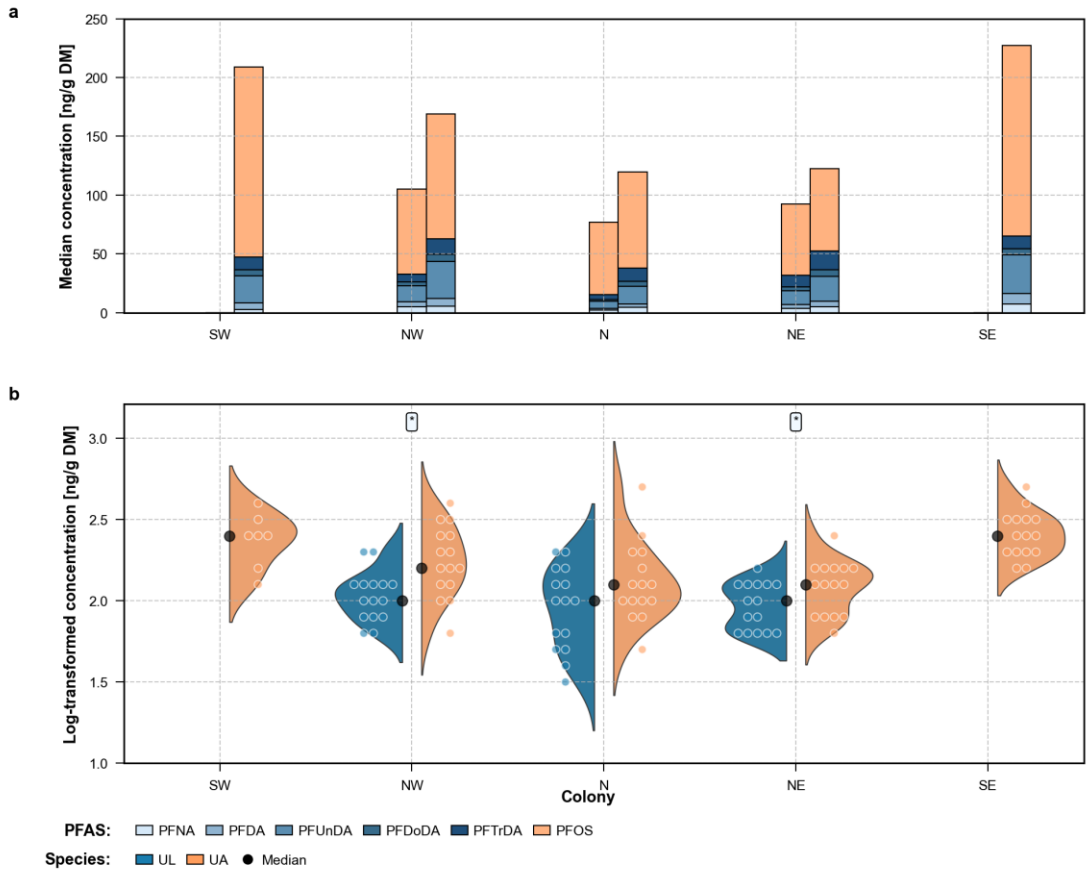

Figure 3-2. PFAS composition and concentrations in Icelandic guillemots across species and colonies. Per- and polyfluoroalkyl substance (PFAS) profiles are compared between Brünnich's guillemots (*Uria lomvia*, UL) and common guillemots (*Uria aalge*, UA) across five colonies in Iceland (NW [northwest], N [north], NE [northeast], SW [southwest], and SE [southeast]). a, Median PFAS concentrations of five long-chain perfluoroalkyl carboxylic acids (C9–C13 PFCAs) and perfluorooctane sulfonate (PFOS, linear and branched). Left: UL; right: UA. b, Log-transformed PFAS concentrations (including C9–C13 PFCAs and PFOS) shown as split-violin plots. Each data point represents an individual bird, while the split-violin shapes reflect the overall distribution for each colony and species. Black dots indicate median values for each species at each colony, and asterisks represent significance levels between species at the sympatric colony (*$p \leq 0.05$).

Table 3-1. Detection rates and concentration ranges of PFAS in UA and UL samples.

Compound	UL				UA			
	DF [%]	Median	Min. [ng/g DM]	Max.	DF [%]	Median	Min. [ng/g DM]	Max.
PFPeA	n.d.	< MDL	< MDL	< MDL	n.d.	< MDL	< MDL	< MDL
PFHxA	n.d.	< MDL	< MDL	< MDL	n.d.	< MDL	< MDL	< MDL
PFHpA	49	0.1	< MDL	0.9	27	0.1	< MDL	0.4
PFOA	47	0.4	< MDL	1.8	40	0.5	< MDL	2.8
PFNA	100	3.4	0.9	16.5	100	4.4	1.1	24.2
PFDA	100	2.7	0.4	15.5	100	5.6	1.0	21.5
PFUnDA	100	10	1.3	48.1	100	23.3	5.9	95.5
PFDoDA	100	2.4	0.3	9.3	100	5	1.6	17.9
PFTrDA	100	6.6	1.2	20.4	100	12.9	4.2	38.7
PFBS	33	< MDL	< MDL	0.1	21	< MDL	< MDL	0.2
PFHxS	27	0.4	< MDL	1.2	40	0.4	< MDL	1.7
PFHpS	7	1.9	0.6	1.9	4	2.2	1.6	5.0
PFOS	100	69.8	22.8	203	100	103	23.1	409.7
PFDS	69	1.5	< MDL	12.7	70	0.7	< MDL	7.0
HFPO-DA	n.d.	< MDL	< MDL	< MDL	n.d.	< MDL	< MDL	< MDL

DF: Detection Frequency

n.d.: not detectable

To identify the underlying exposure patterns driving PFAS variability within individuals, we investigated how PFAS covary using PCA. PCA revealed two main sources of variability in PFAS exposure patterns. The first principal component (PC1), which was mainly driven by long-chain PFCAs (C9-C13), explained 79% of the variation. The second component (PC2) was driven by PFOS, which varied independently from the other compounds, and accounted for an additional 13% of the variability (detailed results in Appendix A, Fig. A1). Based on these distinct patterns, coordinated PFCA behaviour versus independent PFOS behaviour, we applied *z*-scores, denoted as z_{PFCA} (for long-chain PFCAs) and z_{PFOS} (for PFOS), to measure how much each individual bird expresses these different exposure patterns. z_{PFCA} ranged from -2.3 to 2.9 across all birds. Northernmost UA showed predominantly negative *z*-scores (median: -0.6 to 0.2) with relatively constrained variability. In contrast, northernmost UL exhibited predominantly positive *z*-scores (median: 0.3 to 1.1) with greater

variability in pattern expression. z_{PFOS} ranged from -2.1 to 3.4. Southernmost UA showed elevated positive *z*-scores (median: 0.7 to 0.8) with high variability in PFOS pattern expression (max values, SW: 3.4; SE:2.7). Northernmost populations of both species showed more constrained PFOS patterns, exhibiting predominantly negative *z*-scores across colonies (median, UA: -0.7 to -0.2; UL: -0.5 to 0.4).

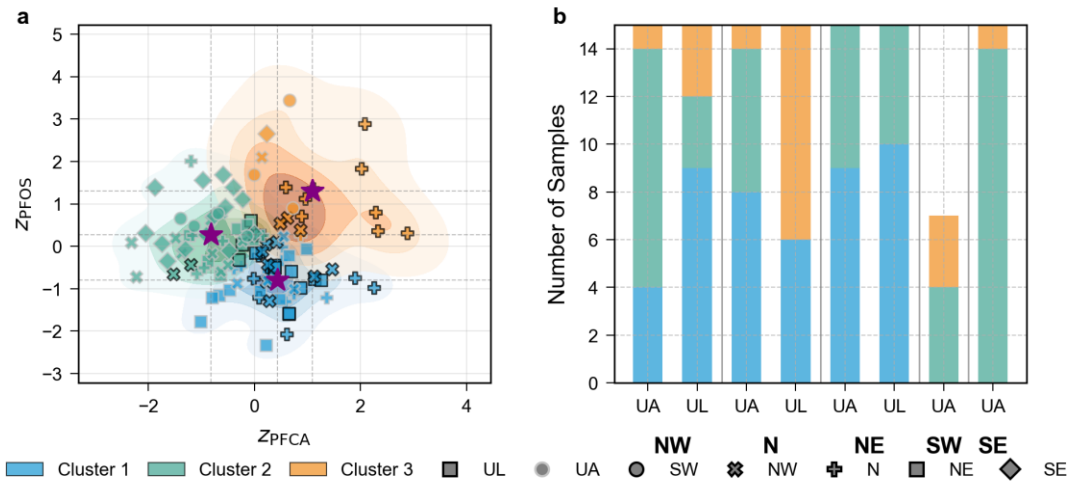

Figure 3-3. Clustering of PFAS variability in common and Brünnich's guillemots. a, *K*-means clustering based on standardised variability (z-scores) in long-chain PFCAs (z_{PFCA}, C9-C13) and PFOS (z_{PFOS}). The zero point on each axis represents the mean variability, with positive and negative values indicating higher and lower variability than the mean, respectively. Each point represents an individual seabird, with edge colours denoting species (black: *Uria lomvia* [UL]; white: *Uria aalge* [UA]), shapes indicating colony location, and fill colours representing cluster assignment. Purple stars mark cluster centroids. b, Colony-level distribution of cluster membership, shown as the proportion of individuals from each species assigned to each cluster at each colony. Colony codes: NW, northwest; N, north; NE, northeast; SW, southwest; and SE, southeast.

To categorize birds according to their PFAS exposure variability profiles, we performed *k*-means clustering analysis. *k*-means clustering analysis ($k = 3$) identified three distinct patterns in PFAS exposure variability across guillemot populations (Fig. 3-3), with an overall silhouette score of 0.35. The first and largest cluster ($n = 51$, silhouette score: 0.32) was centred at (0.4 ± 0.6 z_{PFCA}, -0.7 ± 0.6 z_{PFOS}), indicating variable PFCA variability but consistently low PFOS variability. The second cluster ($n = 44$, silhouette score: 0.37) displayed the opposite pattern, with consistently low PFCA variability but more variable PFOS variability, centred at (-0.9 ± 0.6 z_{PFCA}, 0.3 ± 0.7 z_{PFOS}). The

smallest cluster (n = 17, silhouette score: 0.23) showed high variability in both PFAS classes, centred at markedly positive values (1.1 ± 0.8 z_{PFCA}, 1.4 ± 0.9 z_{PFOS}).

PFAS variability patterns showed a clear north-south gradient, with Cluster 1 (variable PFCAs, low PFOS variability) dominating northern colonies and Cluster 2 (low PFCA, variable PFOS variability) predominating southern colonies. Species distributions varied by location: at NW colony, UA individuals mainly fell into Cluster 2 while UL individuals primarily grouped in Cluster 1; at colony N, both species shared representation in Cluster 1 but diverged in secondary patterns (UA in Cluster 2, UL in Cluster 3); and at NE colony, both species predominantly occupied Cluster 1 with minimal divergence.

3.3.2 Isotopic Consistency Across Tissues

Blood cell, $\delta^{13}C$ values showed a north-south gradient ranging from -22‰ to -19‰, with more negative values in northern colonies and more positive values in southern colonies (Fig. 3-4). Plasma $\delta^{13}C$ patterns resembled those of the cell, but with slightly more negative overall values. Blood $\delta^{15}N$ values ranged from 11‰ to 14‰, and plasma from 11‰ to 15‰. Both tissues displayed the highest $\delta^{15}N$ values in the SE colony. Find detailed statistical results in Appendix A (Table A7).

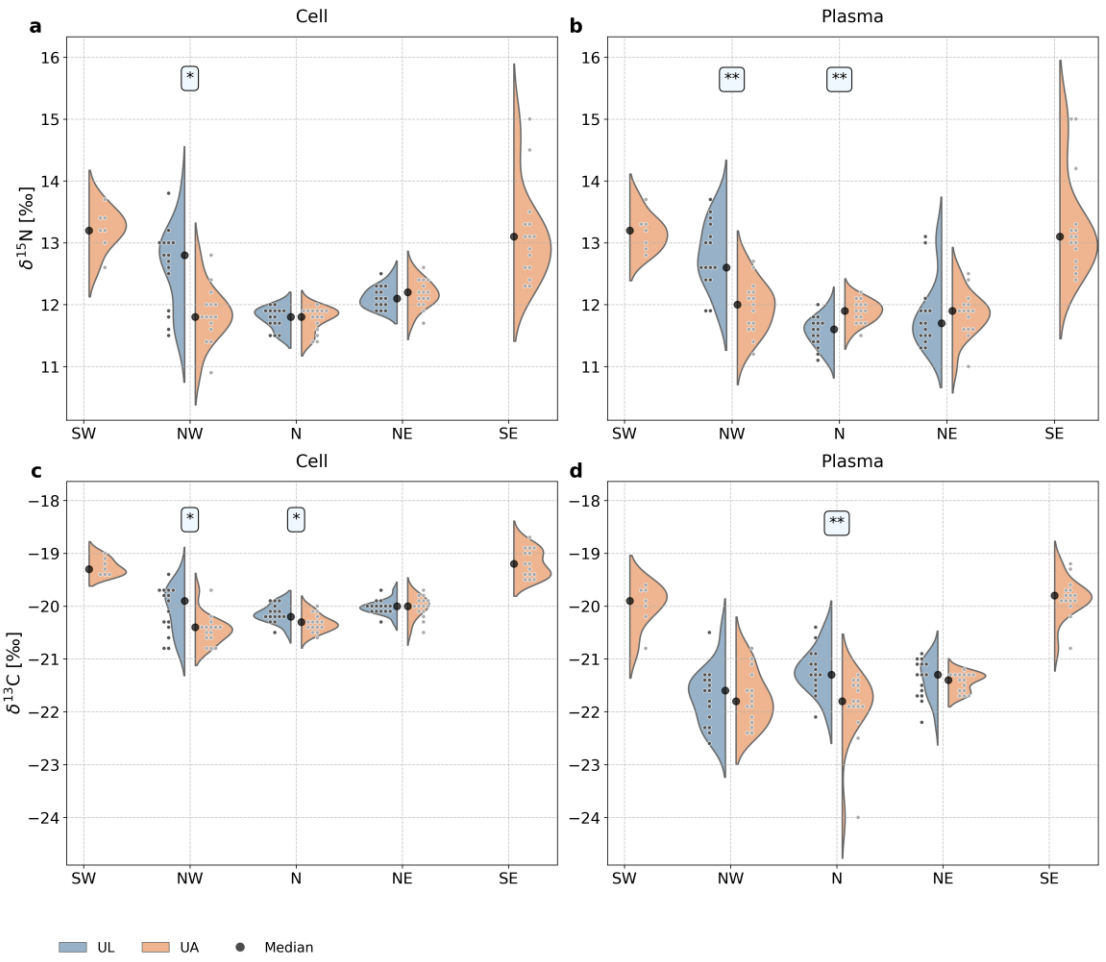

Figure 3-4. **Stable isotope composition of guillemot tissues across Icelandic colonies.** Split violin plots show the distribution of nitrogen (δ15N; a, b) and carbon (δ13C; c, d) isotope values in red blood cells (a, c) and plasma (b, d) from Brünnich's guillemots (Uria lomvia, UL) and common guillemots (Uria aalge, UA) across five geographic colonies: southwest (SW), northwest (NW), north (N), northeast (NE), and southeast (SE). Violin plots display kernel density estimates with individual data points overlaid; black dots represent the median. Asterisks denote statistical significance of between-species comparisons at sympatric colonies (*p < 0.05, **p < 0.01).

To assess foraging consistency during the breeding season, we examined isotopic relationships between plasma and red blood cells. Both $\delta^{13}C$ ($r = 0.65$, $p < 0.001$) and $\delta^{15}N$ ($r = 0.70$, $p < 0.001$) values showed significant positive correlations between tissues, indicating temporal consistency in foraging patterns. To quantify this consistency across both isotopes simultaneously, we applied PCA to the dual-tissue isotope data, capturing the shared variability between plasma and red blood cell measurements. We then transformed PC1 scores into *z*-scores, denoted as $\delta^{15}N_{consist}$ and $\delta^{13}C_{consist}$. Stable isotope consistency patterns varied across species and colonies. For nitrogen ($\delta^{15}N_{consist}$), UA breeding at southernmost colonies showed predominantly

positive *z*-scores (median SE: 1.3, SW: 1.4), indicating more positive $\delta^{15}N$ values consistently across both tissues. In contrast, northernmost colonies of both species exhibited negative *z*-scores (ranging from -0.9 to -0.2), reflecting more negative $\delta^{15}N$ values across tissues. Carbon isotope consistency ($\delta^{13}C_{consist}$) showed similar geographic patterns, with UA from southernmost colonies displaying positive *z*-scores (median SE: 2.0, SW: 1.6) indicating consistently more positive $\delta^{13}C$ values, while northern populations of both species showed negative *z*-scores (ranging from -0.9 to -0.1), reflecting consistently more negative $\delta^{13}C$ values across plasma and cell tissues. Both isotope systems demonstrated consistent north-south gradients, with UL showing relatively similar patterns to northernmost UA.

3.3.3 Bivariate Segmented Regression

The bivariate segmented regression analyses revealed that PFCA and PFOS variability patterns respond differently to oceanographic thresholds (Table 3-2). Statistical breakpoints ($\delta^{13}C_{consist}$ = 0.19, $\delta^{15}N_{consist}$ = 0.00) delineated three distinct foraging habitats in isotopic space: Arctic-influenced, niche partitioning, and Atlantic-influenced waters (Fig. 3-5). PFOS variability (z_{PFOS}) showed a clear oceanographic threshold effect, with a statistically significant shift at $\delta^{13}C_{consist}$ = 0.19 ($p < 0.01$). Mean Z_{PFOS} scores were negative in Arctic-influenced habitats, indicating constrained variability, but strongly positive in Atlantic-influenced habitats, reflecting more variable patterns. This habitat effect accounted for 66% of the total model influence on PFOS variability. In contrast, PFCA variability (z_{PFCA}) showed a more gradual transition across the oceanographic gradient, with non-significant threshold effects. Mean z_{PFCA} scores were positive in Arctic waters but became increasingly negative in Atlantic waters. While not statistically significant, the $\delta^{15}N_{consist}$ threshold accounted for 55% of the total model effect. The niche partitioning segment contained predominantly UL individuals from the NW colony, exhibiting negative values for both z_{PFCA} and z_{PFOS}. These contrasting patterns demonstrate that PFCA and PFOS respond to different ecological drivers: PFCA variability is more influenced by trophic position ($\delta^{15}N_{consist}$), while PFOS variability is predominantly controlled by habitat factors ($\delta^{13}C_{consist}$). Find detailed statistical results in Appendix A (Table A8-9).

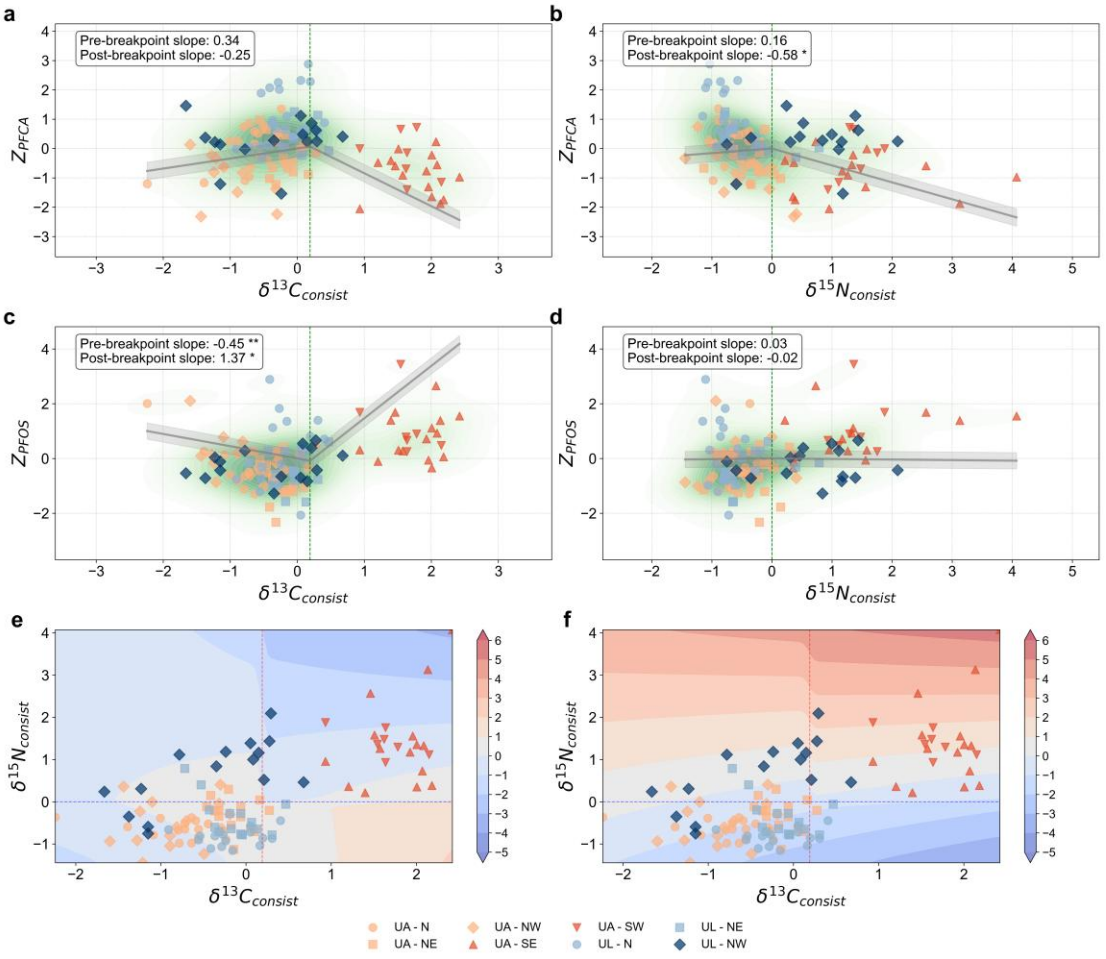

Figure 3-5. Segmented regressions and interaction effects of foraging consistency on PFAS bioaccumulation in guillemots. a–d, Segmented regression relationships between PFAS variability (z-scores for long-chain PFCAs [a, b] and PFOS [c, d]) and isotopic foraging consistency metrics (δ13C [a, c] and δ15N [b, d]). Vertical dashed green lines indicate identified breakpoints, with pre- and post-breakpoint slopes annotated (asterisks denote significance: *$p < 0.05$, **$p < 0.01$). Shade represents 95% confidence intervals. e–f, Contour plots illustrating two-way interactions between δ13Cconsist and δ15Nconsist for PFCAs (e) and PFOS (f). Dashed lines mark identified breakpoints (δ13Cconsist = 0.19, vertical; δ15Nconsist = 0.0, horizontal), delineating four foraging strategy quadrants: Arctic-influenced habitat specialists (δ13Cconsist < 0.19 and δ15Nconsist < 0.0), niche partitioning within Arctic-influenced waters (δ13Cconsist < 0.19 and δ15Nconsist > 0.0), Atlantic-influenced generalists (δ13Cconsist > 0.19 and δ15Nconsist > 0.0), and individuals with high carbon but low nitrogen consistency (δ13Cconsist > 0.19 and δ15Nconsist < 0.0). Colour gradients represent predicted PFAS z-scores ranging from −3.0 (blue) to 4.0 (red). Species are distinguished by colours and breeding colonies by marker shapes. UA: Uria aalge, common guillemots; UL: Uria lomvia, Brünnich's guillemots. Five geographic colonies: southwest (SW), northwest (NW), north (N), northeast (NE), and southeast (SE).

Table 3-2. Bivariate Segmented Regression Analysis of Isotopic Indicators' Influence on PFAS Variability Patterns.

Response Variable		PFCA (z_{PFCA})	PFOS (z_{PFOS})
Model Performance	R^2 (Training)	0.17	0.30
	R^2 (Testing)	0.06	0.16
	RMSE (Training)	0.86	0.82
	RMSE (Testing)	1.10	1.03
Breakpoints	$\delta^{13}C_{consist}$	0.19	0.19
	$\delta^{15}N_{consist}$	0.00	0.00
Coefficients	Intercept	0.32 (0.16)	**-0.42 ****
	$\delta^{13}C_{consist}$	0.23 (0.17)	-0.22 (0.06)
	$\delta^{13}C_{consist}$ segment	-0.06 (0.60)	**1.16 ****
(*p*-value)	$\delta^{15}N_{consist}$	-0.09 (0.70)	0.14 (0.60)
	$\delta^{15}N_{consist}$ segment	-0.64 (0.25)	-0.12 (0.65)
	$\delta^{13}C_{consist}$ $\delta^{15}N_{consist}$	-0.15 (0.20)	**0.13 ***
Segment Combinations	Arctic-influenced	0.21	-0.28
	Niche Partitioning	-0.32	-0.40
(mean)	Atlantic-influenced	0.51	0.80

Significance levels: *** $p < 0.001$, ** $p < 0.01$, * $p < 0.05$

3.4 Discussion

PFAS bioaccumulation patterns in marine predators reflect the dynamic integration between environmental exposure pathways and trophic transfer processes [5,9]. Whereas previous studies have treated variability as statistical noise, our approach recognises that variability as ecologically informative, revealing aspects of contaminant pathways that mean-based analyses may miss [5,9,58]. Our integrated dual-isotope framework ($\delta^{13}C_{consist}$ and $\delta^{15}N_{consist}$ scores) allows us to interpret PFAS variability as an ecological signal, showing how foraging patterns influence contamination dynamics. Despite inherent methodological limitations as discussed later, this approach offers insights into the ecological drivers of contaminant exposure [43,126]. Our variability-based framework demonstrates broader applicability beyond PFAS, potentially revealing ecological processes governing other persistent contaminants in marine food webs where spatial heterogeneity and foraging specialisation create measurable variability patterns. For instance, the segmented regression analysis (Table 3-2, Fig. 3-5) identified significant isotopic thresholds aligning with Arctic-Atlantic oceanographic regimes. These thresholds reveal how variability patterns shift across these oceanographic gradients even when mean concentrations might not show clear transitions. Similarly, cluster analysis (Fig. 3-3) identified

habitat-specific variability differences between sympatric species, with pronounced niche separation at the NW colony that traditional approaches would mask. These findings demonstrate how variability patterns uncover ecological drivers, such as the different influences of trophic position on long-chain PFCAs and habitat use on PFOS, thus contributing to our understanding of contaminant dynamics in rapidly changing marine ecosystems.

3.4.1 PFAS Variability as Structured Ecological Signal

Our hypotheses predicted that (1) PFAS exposure variability contains structured ecological signals reflecting foraging strategies and oceanographic influences, and (2) UL and UA would exhibit distinct variability profiles, with UL showing more constrained patterns and UA exhibiting broader variability. The results provide support for structured ecological signals while revealing that species differences are compound- and habitat-dependent rather than universally expressed.

k-means clustering revealed three distinct variability patterns with clear geographic organisation (Fig. 3-3), while significant threshold effects at Arctic-Atlantic transitions ($\delta^{13}C_{consist} = 0.19$, $\delta^{15}N_{consist} = 0.00$) mark ecological boundaries. The temporal consistency in foraging behaviour during breeding (plasma-cell isotope correlations: $r = 0.65$-0.70) indicates that individuals maintain relatively stable foraging patterns over tissue integration periods, enabling confident interpretation of relationships between current foraging indicators and PFAS variability patterns despite temporal mismatches between isotopic integration (weeks - months) and PFAS accumulation (years).

As expected from previously published telemetry data [127], these geographic patterns demonstrate that PFAS variability reflects structured ecological signals rather than statistical noise. Both guillemot species breeding in northern Iceland exhibited high site fidelity by foraging in cold, less saline Arctic waters, reflected in more negative $\delta^{13}C_{consist}$ and $\delta^{15}N_{consist}$ scores (Fig. 3-4) and primarily associated with constrained PFOS variability (Fig. 3-3). In contrast, southern Icelandic UA foraged within warmer, more saline Atlantic waters (evidenced by more positive isotopic scores), demonstrating constrained PFCA variability yet more variable PFOS patterns. This compound-specific response validates distinct bioaccumulation mechanisms operating within the sister species.

While these broad-scale patterns demonstrate how water masses influence PFAS variability, our detailed analysis identified fine-scale habitat-specific behavioural adaptations that generated notable differences from expected patterns. At the NW colony, the variability patterns of both UA and UL distributed across three clusters, with UL showing predominantly constrained PFOS variability whereas UA showed constrained PFCA variability (Fig. 3-3), reflecting their differences in foraging strategies. As shown in our tracking data [127], oceanographic heterogeneity at the interface between the warm Irminger Current and cold East Greenland Current enabled distinct foraging opportunities where UL foraged more frequently in glacial fjords and along the marginal ice zone compared to UA [87], while they also showed substantial overlaps in their use of other habitat features such as water depth. This pattern suggests that species-specific foraging behaviours may influence compound-specific variability patterns. While the mechanisms remain to be fully elucidated, the species-compound coupling demonstrates that environmental heterogeneity enables the expression of different variability patterns rather than simply creating broad variability differences. At the N colony, while both species shared more similar foraging strategies and habitat use [127], UA showed more defined PFAS variability patterns compared to UL (Fig. 3-3). Within this colony, both UA and UL were associated with constrained PFOS variability. However, a considerable portion of UA showed constrained PFCA variability, whereas more than half of the observed UL showed less defined variability (Fig. 3-3). Diel vertical migration of marine prey provides the ecological foundation for how depth- and time-specific foraging may expose the two species to different prey assemblages and contamination sources [128,129]. The documented differences between species, UL performing nocturnal foraging and shallower diving while UA dived to deeper depths throughout the day [127], position them to encounter different components of the vertically migrating prey community. This temporal-depth decoupling potentially creates the observed PFAS variability patterns, particularly explaining UL's less defined variability. At the NE colony, the variability patterns were the most uniform, as both UA and UL are predominantly associated with constrained PFOS variability. Within NE, no niche partitioning was observed between species [87]. This ecological convergence reflects both species accessing similar prey resources within Arctic food-web structures and creates homogeneous exposure environments.

In contrast, the SW and SE colonies demonstrate how trophic magnification processes create compound-specific uniform variability patterns despite isotopic diversity. UA at these colonies exhibited the highest $\delta^{15}N$ values across both tissues (Fig. 3-4), indicating foraging at relatively high trophic levels within Atlantic-influenced waters. Correspondingly, the highest PFOS concentrations were observed within these colonies (Fig. 3-2), indicating enhanced biomagnification processes during high-trophic-level foraging [9,28]. This enhanced biomagnification creates compound-specific responses through different mechanisms. For PFOS, the elevated concentrations enable greater detection of inter-individual variability, resulting in more variable PFOS patterns. For PFCAs, however, the intense biomagnification results in competitive protein binding where PFOS consistently outcompetes PFCAs for limited binding sites regardless of prey diversity consumed [8,100]. This competitive dominance suppresses PFCA accumulation and constrains PFCA variability, creating uniform PFCA patterns. The result is compound-specific variability patterns where bioaccumulation intensity differentially affects PFOS and PFCA detectability through distinct mechanisms, concentration-enhanced detection for PFOS versus competition-mediated suppression for PFCAs. On the other hand, birds at Arctic-influenced colonies foraged on lower trophic sources with reduced biomagnification compared to Atlantic systems, creating contrasting effects on variability patterns. For PFOS, lower concentrations from reduced biomagnification constrain detectable inter-individual variability, creating uniform patterns. For PFCAs, the absence of intense biomagnification prevents competitive protein binding, making PFCA variability more detectable rather than being biochemically suppressed. Arctic systems thus preserve ecological signals as primary drivers of PFCA variability while PFOS variability becomes constrained by both ecological similarity and concentration-dependent detection. This represents ecological signal preservation rather than the biochemical masking observed in Atlantic systems.

3.4.2 Methodological Considerations

Our approach of using temporal consistency in isotopic values ($\delta^{13}C_{consist}$ scores and $\delta^{15}N_{consist}$ scores) for foraging behaviour provides a framework for interpreting PFAS variability patterns across oceanographic gradients. While these consistency scores offer insights into foraging habits during the breeding season, several methodological

limitations should be considered when interpreting the results. One consideration is the temporal mismatch between isotope turnover rates (weeks to months) and PFAS persistence (years in some cases). While the isotopes analysed in the two blood fractions reflect recent foraging behaviour, part of the detected PFAS likely accumulated before the breeding season. This temporal integration is particularly relevant for legacy compounds like PFOS, which has a half-life of several years in seabirds [93]. Additionally, isotopic baselines can vary substantially across oceanographic regions, seasons, and even small spatial scales [130,131]. Without direct measurements of baseline isotopic values across our study area, we cannot definitively attribute differences in isotopic values to trophic or habitat factors versus baseline shifts. For example, $\delta^{15}N$ values may reflect differences in baseline nitrogen sources rather than actual trophic positions [132]. Physiological factors unrelated to diet can also influence both isotopic values and PFAS accumulation. Individual variation in metabolic rates, growth, reproductive status, and detoxification capacity may affect both isotopic incorporation and PFAS retention independently, potentially creating correlations that do not reflect ecological processes. Finally, our correlative approach cannot establish causation between isotopic patterns and PFAS variability. While our 2018 breeding season data capture apparent habitat associations, these relationships require experimental validation to confirm the mechanistic links between foraging ecology and PFAS accumulation patterns. Nevertheless, several methodological advances could address these limitations. Isotope analysis of tissues formed before the breeding season and inclusion of more sophisticated analyses such as compound specific isotope analyses that can provide more detailed insight into foraging and physiology compared to bulk stable isotope analyses [104,133-137]. Furthermore, baseline corrections across different oceanographic regions could improve the comparability of isotopic measurements between Arctic and Atlantic waters [138].

3.4.3 Conclusion and Implications

Our integrated analysis highlights how PFAS exposure variability in marine predators is structured by a combination of oceanographic features, foraging ecology, and compound-specific behaviour. Spatial habitat factors predominantly shape PFOS variability, with pronounced transitions at Arctic-Atlantic boundaries, while long-chain PFAC variations aligns with trophic indicators, reflecting foraging position within food

webs. These patterns point to the influence of both large-scale oceanographic gradients and colony-level foraging behaviours in generating local variation in exposure. The distinct PFCA and PFOS responses reflect their unique physicochemical properties and biological interactions. Our variability-focused approach reveals ecological dimensions of contaminant exposure that mean-based methods typically miss, though temporal mismatches between isotopic integration and PFAS persistence require careful interpretation. As climate change shifts ocean conditions, the oceanographic drivers of PFAS variability we identify will likely alter contaminant risks for marine predators. As demonstrated in this study, this framework offers potential for tracking contaminant pathways and for informing conservation strategies in rapidly changing polar and subpolar marine ecosystems.

Acknowledgments

This paper is an output of Project LOMVIA (BMBF Grant No. 03V01459) and Project EISPAC (BMBF Grant No. 03F0809A), both of which are part of the Changing Arctic Ocean Programme. Additional funding was provided by UKRI/NERC (Grant Nos. NE/R012660/1 and NE/R012857/1). R.S. received a stipend from the Max Planck Institute of Geoanthropology. A permit was provided by the Icelandic Institute of Natural History and animal ethics was overseen by BAS AWERB.

Chapter 4: Contamination Niche: Foraging Strategies Structure PFAS Exposure in Seabirds

Note: This chapter is currently under preparation for submission in *Environmental Science & Technology*.

Shen, R., Vassão, D.G., Ratcliffe, N., & Larsen, T. (2025).

Abstract

Understanding contaminant accumulation in marine top predators requires moving beyond one-dimensional trophic models to examine how multidimensional foraging strategies shape exposure patterns. We introduce a 'contamination niche' framework and apply it to per- and polyfluoroalkyl substances (PFAS) exposure in two sympatric guillemot species (*Uria lomvia* and *Uria aalge*) breeding across five Icelandic colonies influenced by Arctic and Atlantic water masses. We analysed PFAS concentrations and stable isotope ratios ($\delta^{13}C$, $\delta^{15}N$) in blood plasma and red blood cells from 112 seabirds sampled at five breeding colonies around Iceland during June-July 2018 to evaluate how spatial, temporal, and dietary dimensions of foraging behaviour influence contamination patterns. Clustering analysis of PFAS concentrations identified three exposure groups with distinct compositional profiles: high-exposure individuals ($n = 36$) exhibited exclusively PFOS-dominated patterns, intermediate-exposure individuals ($n = 62$) showed predominantly population-average patterns (79.0% conditional probability), and low-exposure individuals ($n = 14$) displayed PFCA-enriched profiles (78.6%) with complete absence of PFOS-dominance. Multidimensional foraging strategies, integrating water mass utilisation, temporal consistency, and trophic position, shape these contamination profiles. Three discrete contamination niches emerged from these exposure-foraging associations: High-Exposure Atlantic Foragers (Atlantic waters, higher trophic resources, strong temporal consistency), Low-Exposure Arctic Foragers (Arctic waters, lower trophic resources, temporal variability), and Intermediate-Exposure Mixed Foragers (intermediate values across all dimensions). These contamination niches represent emergent properties of multidimensional ecological strategies rather than simple reflections of geographic proximity to sources or trophic position alone. The framework provides potential predictive capacity for identifying vulnerable populations based on foraging ecology, enabling proactive monitoring that targets ecological vulnerability rather than geographic proximity to contamination sources and offers mechanistic understanding necessary for anticipating how climate-driven shifts in prey distributions may alter contamination dynamics in Arctic marine ecosystems.

Keywords: Contamination niche; ecological niche; PFAS; guillemots; trophic ecology; bioaccumulation

4.1 Introduction

Chemical exposure patterns in marine ecosystems constitute more than mere contamination gradients; rather, they represent emergent ecological structures shaped by behavioural adaptations and resource partitioning. Persistent pollutants such as per- and polyfluoroalkyl substances (PFAS) exhibit non-random distribution patterns in marine predators that parallel resource partitioning, suggesting that contamination follows organising principles analogous to those governing ecological niches [60,64,72,74]. This phenomenon is particularly evident in seabirds, where populations occupying equivalent trophic positions display distinct PFAS profiles that persist across temporal scales and correspond with specific foraging strategies [62,63]. We introduce the term 'contamination niche' to conceptualise the characteristic pattern of chemical exposure that results from an organism's specific ecological strategies. Just as ecological niches describe how species partition resources through their behaviours and adaptations, contamination niches elucidate how organisms partition chemical exposure through these same ecological mechanisms.

Chemical exposure patterns comprise three distinct yet interconnected features: concentration (magnitude of accumulation), composition (relative proportions of different compounds), and variability (distribution within populations). While concentration aspects have dominated research through trophic magnification studies [31,46], both compositional profiles and variability patterns remain largely unexplored. Our previous investigation (Chapter 3) addressed this methodological gap by examining PFAS variability patterns within two sympatric seabirds, revealing clear ecological signals rather than statistical noise. The findings demonstrated that PFOS variability correlates strongly with spatial indicators ($\delta^{13}C$), whereas PFCA variability corresponds significantly with trophic position ($\delta^{15}N$). Seabirds foraging in shared waters exhibit consistent variability patterns but display distinct threshold effects in the relationship between isotopic consistency and PFAS variability. These structured variability patterns suggest that contamination follows organising principles that parallel ecological niche partitioning. A comprehensive approach integrating multiple dimensions, concentration, composition, and variability, is now required to elucidate the ecological factors underlying chemical exposure patterns.

Seabirds represent particularly valuable sentinel species for investigating these multidimensional contamination patterns. As marine apex predators, they consistently exhibit some of the highest PFAS concentrations documented in marine ecosystems [60,139]. These elevated exposure levels raise concerns regarding reproductive impairment, immune dysfunction, and metabolic disruption across seabird populations [140,141]. Colonial seabirds constitute an exceptional model system for examining contamination niches due to their well-defined spatial constraints during breeding seasons, taxonomically diverse yet ecologically comparable communities, and clearly delineated foraging strategies that can be quantified through multiple complementary methodologies. Their central-place foraging behaviour during breeding periods creates natural experiments in resource partitioning, as sympatric species must differentiate their ecological strategies while operating within similar spatial constraints [142,143]. Additionally, seabird tissues provide integrated signals of both contaminant accumulation and isotopic niche parameters across multiple temporal scales, from recent foraging trips to longer-term dietary patterns, allowing for robust characterisation of ecological-contaminant relationships [42,90].

Stable isotope analysis has transformed ecological investigations by providing time-integrated measures of resource utilisation and trophic relationships. Carbon isotope ratios ($\delta^{13}C$) primarily reflect basal carbon sources and habitat utilisation, with distinct values associated with different water masses, more negative values typically indicating colder, less saline Arctic-influenced waters, whereas less negative values characterise warmer, more saline Atlantic-influenced waters [144]. Nitrogen isotope ratios ($\delta^{15}N$) typically exhibit stepwise enrichment with trophic transfers (approximately 3-4‰ per trophic level in many systems), enabling estimates of a consumer's relative position within food webs when appropriate baselines and discrimination factors are applied [32,145]. The temporal integration of isotopic values varies by tissue type, with blood plasma capturing recent dietary inputs (3-5 days) while red blood cells reflect intermediate-term foraging patterns (3-4 weeks), thereby allowing ecologists to distinguish between ephemeral and persistent feeding strategies [42,90].

The concept of isotopic niche has operationalised resource partitioning through statistical metrics such as standard ellipse areas [33,138], revealing multidimensional

patterns of resource use within ecosystems [39,40,146]. Strong correlations between tissue-specific isotopic values indicate temporal consistency in foraging behaviours, while weak correlations suggest shifts in resource utilisation, particularly valuable for evaluating how foraging strategies influence contaminant exposure patterns. Although isotopic niche frameworks have substantially advanced understanding of resource partitioning, the application of similar multidimensional analytical approaches to PFAS provides a methodological opportunity to elucidate previously unrecognised patterns in contaminant exposure. Examining whether PFAS accumulation follows comparable ecological structuring principles may reveal how chemical properties interact with foraging strategies to create predictable exposure outcomes, thereby enhancing our capacity to identify vulnerable populations and anticipate contamination dynamics in changing ecosystems.

We propose an analytical framework that examines PFAS exposure through three integrated ecological dimensions that shape seabird foraging during breeding seasons. The spatial dimension considers how colony location relative to distinct marine habitats influences exposure to different water masses and associated contaminant sources. The temporal dimension addresses how breeding constraints create time-dependent foraging patterns that affect exposure duration and frequency. The dietary dimension focuses on how prey specialisation, versus generalisation, influences the compositional profiles of accumulated contaminants. This integrated approach allows for examination of how these dimensions synergistically structure contamination patterns beyond what can be explained by trophic position alone.

The unique position of Icelandic guillemot populations at the intersection of Arctic and Atlantic water masses exposes them to contrasting prey communities and contaminant regimes, providing an ideal context for investigating contamination niches. Iceland's geographical situation creates pronounced oceanographic gradients with distinct trophic structures and chemical profiles [147]. Two sympatric guillemot species (*Uria lomvia* and *Uria aalge*, hereafter UL and UA) occupy comparable trophic positions while exhibiting differential foraging strategies: UA predominantly exploits Atlantic-influenced environments, whereas UL primarily utilises Arctic-influenced waters [88,148]. The distribution of both species across multiple colonies spanning

these distinct marine habitats establishes a robust comparative framework for examining the ecological structuring of contamination patterns [121].

This investigation addresses an important knowledge gap by integrating multivariate PFAS profiling with niche-based stable isotope analysis to test whether specific foraging strategies create distinct patterns of chemical exposure across seabird populations. Our approach examines whether: (1) distinct PFAS exposure clusters result from concentration data; (2) these clusters align with isotopic niches, species identity, and colony location in ways that suggest discrete contamination niches; and (3) structured relationships exist between PFAS concentration patterns and compound composition that reveal underlying ecological mechanisms, thus building on previous findings that PFAS variability reflects ecological thresholds. By examining these relationships across spatial, temporal, and dietary dimensions, this investigation addresses whether PFAS accumulation patterns in seabirds are structured according to ecological principles analogous to those governing resource partitioning. The outcomes of this research contribute to a more comprehensive understanding of contaminant dynamics in marine ecosystems, particularly in regions experiencing rapid environmental change.

4.2 Methods and Materials

4.2.1 Data Sources and Study Design

This study utilises datasets from Bonnet-Lebrun *et al.* [87] and Chapter 3, which include blood cell and plasma samples from common guillemots (UA) and Brünnich's guillemots (UL) collected across Icelandic colonies during the 2018 breeding season. The sampling locations encompassed diverse oceanographic influences along both north-south and east-west gradients. Three northernmost colonies (NW, N, NE) harboured both UA and UL populations, while two southernmost colonies (SE, SW) harboured UA only. We separated blood samples into cells and plasma to evaluate guillemot foraging across different temporal scales. We measured PFAS concentrations in plasma, given the strong binding affinity of these compounds to albumin, a primary plasma protein. This study was conducted concurrently with an analysis examining foraging strategies in these same populations, using identical study sites and field

methods. Sampling protocols, PFAS extraction/quantification (*via* LC-MS/MS), and stable isotope ($\delta^{13}C$, $\delta^{15}N$) analysis followed methodologies detailed in Chapter 3.

PFAS analysis was conducted at Helmholtz-Zentrum Hereon (Germany) using HPLC-MS/MS with electrospray ionization (MRM mode). Plasma samples, fortified with ^{13}C-labeled internal standards, targeted 14 compounds: nine PFCAs (C5-C13), four PFSAs (C4, C6, C8, and C10), and HFPO-DA (Table A1, Appendix A). Separation employed a C18 column with a water-methanol/ammonium acetate gradient, achieving a detection limit of 0.1 ng/g dry weight. Modified extraction protocols and QA/QC details are provided in Appendix A. Elemental content and bulk isotope values of blood tissues were determined at the Stable Isotope Facility of the Experimental Ecology Group, GEOMAR, Kiel with a customised, high sensitivity elemental analyser connected to a stable isotope ratio mass spectrometer (DeltaPlus Advantage, Thermo Fisher Scientific, Germany) as described by Hansen and Sommer. The standard deviations for $\delta^{13}C$ and $\delta^{15}N$ ranged from ± 0.15‰ to ± 0.25‰ ($n = 3$). The isotope data are expressed in delta (δ) notation:

$$\delta = \left(\frac{R_{sample}}{R_{standard}} - 1\right) \times 1000$$

Where R_{sample} is the ratio of the heavy to light isotope in the sample, and $R_{standard}$ is the ratio of the heavy to light isotope in the standard. To express the isotopic data as per mil (‰), they are multiplied by 1000. The isotope ratios are expressed relative to Vienna Pee Dee Belemnite (VPDB) for carbon and atmospheric air for nitrogen.

4.2.2 Statistical Analysis

All statistical analyses were performed using Python version 3.9 with associated libraries including Pandas 1.5.3, NumPy 1.24.3, SciPy 1.10.1, Scikit-learn 1.2.2, Statsmodels 0.13.5, Matplotlib 3.7.1, and Seaborn 0.12.2. Prior to analysis, PFAS concentrations were log-transformed to approximate normal distributions.

We used three distinct *k*-means clustering approaches to identify patterns in PFAS exposure and ecological niches. By analysing these dimensions separately and then testing their associations, we assess whether contamination patterns align with ecological niche structure. These approaches target complementary dimensions: (1)

PFAS exposure clusters identify groups based on overall contamination magnitude and concentration patterns; (2) structural compositional score (SCS) clusters characterise relative proportions of PFAS compound classes (long-chain PFCAs vs. PFOS) independent of total exposure levels; and (3) isotopic foraging clusters delineate groups based on spatial, temporal, and dietary foraging patterns captured by stable isotope ratios. For each clustering approach, principal component analysis (PCA) was first applied to log-transformed data (PFAS concentrations, structural compositional scores, or stable isotope values) to reduce dimensionality, followed by *k*-means clustering of the resulting principal components. Based on the oceanographic context of Icelandic waters, where Arctic and Atlantic influences create spatial and ecological gradients [84,89], and the documented foraging differences between guillemot species [87,88,127], we tested k = 2, 3, and 4 cluster solutions to identify ecologically meaningful groupings. The three-cluster solution (k = 3) was selected as optimal by maximising both silhouette scores and Calinski-Harabasz indices. Cluster robustness was validated through geometric properties (centroid dispersion, point density) and distributional overlap assessment (Bhattacharyya coefficients).

To characterise multidimensional patterns in both PFAS composition and foraging behaviour, we employed principal component analysis (PCA) to derive variance-weighted scores. For each sample i and principal component j, scores were calculated as:

$$S_{ij} = \left(\sum_{k=1}^{p} Z_{ik} \times L_{kj}\right) \times \sqrt{\lambda_j}$$

Where Z_{ik} is the standardised value (z-score) of variable k for sample i, L_{kj} is the loading of variable k on principal component j, and λ_j is the eigenvalue (explained variance) of component j. This weighting approach emphasises dimensions with greater explanatory power while maintaining interpretability across different data types.

For structural compositional score (SCS), PFAS concentrations were standardised using robust scaling prior to PCA. Two principal component scores were derived: SCS_{PFCA} representing variation in long-chain PFCA (PC1: PFNA, PFDA, PFUnDA, PFDoDA, PFTrDA) and SCS_{PFOS} representing variation in PFOS (PC2). These scores characterise

the relative proportions of PFAS compound classes rather than absolute concentrations, enabling identification of compositional patterns independent of exposure magnitude.

We visualised intra-cluster distributions using kernel density estimation (KDE) contours for continuous variables (PFAS concentrations, isotope values) and employed bar plots to represent categorical ecological factors. To assess ecological associations, we performed Pearson's χ^2 tests with effect sizes quantified using Cramér's *V*. Given the exploratory nature of our analyses, we considered *p*-values significant at $\alpha = 0.05$ without adjustment for multiple comparisons.

For isotopic characterisation, we calculated tissue-specific differences (Δ values) between plasma and cellular fractions for both $\delta^{13}C$ and $\delta^{15}N$. Sample-size-corrected Standard Ellipse Areas (SEA_c) were computed following Jackson *et al.* [138] from the covariance matrix of isotopic values, representing the core 40% of bivariate variation (see Appendix B, Equation B1 for details). SEA_c provides a robust measure of isotopic niche width that accounts for small sample sizes and enables comparison across groups with different sample sizes.

Conditional probabilities quantifying associations between isotopic foraging patterns (SI clusters) and PFAS structural profiles (SCS clusters) were calculated using the standard definition of conditional probability:

$$P(SCS = j \mid SI = i) = n(SCS = j \cap SI = i) / n(SI = i)$$

where $P(SCS = j \mid SI = i)$ represents the probability of a bird exhibiting PFAS structural profile j given its isotopic foraging pattern i, $n(SCS = j \cap SI = i)$ is the count of individuals belonging to both clusters, and $n(SI = i)$ is the total count of individuals in isotopic cluster i. These relationships were visualized using alluvial diagrams, with 95% confidence intervals estimated through 1000-iteration bootstrap resampling. Chi-square analysis was performed to test for significant associations between cluster memberships, with standardised residuals calculated to identify specific significant relationships.

4.3 Results

We tested whether PFAS exposure in Icelandic seabird populations conforms to the contamination niche framework through three complementary analyses. First, we identified discrete PFAS exposure clusters and characterised their isotopic variances to assess whether concentration patterns correspond to distinct foraging strategies (Section 4.3.1). Second, we examined how these exposure magnitudes relate to compositional patterns through structural analysis, testing whether exposure clusters exhibit characteristic PFAS profiles (Section 4.3.2). Finally, we quantified the associations between multidimensional foraging strategies and contamination patterns to determine whether specific ecological behaviours shape exposure outcomes (Section 4.3.3). Together, these approaches evaluate whether PFAS exposure is ecologically structured according to principles analogous to resource partitioning, or whether exposure patterns reflect stochastic variation.

4.3.1 Identifying Discrete PFAS Exposure Patterns

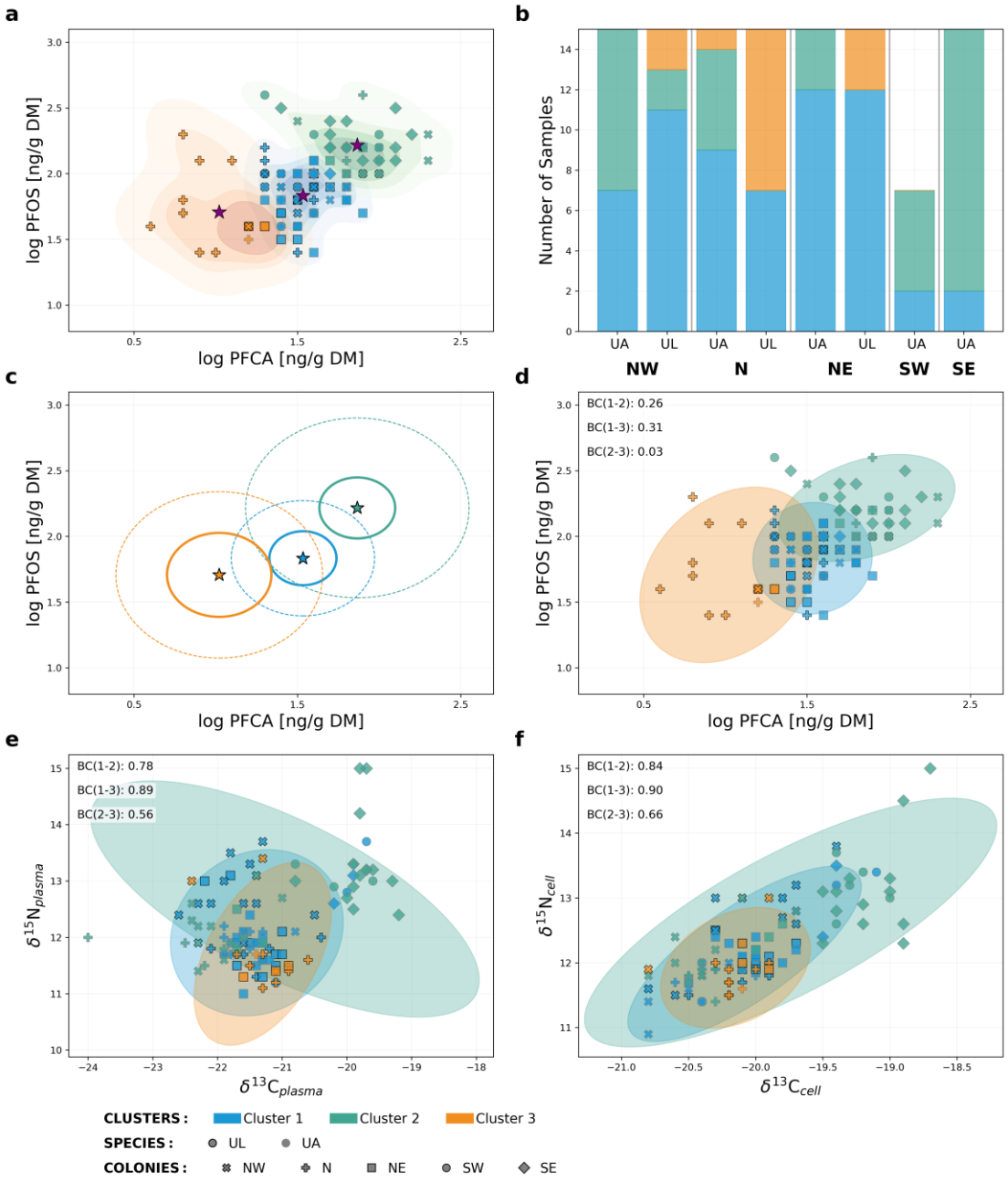

Figure 4-1. PFAS exposure clusters and their ecological characteristics. Panels a-b: Three exposure clusters identified from log-transformed PFCA and PFOS concentrations (Panel a) show distinct taxonomic and geographic distributions (Panel b). Panels c-d: Cluster validation through geometric properties (Panel c) and Bhattacharyya coefficient overlap analysis in concentration space (Panel d, $BC < 0.31$). Panels e-f: Isotopic characterisation of PFAS-defined clusters in plasma (e) and red blood cells (f). Standard ellipses represent isotopic variance within exposure groups (SEA values in Table 4-1). Symbols: colony locations (NW, N, NE, SW, SE); species (black edge: UL, gray: UA); cluster assignment (colours and contours). Purple stars: cluster centroids. Note that only in the northernmost colonies (NW, N, NE) do both species coexist, while southern colonies (SW, SE) contain only UA individuals.

Principal component analysis followed *k*-means clustering of log-transformed PFCA and PFOS concentrations identified three exposure clusters (Fig. 4-1a). Cluster validation indicated moderate internal cohesion (Silhouette Score: 0.39), yet Bhattacharyya coefficient analysis revealed low distributional overlap between clusters in PFAS concentration space ($BC < 0.31$ for all pairwise comparisons, Fig. 4-1d), with the most pronounced separation between Clusters 2 and 3 ($BC = 0.15$). Additional cluster validation statistics are provided in Supplementary Information (Appendix B, Table B1).

The three clusters exhibited differentiated concentration profiles spanning 0.5-0.9 log units. Each cluster exhibited distinct PFAS concentration profiles. High-exposure individuals (Cluster 2, $n = 36$) showed mean log PFCA of 1.87 ± 0.22 ng/g DM and mean log PFOS of 2.22 ± 0.16 ng/g DM. Intermediate-exposure individuals (Cluster 1, $n = 62$) exhibited mean log PFCA of 1.53 ± 0.15 ng/g DM and mean log PFOS of 1.83 ± 0.17 ng/g DM. Low-exposure individuals (Cluster 3, $n = 14$) displayed mean log PFCA of 1.02 ± 0.21 ng/g DM and mean log PFOS of 1.71 ± 0.26 ng/g DM.

To examine the ecological context underlying these exposure patterns, we analysed the isotopic characteristics of individuals within each cluster. We note that the absence of site-specific baseline isotopic values limits our interpretation to broad foraging patterns rather than precise niche quantification. Nevertheless, systematic differences were evident among clusters in isotopic variance (Fig. 4-1e-f, Table 4-1). Individuals in the high-exposure cluster (Cluster 2, $n = 36$) displayed high isotopic values across both tissue types (Table 4-1), indicating exploitation of warmer, more saline Atlantic-influenced waters and higher trophic-level resources. These birds, predominantly from SE and NW colonies (Fig. 4-1b), exhibited the broadest isotopic variance (Table 4-1, SEA_c), consistent with diverse foraging patterns within this exposure group. Strong tissue correlations for both $\delta^{13}C$ ($r = 0.87$, $p < 0.001$) and $\delta^{15}N$ ($r = 0.85$, $p < 0.001$) indicated temporal consistency in foraging throughout the breeding season. In contrast, individuals in the low-exposure cluster (Cluster 3, $n = 14$) showed the lowest isotopic values (Table 4-1), reflecting exploitation of colder, Arctic-influenced waters and lower trophic-level prey. These birds, concentrated in the northernmost colonies (NW, N, NE; Fig. 4-1b), displayed the narrowest isotopic niche variance (Table 4-1, SEA_c), suggesting more uniform foraging approaches within

Arctic marine ecosystems. Weaker tissue correlations, particularly for $\delta^{13}C$ ($r = 0.64$, $p < 0.05$), indicated some temporal shifts in foraging habitat during the breeding season. Individuals in the intermediate-exposure cluster (Cluster 1, $n = 62$) showed more even distribution across colonies (Fig. 4-1b) and occupied an intermediate position in both isotopic values and variance (Table 4-1, SEA_c), with moderate tissue correlations ($\delta^{13}C$: $r = 0.50$, $p < 0.001$; $\delta^{15}N$: $r = 0.72$, $p < 0.001$) suggesting temporal foraging consistency. This cluster showed more balanced species composition and even distribution across colonies (Fig. 4-1b). Chi-square analyses confirmed that these taxonomic and spatial patterns were statistically robust. Strong associations existed between cluster membership and both species identity ($\chi^2 = 34.11$ combined, $p < 0.001$) and colony location ($\chi^2 = 35.13$ combined, $p < 0.001$), with no significant interaction ($\chi^2 = 10.68$, $p = 0.28$; Table 4-1). Effect sizes ranged from medium to large (Cramér's $V = 0.41$-1.08 for significant associations), indicating that species and geographic factors substantially influence exposure cluster assignment.

Despite these systematic differences in mean isotopic values and variance patterns, Bhattacharyya coefficient analysis revealed substantial isotopic overlap between PFAS-defined exposure clusters (Fig. 4-1e-f). In contrast to the low overlap observed in PFAS concentration space ($BC < 0.31$), isotopic values showed high overlap across both tissue types ($BC > 0.50$ for all pairwise comparisons in plasma and cells). This discrepancy indicates that PFAS exposure clusters defined by concentration profiles are not strongly differentiated by mean $\delta^{13}C$ and $\delta^{15}N$ values alone. The limited isotopic separation suggests that exposure patterns may be structured by foraging dimensions beyond simple trophic position and habitat use, such as fine-scale prey selection not fully captured by bulk isotopic measurements.

Table 4-1. Isotopic and ecological characteristics of PFAS exposure clusters identified through concentration-based clustering.

Parameter	Cluster 1	Cluster 2	Cluster 3
Sample Size (*n*)	62	36	14
PFAS Concentrations [ng/g DM]			
Log PFCA Mean ± SD	1.53 ± 0.15	1.87 ± 0.22	1.02 ± 0.21
Log PFOS Mean ± SD	1.83 ± 0.17	2.22 ± 0.16	1.71 ± 0.26
Corrected Standard Ellipse Area (SEAc) [‰^{2}]			
Plasma	6.25	14.82	5.16
Cell	2.40	5.98	1.68
Mean Isotope Values [‰]			
$\delta^{13}C_{plasma}$	-21.39	-20.96	-21.3
$\delta^{13}C_{cell}$	-20.08	-19.74	-20.15
$\delta^{15}N_{plasma}$	12.08	12.68	11.71
$\delta^{15}N_{cell}$	12.14	12.62	11.92
Tissue Differences [‰]			
$\Delta\delta^{13}C$ Mean ± SD	-1.31 ± 0.48	-1.22 ± 0.75	-1.15 ± 0.34
$\Delta\delta^{15}N$ Mean ± SD	-0.06 ± 0.44	0.06 ± 0.46	-0.21 ± 0.55
Tissue Correlations			
$\delta^{13}C$ Correlation (*r*)	0.50***	0.87***	0.64*
$\delta^{15}N$ Correlation (*r*)	0.72***	0.85***	0.57*
Distribution Test			
Species-Colony interaction χ^2	5.08 ($p = 0.28$)	5.51 ($p = 0.24$)	0.60 ($p = 0.74$)
Effect size (Cramér's *V*)	-	-	-
Colony distribution χ^2	9.12 ($p = 0.06$)	24.06***	11.07**
Effect size (Cramér's *V*)	-	0.41	0.45
Species distribution χ^2	1.74 ($p = 0.19$)	17.95***	16.16***
Effect size (Cramér's *V*)	-	0.71	1.08

Notes:
DM = Dry mass
All isotopic values are reported in per mil (‰) relative to international standards.
Δ values represent the difference between plasma and cell isotope measurements.
Significance levels: * $p < 0.05$, ** $p < 0.01$, *** $p < 0.001$, - = not significant/not applicable

4.3.2 Structure Analysis: Linking PFAS Exposure to Chemical Composition

Next, we examined how exposure magnitude (absolute PFAS concentrations) relates to compositional patterns (relative proportions between PFAS classes). While absolute PFAS concentrations may fluctuate with cumulative exposure duration and intensity, compositional profiles, the relative proportions of PFAS classes, may remain characteristic of specific foraging strategies.

We derived structural compositional scores (SCS) through principal component analysis of log-transformed PFAS concentrations, creating composite metrics that emphasise systematic variation in compound proportions while retaining information about concentration magnitude. *k*-means clustering of these SCS distinguished three distinct PFAS structural profiles (Overall Silhouette Score: 0.36; Calinski-Harabasz Score: 86.27; Fig. 4-2a-b; Appendix B, Table B2).

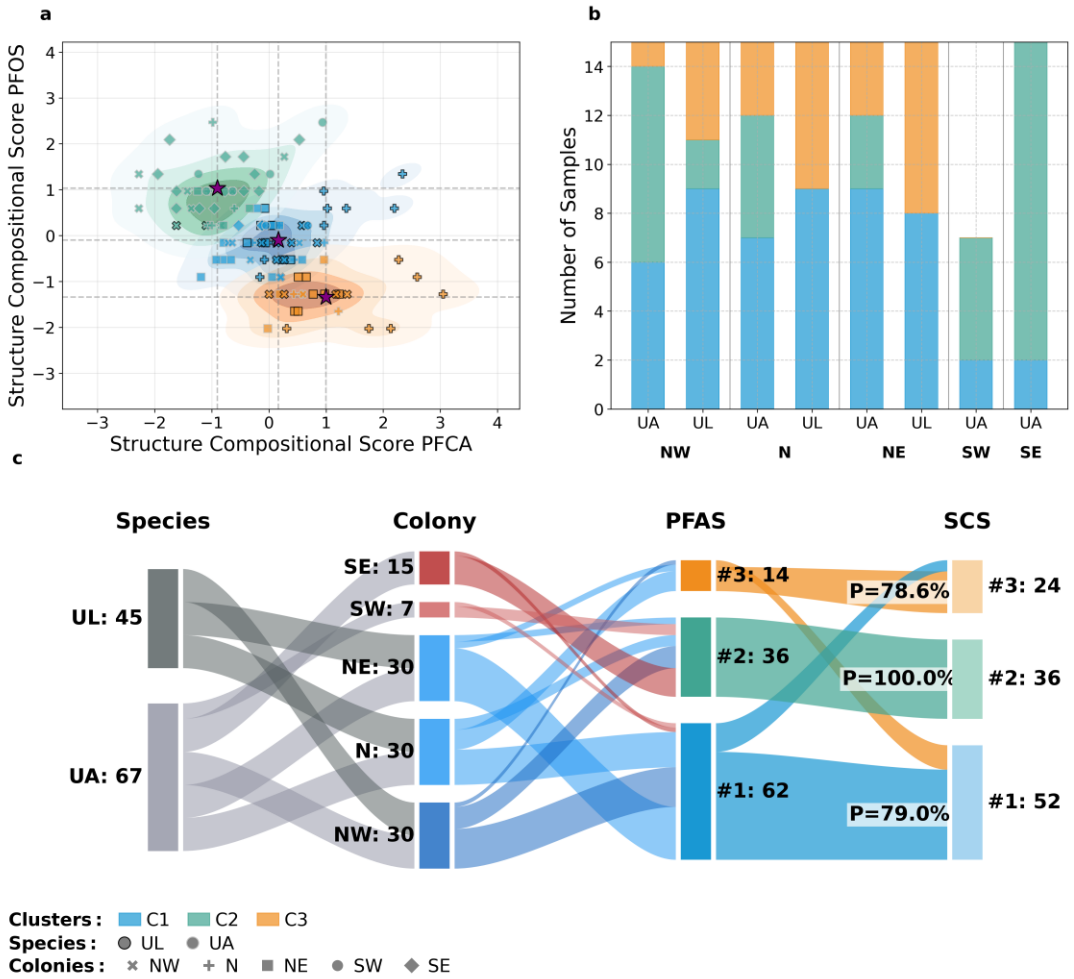

Figure 4-2. Structural compositional profiles of PFAS and their relationship to exposure clusters. Panel a: Three structural profiles identified through *k*-means clustering of structural compositional scores (SCS) in PFCA-PFOS space: population-average (SCS Cluster 1, blue), PFOS-dominated (SCS Cluster 2, orange), and PFCA-dominated (SCS Cluster 3, green). Density contours show cluster distributions, with purple stars marking centroids. Panel b: Cluster composition by colony location and species (UA: *Uria aalge*; UL: *Uria lomvia*). Panel c: Alluvial diagram showing conditional probability flows from PFAS exposure clusters (Section 4.3.1) to structural profiles. Stream width represents sample count. Symbols indicate colony locations and species as in Figure 4-1.SCS Cluster 1 ($n = 52$) exhibited near population-average proportions for both PFCA and PFOS classes (Fig. 4-2a), representing an intermediate structural profile. This cluster showed relatively even species representation and predominant distribution in northernmost colonies (Fig. 4-2b, Appendix B, Table B2). SCS Cluster 2 ($n = 36$) displayed PFOS-dominated profiles characterised by higher-than-average relative PFOS abundance and correspondingly lower PFCA proportions. This cluster contained primarily UA individuals and concentrated in SE and NW colonies (Fig. 4-2b; Appendix B, Table B2). SCS Cluster 3 ($n = 24$) showed PFCA-dominated profiles with higher-than-average relative PFCA abundance and lower PFOS proportions (Fig. 4-2a; Appendix B, Table B2), occupied predominantly by UL individuals from northernmost colonies.

We calculated conditional probabilities *P(SCS | PFAS)* to determine whether each PFAS exposure cluster exhibits characteristic structural profiles in terms of relative compound proportions (Fig. 4-2c). These analyses revealed systematic associations supporting the

contamination niche framework. The high-exposure cluster (PFAS Cluster 2) showed complete association with PFOS-dominated structural profiles, with 100% (95% CI: 90.4-100%) conditional probability of individuals belonging to SCS Cluster 2. This correspondence suggests that the ecological factors shaping elevated PFAS exposure preferentially enhance PFOS uptake or retention relative to PFCAs, rather than uniformly increasing all compound classes. Such selectivity likely reflects the combined effects of PFOS bioavailability in specific habitats and differential biomagnification properties in associated prey assemblages.

The intermediate-exposure cluster (PFAS Cluster 1) demonstrated conditional probabilities of 79.0% (95% CI: 67.4-87.3%) for population-average profiles (SCS Cluster 1) and 21.0% (95% CI: 12.7-32.6%) for PFCA-dominated patterns (SCS Cluster 3). This distribution suggests that intermediate exposure levels can arise through diverse compositional pathways, indicating mixed foraging strategies. The low-exposure cluster (PFAS Cluster 3) exhibited conditional probabilities of 78.6% (95% CI: 52.4-92.4%) for PFCA-dominated structural patterns (SCS Cluster 3) and 21.4% (95% CI: 7.6-47.6%) for population-average patterns (SCS Cluster 1). The complete absence of PFOS-dominated patterns in this cluster distinguishes low-exposure individuals from other groups, suggesting that specific foraging strategies avoid PFOS-rich contamination sources.

4.3.3 Ecological Drivers: Foraging Strategies as Predictors of Contamination Patterns

The systematic associations between exposure magnitude and structural profiles indicate underlying ecological organisation. We therefore examined whether multidimensional foraging strategies, integrating spatial, temporal, and dietary components through isotopic consistency metrics rather than mean isotopic values, predict these contamination patterns. This analysis integrates the exposure clusters (Section 4.3.1) and structural profiles (Section 4.3.2) with foraging ecology to define discrete contamination niches.

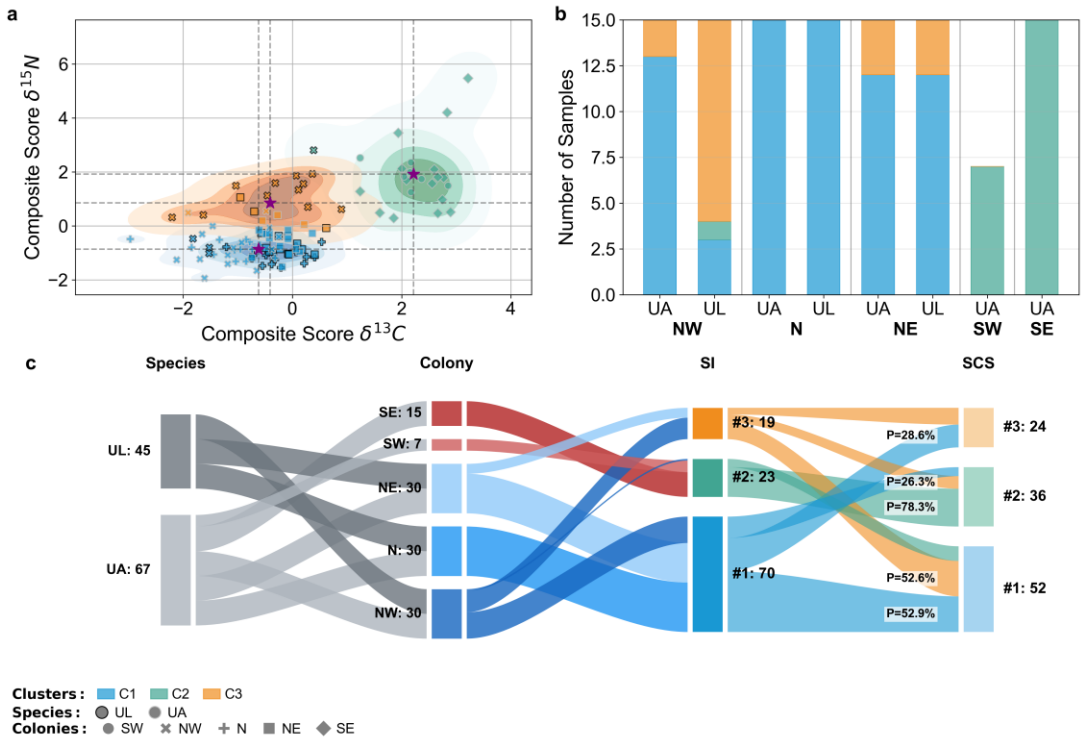

Figure 4-3. Foraging strategies predict contamination patterns, defining three discrete contamination niches. Panel a: Three isotopic foraging clusters based on temporal consistency in habitat use ($\delta^{13}C_{consist}$) and trophic position ($\delta^{15}N_{consist}$): Arctic-influenced (SI Cluster 1, blue), Atlantic-influenced (SI Cluster 2, orange), and mixed patterns (SI Cluster 3, green). Density contours show distributions with purple stars marking centroids. Panel b: Foraging cluster composition by colony and species (UA: *Uria aalge*; UL: *Uria lomvia*). Panel c: Conditional probability flows from foraging strategies to PFAS structural profiles. Stream width represents probability strength.

We quantified foraging consistency through composite scores ($\delta^{13}C_{consist}$ and $\delta^{15}N_{consist}$) that capture temporal stability in habitat use and trophic resources based on correlations between plasma and red blood cell isotope values (see Methods). *k*-means cluster analysis of these consistency metrics identified three distinct foraging patterns (Overall Silhouette Score: 0.46; Calinski-Harabasz Score: 151.89; Fig. 4-3a; Appendix B, Table B3).

Isotope Cluster 1 (n = 70) captured Arctic-influenced foraging, characterised by negative $\delta^{13}C_{consist}$ and negative $\delta^{15}N_{consist}$ scores, corresponding to consistent exploitation of colder, less saline Arctic-influenced waters with lower-trophic-level resources. Isotope Cluster 2 (n = 23) represented Atlantic-influenced foraging, with positive $\delta^{13}C_{consist}$ and positive $\delta^{15}N_{consist}$ scores, indicating consistent exploitation of warmer, more saline Atlantic-influenced waters with higher-trophic-level resources.

Isotope Cluster 3 (n = 19) showed mixed foraging patterns, combining negative $\delta^{13}C_{consist}$ scores (Arctic water influence) with positive $\delta^{15}N_{consist}$ values (relatively-higher-trophic-level resource use), suggesting temporal variability in foraging strategies.

Conditional probability analysis revealed distinct associations between isotopic foraging patterns and PFAS structural profiles (Fig. 4-3c, Table 4-2). Chi-square analysis confirmed substantial overall association (χ^2 = 29.83, p < 0.001, df = 4, Cramér's V = 0.37), with standardised residuals identifying specific significant relationships.

Atlantic-influenced foraging strategies (SI Cluster 2) showed strong association with high contamination exposure, exhibiting 78.3% (95% CI: 56.3-92.5%) probability of PFOS-dominated structural patterns (SCS Cluster 2; Table 4-2). The complete absence of PFCA-dominated patterns indicates that this foraging strategy consistently shapes specific contamination outcomes rather than variable exposure. These birds represent a High-Exposure Atlantic Forager contamination niche. Arctic-influenced foraging strategies (SI Cluster 1) shaped more diverse but systematically structured exposure outcomes. These birds showed highest probability (52.9%) of population-average PFAS profiles (SCS Cluster 1) and moderate probability (28.6%) of PFCA-dominated patterns (SCS Cluster 3), together characterising a Low-Exposure Arctic Forager contamination niche. These birds showed significant underrepresentation of PFOS-dominated patterns (18.6%, Table 4-2), suggesting either lower environmental PFOS concentrations in Arctic-influenced waters or prey communities with different PFAS retention characteristics. Mixed foraging patterns (SI Cluster 3) created intermediate exposure outcomes with moderate probabilities distributed across all structural profile types: 52.6% for population-average patterns, 26.3% for PFOS-dominated patterns, and 21.1% for PFCA-dominated patterns. This distribution reflects the Intermediate-Exposure Mixed Forager contamination niche, where temporal variability in foraging strategies produces variable contamination outcomes.

Table 2-2. Associations Between Isotopic Foraging Patterns and PFAS Structural Profiles.

Foraging Strategy Cluster	PFAS Structural Cluster	Conditional Probability [%]	95% CI [%]	Standardised Residual	Contamination Niche Association
Arctic-influenced foraging (SI 1)	near population-average (SCS 1)	52.9	41.5-64.9	0.79	Low-Exposure Arctic Foragers
	PFOS-dominated (SCS 2)	18.6	10.1-27.9	-2.00*	Under-represented
	PFCA-dominated (SCS 3)	28.6	18.4-38.7	1.29	Low-Exposure Arctic Foragers
Atlantic-influenced foraging (SI 2)	near population-average (SCS 1)	21.7	6.2-40.5	-1.74	Intermediate-Exposure Mixed
	PFOS-dominated (SCS 2)	78.3	59.5-93.8	3.90*	High-Exposure Atlantic Foragers
	PFCA-dominated (SCS 3)	0	-	-2.22*	Absent
Mixed foraging patterns (SI 3)	near population-average (SCS 1)	52.6	30.4-75.0	0.4	Intermediate-Exposure Mixed
	PFOS-dominated (SCS 2)	26.3	6.2-46.2	-0.45	Variable exposure
	PFCA-dominated (SCS 3)	21.1	5.3-41.2	-0.04	Low-Exposure Arctic influence

*Asterisks indicate standardized residuals with absolute values >2.0, representing significant contributions to the chi-square statistic.

4.4 Discussion

Our investigation examined how breeding season foraging behaviours across spatial, temporal, and dietary dimensions contribute to PFAS exposure patterns in guillemots. Building upon our previous work that identified variability patterns in PFAS profiles as indicators of ecological thresholds and foraging specialisation (Chapter 3), this study extends the analysis to concentration and compositional features. Together, these three dimensions—variability, concentration, and composition—form a comprehensive contamination niche framework that parallels ecological niche theory in how specific foraging strategies create distinct patterns of chemical exposure across seabird populations. Results support this conceptual framework and demonstrate that PFAS accumulation in seabirds follows distinct, non-random patterns reflecting these multidimensional foraging strategies alongside trophic position. The three differentiated PFAS exposure clusters—High-Exposure Atlantic Foragers, Intermediate-Exposure Mixed Foragers, and Low-Exposure Arctic Foragers—represent contamination niches associated with specific ecological strategies, extending traditional one-dimensional trophic magnification models.

4.4.1 Foraging Strategies and Contamination Niche Occupancy

The two guillemot species exhibited overlapping but distinguishable distributions across contamination niches, shaped by interactions between species-typical foraging tendencies and local oceanographic conditions. UL disproportionately represented the Low-Exposure Arctic-influenced niche while UA dominated the High-Exposure Atlantic-influenced niche. Both species showed substantial presence in the Intermediate-Exposure niche. The distinction lies not in exclusive niche occupancy but in isotopic variance: UL exhibited narrower variance within exposure clusters (Table 4-1, Cluster 3) compared to UA (Table 4-1, Cluster 2). This narrower variance in UL indicates that during breeding season individuals facing similar central-place foraging constraints converge on similar prey resources, consistent with foraging within relatively homogeneous Arctic-influenced waters [37]. In contrast, UA's broader variance suggests exploitation of prey across more heterogeneous water masses where both prey distributions and baseline isotopic values vary [84,144].

Substantial within-species geographic variation demonstrates that local oceanographic context modulates species-typical patterns. Among UL, western and northern colonies (NW, N) disproportionately occupied the Low-Exposure Arctic-influenced niche, while eastern populations (NE) showed greater overlap with UA in the Intermediate-Exposure niche, reflecting fine-scale differences in prey community structure. Among UA, southern colonies (SW, SE) exhibited 2.3× higher PFOS exposure than northern colonies (NE). These geographic patterns indicate that contamination outcomes result from exploitation of locally available prey assemblages, consistent with tracking studies demonstrating behavioural and spatial partitioning within sympatric colonies [87,127].

The distinct compositional profiles (Figure 4-2) observed across contamination niches correspond to different prey-contaminant pathways documented in the literature. UL predominantly consume invertebrates and forage at greater depths [88,148], accessing benthic prey assemblages where lower trophic level organisms and invertebrate-dominated pathways show reduced PFOS biomagnification efficiency, resulting in PFCA-enriched compositional profiles [56]. This corresponds to the lower total PFAS concentrations and relatively higher PFCA proportions characteristic of the Low-Exposure Arctic niche. In contrast, UA predominantly exploit pelagic fish such as capelin (*Mallotus villosus*) and sand lance (*Ammodytes* spp.) in shallower waters [88,111], accessing prey where PFOS biomagnifies more efficiently through fish-based food webs [149,150]. This corresponds to the PFOS-dominated profiles and elevated concentrations characteristic of the High-Exposure Atlantic-influenced niche. The magnitude of within-species variation and species overlap in intermediate niches emphasizes that foraging flexibility within locally available prey assemblages, not taxonomic identity alone, determines exposure outcomes [151,152].

4.4.2 Habitat Influences on PFAS Profiles

The distinct geographic patterns in contamination niches correspond to fundamental differences in food-web structure between oceanographic regimes, illustrating the spatial dimension of the contamination niche framework. This spatial differentiation is evident in both isotopic values (lower $\delta^{13}C$ in northern sites) and PFAS profiles (PFOS dominance in southern sites, higher proportion of PFCAs in northern sites).

Atlantic-influenced waters around Iceland support higher and more consistent primary and secondary production compared to Arctic-influenced northern waters [84,86], with different seasonal patterns and prey availability [85,89]. These characteristics are associated with different PFAS accumulation patterns, including higher PFOS concentrations in seabirds foraging in these waters [9,150]. While we cannot establish causation from correlative data, the systematic co-occurrence of Atlantic foraging patterns, PFOS dominance, and higher trophic positioning suggests mechanistic linkages. These food-web characteristics create conditions favourable for PFOS biomagnification: background water concentrations contribute to initial exposure levels, but the biomagnification potential through fish-dominated food webs substantially amplifies PFOS accumulation [153-155]. Guillemots exploiting these southern waters consequently exhibit elevated total PFAS concentrations with PFOS-dominated compositional profiles, regardless of species identity. In contrast, Arctic-influenced waters support different prey communities, including greater availability of invertebrate prey and ice-associated species [29,156], with more pronounced seasonal variation in productivity [37,54]. These regional food-web characteristics correspond to different PFAS accumulation patterns: guillemots foraging in these waters show lower total PFAS concentrations with proportionally elevated long-chain PFCAs. The intersection of horizontal oceanographic gradients with vertical foraging stratification creates multidimensional exposure boundaries, where even sympatric colonies show contamination differentiation based on depth-specific prey exploitation within regionally available food webs [127].

4.4.3 Temporal Dimensions of Contamination Niches

Analysis of temporal dimensions in contamination niches indicates that PFAS exposure patterns reflect not only where guillemots forage but also how consistently they do so over time, addressing the temporal dimension of the framework. The strength of correlations between plasma and red blood cell isotope values provided insight into temporal foraging consistency. The High-Exposure Atlantic Foragers (Fig. 4-2, Cluster 2) exhibited strong correlations between plasma and red blood cell isotope values, along with minimal isotopic shifts in nitrogen resources (Table 4-1), indicating highly consistent foraging strategies maintained over weeks. This temporal consistency in foraging behaviour corresponds to their elevated and stable PFAS exposure,

particularly their PFOS-dominated profiles. The continuous exploitation of similar prey resources in Atlantic-influenced waters creates predictable, persistent exposure pathways that facilitate higher bioaccumulation over time.

Both Intermediate-Exposure Mixed Foragers and Low-Exposure Arctic Foragers displayed relatively weaker tissue correlations, particularly for carbon isotopes (Table 4-1), indicating temporally variable foraging grounds. These Arctic Foragers also exhibited a negative nitrogen isotope shift (Table 4-1), suggesting a recent move toward lower-trophic-level prey. These temporal shifts may disrupt bioaccumulation by reducing exposure duration to contaminated resources, indicating that *when* organisms forage (temporal consistency versus seasonal variability) structures exposure outcomes alongside *where* (habitat use) and *what* (diet) they forage.

4.4.4 Interactions Among Spatial, Temporal, and Dietary Dimensions

The contamination niches identified emerge from multidimensional interactions among spatial, temporal, and dietary components rather than from single dominant factors. The necessity of this integrated framework becomes evident when considering simpler alternatives. Trophic position alone cannot explain observed patterns, as PFAS-defined exposure clusters showed high isotopic overlap, indicating that $\delta^{15}N$ values inadequately differentiate exposure outcomes. Similarly, spatial factors alone are insufficient: within Arctic-influenced northern colonies, UL and UA populations exhibited fundamentally different contamination profiles despite geographic proximity. Species identity provides an incomplete explanation, as both species occupied intermediate contamination patterns and substantial within-species variation exceeded between-species differences in several colonies. Integration of spatial, temporal, and dietary dimensions reveals systematic patterns in contamination that single-factor approaches cannot detect.

These multidimensional interactions align with Hutchinson's niche theory, which posits that ecological niches are inherently multidimensional with interactive properties among constituent dimensions [74,76]. In the context of contaminant exposure, dimensional interactions generate emergent patterns unpredictable from single-factor analyses. The High-Exposure Atlantic niche exemplifies synergistic interactions where spatial factors (Atlantic-influenced waters with PFOS-rich food webs) combine with

dietary parameters (higher-trophic-position prey) and temporal consistency (consistent exploitation) to facilitate efficient PFOS bioaccumulation. In contrast, the Low-Exposure Arctic niche demonstrates how Arctic-influenced waters supporting invertebrate-dominated food webs interact with temporal variability in foraging to attenuate bioaccumulation processes, explaining both reduced concentrations and distinctive compositional patterns. Such dimensional interactions correspond with theoretical models predicting amplification effects when exposure consistency interacts with trophic factors [25], and bioaccumulation disruption through dietary variability [126].

These findings integrate with our previous demonstration that PFAS variability patterns reflect ecological thresholds (Chapter 3), revealing that all three components of chemical exposure—variability, concentration, and composition—are ecologically structured. The High-Exposure Atlantic niche combines low within-group PFAS variability indicative of dietary specialisation, elevated absolute concentrations reflecting bioaccumulation intensity, and PFOS-dominated composition characteristic of fish-based food webs. The Low-Exposure Arctic niche exhibits higher PFAS variability suggesting dietary flexibility, lower absolute concentrations, and PFCA-enriched composition associated with invertebrate pathways. This three-dimensional characterisation provides more complete description of contamination outcomes than any single metric alone, demonstrating that contamination niches manifest as properties arising from specific configurations of where, when, and what seabirds forage. This framework extends recent theoretical developments in ecotoxicology emphasising multidimensional perspectives for evaluating contaminant dynamics in food webs [65].

4.4.5 Limitations and Future Directions

While our study identified discrete contamination niches shaped by multidimensional foraging strategies, several limitations warrant consideration. First, sampling during a single breeding season precludes assessing interannual variability in contamination patterns. Future studies should examine niche stability across years to determine whether the observed patterns persist over longer time scales. Second, focusing on adult breeders excludes other life stages (e.g. juveniles, non-breeders) that occupy distinct niches. Expanding analyses to these groups would clarify how contamination dynamics

vary demographically. Third, blood tissues reflect relatively recent exposure and foraging (weeks), whereas long-term accumulation patterns in slower-turnover tissues remain unexplored with the caveat that some tissues such as feathers are best suited for isotopic, but not PFAS, analyses. Multi-tissue sampling could resolve temporal scales of niche formation.

Bulk isotope analysis, while effective, limits the resolution of fine-scale exposure pathways. Compound-specific isotope analysis (CSIA) could expand the temporal, spatial, and dietary dimensions explored here by more precisely delineating foraging habitats and differentiating between baseline isotopic shifts and actual trophic position changes. To strengthen the connection between seabird contamination patterns and their ecological drivers, concurrent prey sampling would establish site-specific isotopic baselines and PFAS profiles. Longitudinal studies tracking seasonal and inter-annual variations are also critical to assess niche persistence. Finally, non-targeted PFAS screening could reveal previously unidentified compounds contributing to the observed patterns, particularly as industrial practices evolve in response to regulatory changes.

4.4.6 Conclusions

Findings contribute to a framework connecting ecological niche theory with contaminant exposure patterns in marine ecosystems. By demonstrating how multidimensional foraging strategies correspond to distinct contamination niches, this study expands established trophic magnification models with additional ecological dimensions. The progression from one-dimensional trophic magnification models to the multidimensional contamination niche framework represents an important theoretical advancement in contaminant research, aligning with recent calls for more integrative approaches to ecotoxicology [65,66].

This framework provides both explanatory power for observed patterns and predictive capacity for assessing vulnerability in unstudied populations. Species or populations exhibiting Atlantic-oriented foraging strategies face disproportionate PFOS exposure regardless of colony proximity to contamination sources, while Arctic-oriented foragers accumulate distinct PFCA-dominated profiles despite lower overall exposure. Such foraging-based predictions enable more efficient monitoring programmes that target ecological vulnerability rather than geographic proximity to sources. By recognising

contamination as an emergent property of ecological specialisation rather than merely a function of environmental concentrations, this framework provides the mechanistic understanding necessary for anticipating how climate-driven shifts in prey distributions may alter contamination dynamics in Arctic marine ecosystems. This represents a shift from reactive monitoring of contamination hotspots toward proactive identification of vulnerable populations based on their foraging ecology, enabling more targeted conservation efforts for species whose specialised ecological niches predispose them to disproportionate chemical exposure.

Acknowledgments

This paper is an output of Project LOMVIA (BMBF Grant No. 03V01459) and Project EISPAC (BMBF Grant No. 03F0809A), both of which are part of the Changing Arctic Ocean Programme. Additional funding was provided by UKRI/NERC (Grant Nos. NE/R012660/1 and NE/R012857/1). R.S. received a stipend from the Max Planck Institute of Geoanthropology. A permit was provided by the Icelandic Institute of Natural History and animal ethics was overseen by BAS AWERB.

Chapter 5: General Discussion

Bioaccumulation models have primarily focused on trophic magnification frameworks to explain the patterns of PFAS exposure in marine predators [38,149,157]. This reductionistic approach constrains the holistic integration of the multidimensional ecological processes that structure exposure patterns in marine ecosystems. This thesis addressed three overarching research questions: (1) Do the variability patterns of PFAS exposure exhibit ecological structuring with compound-specific responses to oceanographic gradients? (2) Do the patterns of PFAS exposure form discrete contamination niches corresponding to distinct foraging strategies? (3) Can the integration of variability analysis and niche clustering reveal how marine predators experience chemical exposure through their foraging strategies? The discussion synthesises findings from both studies within a unified theoretical framework, examines the broader implications for understanding contaminant dynamics in marine ecosystems, and proposes future research directions for the integration of contamination science and ecology.

To investigate these questions, I revisited the analytical approaches bridging exposure data with ecological indicators. Early explorations using conventional trophic magnification metrics revealed that the substantial variation in PFAS patterns could not be attributed to measurement error or sampling limitations. This prompted me to develop integrated analytical frameworks combining contaminant profiles with stable isotope values, niche theory, and foraging behaviour—a multidisciplinary approach that required a rethinking of how ecological and chemical data interact. This cross-disciplinary perspective demonstrated the importance of recognising that exposure patterns traditionally considered stochastic noise reflect meaningful ecological processes.

Both chapters provide complementary evidence for the central hypothesis that PFAS exposure in marine predators reflects ecological processes rather than simple environmental availability or trophic position, though important limitations constrain these interpretations. Chapter 3 established that PFAS variability functions as an ecological signal, with PFOS variability exhibiting significant threshold effects across

the Arctic-Atlantic gradient ($p < 0.01$) while PFCA patterns demonstrated non-significant responses to dietary indicators. Chapter 4 revealed that exposure patterns form three discrete contamination niches: High-Exposure Atlantic Foragers, Intermediate-Exposure Mixed Foragers, and Low-Exposure Arctic Foragers, with moderate associations between isotopic foraging patterns and PFAS compositional profiles ($\chi^2 = 29.83$, $p < 0.001$), though isotopic indicators explained only 13% of overall variability. Together, these findings indicate that marine predators' chemical exposure patterns are shaped by integrated foraging strategies spanning spatial, temporal, and dietary dimensions, thereby supporting the development of a contamination-niche framework that advances beyond traditional trophic magnification approaches.

5.1 Ecological Structure of PFAS Exposure

Previous research has identified geographical gradients in PFAS distribution in marine surface waters [18-20], primarily attributing these to transport mechanisms and proximity to industrial sources. These environmental distributions represent regimes of baseline exposure that vary spatially across oceanographic provinces and exhibit relatively slow temporal changes [70]. However, the relationship between these environmental baselines and the contaminant patterns in marine predators is typically non-linear and often varies considerably across species and regions [5,157,158]. Although differences in environmental concentrations contribute to overall exposure levels, our research suggests that ecological processes generate distinct contamination patterns that extend beyond what would be predicted from environmental availability alone. Our findings indicate that ecological factors, including habitat specialisation, prey selection, and temporal foraging consistency, interact with physiological mechanisms to create discrete exposure clusters and compound-specific patterns that reflect foraging strategies rather than simple environmental gradients.

Spatial foraging patterns correspond to discrete contamination regimes that diverge from the predictions of environmental distribution models. Previous studies have documented gradual PFAS concentration gradients across oceanographic regions [18,108], leading to expectations of similarly gradual patterns in marine predators. However, PFOS exposure patterns exhibited discrete threshold effects across Arctic and

Atlantic water mass regimes rather than continuous gradual variation, with a statistically significant transition between oceanographic environments ($p < 0.01$). Atlantic foragers demonstrated PFOS-dominated profiles with a high probability (78.3%), while Arctic-influenced habitats supported diverse compositional profiles, including PFCA-dominated patterns absent from Atlantic waters. These discrete exposure clusters indicate that distinct water mass environments function as ecological filters that structure contaminant exposure in ways not predicted by environmental distribution models alone [159,160]. These findings indicate compound-specific responses across different water mass environments, revealing that oceanographic regimes structure contaminant exposure through distinct ecological processes.

Temporal consistency in foraging behaviour represents an important yet understudied dimension structuring contamination patterns. While temporal aspects of contamination have received limited attention compared to spatial and trophic factors [104], our dual-tissue approach indicates that foraging consistency correlates with more coherent PFAS exposure patterns. Seabirds with temporally consistent foraging strategies during the breeding season exhibited more uniform PFAS profiles, particularly High-Exposure Atlantic Foragers who displayed strong correlations between plasma and red blood cell isotope values ($r > 0.85$) with elevated PFOS-dominated profiles. Although our breeding season sampling provides only a limited temporal window, this contrasts with previous contaminant studies that typically rely on single-tissue measurements [39], potentially missing how short-term foraging consistency may be reflected in accumulation patterns within constrained periods. These findings suggest that contamination patterns reflect not only spatial foraging areas, but also the consistency of resource use during breeding, indicating that specialised foraging strategies create characteristic exposure patterns that merit investigation across broader temporal scales.

Our findings indicate that dietary specialisation influences compound-specific accumulation through mechanisms that extend conventional trophic transfer frameworks. Previous biomagnification studies have emphasised linear relationships between trophic position and contaminant concentration [9,28], but our findings suggest compound-specific responses to foraging ecology. Different PFAS demonstrated distinctive associations with ecological indicators, with PFOS patterns showing stronger correlations with spatial habitat use while PFCA patterns exhibited

non-significant relationships with dietary indicators. The significant association between foraging ecology clusters and PFAS structural profiles ($\chi^2 = 29.83$, $p < 0.001$) indicates that feeding ecology shapes contamination in compound-specific bioaccumulation pathways. Our findings are consistent with potential threshold effects where processes of direct trophic transfer dominate PFCA accumulation at lower trophic positions, while trophic magnification becomes more pronounced for PFOS at higher trophic levels. This extends the framework of Borgå *et al.* [25] that the contaminant flow follows energy pathways through marine food webs, suggesting that protein-binding compounds like PFAS create distinct exposure patterns through mechanisms that vary with ecological context and operate beyond conventional trophic position metrics. These patterns indicate that traditional biomagnification factors have limitations in capturing the multidimensional ecological processes embedded in compound-specific accumulation.

These compound-specific responses become particularly evident when comparing closely related species. Although interspecies differences in contamination patterns are often attributed to physiological factors such as metabolic capacities and protein binding affinities [8], our findings indicate that ecological context influences PFAS exposure patterns as strongly as taxonomic identity. Specifically, the two guillemot species showed complex patterns of convergence and divergence across contamination niches. Both species exhibited balanced representation in Intermediate-Exposure niches (Chapter 4, Fig. 4-1), demonstrating convergence when occupying similar ecological space. However, strong species segregation occurred in extreme niches: UA dominated High-Exposure Atlantic niches while UL disproportionately occupied Low-Exposure Arctic niches. This pattern indicates that while taxonomic identity indicates central tendencies in niche occupancy, both species retain the capacity to occupy intermediate ecological spaces when local conditions permit. Geographic variation in contamination patterns within each species further illustrates the primacy of ecological context over taxonomic identity. Colony-specific foraging specialisations, such as differential exploitation of fjord systems, ice-edge habitats, and water depth zones, generated contamination signatures that reflected local ecological opportunities, consistent with documented resource partitioning effects [87,88]. This within-species ecological differentiation demonstrates that habitat specialisation can be as influential as

taxonomic identity in structuring chemical exposure, indicating that ecological factors substantially modify physiologically based predictions of contamination patterns.

The integration of spatial, temporal, and dietary dimensions reveals that marine predators' foraging strategies shape their exposure patterns. These structured exposure patterns subsequently give rise to discrete contamination niches that parallel ecological specialisation. These patterns indicate limitations in traditional bioaccumulation frameworks and support the development of more ecologically integrated approaches. Current bioaccumulation theory, largely based on trophic magnification factors and biomagnification models [38], has demonstrated limited explanatory power for the substantial variability often observed in field studies. Our findings suggest that marine predators occupy distinct contamination niches defined by their integrated foraging strategies across multiple ecological dimensions. Analogous to how ecological niche theory explains the partitioning of traditional resources by species [72,74], marine predators exhibit structured chemical exposure patterns through similar ecological processes. This perspective reframes contamination variability from statistical noise into potentially meaningful ecological information reflecting specialised foraging behaviours, providing empirical support for the conceptualisation of contamination as an additional dimension of ecological niche space.

This multidimensional approach suggests how different aspects of exposure patterns contribute complementary information about PFAS dynamics in marine predators, with contamination patterns emerging as ecological by-products. Concentration patterns reveal the magnitude of exposure across spatial and resource utilisation gradients, forming discrete clusters rather than continuous distributions. Compositional profiles reflect the qualitative nature of exposure, with characteristic PFAS patterns potentially associated with specific foraging strategies. Variability patterns capture the consistency or heterogeneity of exposure, suggesting possible threshold effects at ecological transitions. Together, these features provide evidence consistent with PFAS exposure in marine predators reflecting ecological processes operating across multiple dimensions of foraging ecology, potentially contributing toward more predictive models of contaminant dynamics in marine ecosystems, though broader validation is needed.

5.2 Mechanistic Foundations and Framework Development

The contamination-niche framework proposes a novel integration of ecological niche theory with contaminant dynamics in marine ecosystems. Rather than viewing chemical exposure through traditional toxicological approaches of concentration and biomagnification, this framework conceptualises contamination patterns as ecological phenomena shaped by the same multidimensional processes that govern resource partitioning and niche differentiation.

The contamination-niche framework extends Hutchinson's [74] concept of the ecological niche as an *n*-dimensional hypervolume to include chemical exposure patterns as an additional dimension of niche space. Just as organisms occupy characteristic positions in resource space through their ecological adaptations, marine predators exhibit distinct positions in an exposure space as a consequence of their integrated foraging strategies across multiple dimensions [75,76]. This theoretical expansion builds upon Schoener's [72] identification of habitat, diet, and temporal activity as primary niche axes by proposing that these same dimensions structure passive exposure patterns, while incorporating Pianka's [73] demonstration that the coexistence of species depends on the differential resource utilisation across a multidimensional niche space.

Traditional approaches to contaminant dynamics have typically treated trophic transfer or trophic magnification as a unified process operating at different scales rather than as potentially interacting mechanisms that might vary in relative importance across ecological gradients [24,38]. The contamination niche framework proposes that discrete contamination niches result from the interaction between trophic-dependent processes and varying food-web architectures.

The scope of the framework encompasses persistent compounds with sufficient retention times to allow for the detection and interpretation of biologically meaningful patterns in tissues, particularly protein-binding contaminants that accumulate predictably through biological matrices. While developed for PFAS, the theoretical principles extend to other persistent contaminants, though compound-specific properties require careful consideration. As demonstrated here, the framework is

suitable for obligate central-place foragers during breeding seasons when spatial and temporal foraging patterns are tightly constrained (e.g. by nesting grounds), as evidenced by threshold effects in PFOS variability and exposure clustering. A systematic validation across marine predator guilds with divergent foraging strategies (e.g. pelagic feeders, benthic specialists, and migratory generalists) is needed to assess the broader ecological relevance of the framework [161].

5.2.1 Mechanistic Basis

The theoretical framework proposes mechanistic pathways through which ecological processes create structured contamination patterns *via* compound-specific bioaccumulation processes. Our analysis indicates that different food-web architectures support distinct accumulation mechanisms, with trophic transfer and magnification varying in relative importance across ecological gradients and compound classes [25,162].

At lower trophic positions, direct trophic transfer dominates accumulation processes, as evidenced by our compositional analyses. Arctic-influenced systems characterised by specialised predator-prey relationships [156] favour direct trophic transfer processes, demonstrated by compositional profiles showing reduced PFOS dominance and PFCA-dominated patterns compared to Atlantic systems. This trophic transfer process operates gradually, producing constrained variability in both PFCA and PFOS that reflects systematic transfer from consistent prey sources. The gradual transfer process results in lower total concentrations, reflecting the lower bioaccumulation efficiency of trophic transfer compared to trophic magnification processes.

At higher trophic positions, trophic magnification processes become dominant, with Atlantic-influenced systems supporting diverse prey assemblages [36] that amplify the magnification processes. The prevalence of trophic magnification is demonstrated by PFOS-dominated compositional profiles, as PFOS demonstrates stronger protein-binding affinities and enhanced magnification potential compared to PFCA [13,163]. This magnification process creates elevated PFOS variability patterns, reflecting multiple exposure pathways and diverse prey sources. Concurrently, more constrained variability patterns observed in PFCA result from competitive binding mechanisms, where predominant PFOS burden suppresses PFCA accumulation. These

amplified magnification processes in Atlantic-influenced systems produce higher total concentrations compared to transfer-dominated systems.

This proposed trophic-dependent transition suggests synergistic compound-specific accumulation patterns where compositional profiles indicate the dominant process, variability patterns potentially reflect the characteristics of that process, and concentration magnitudes demonstrate the relative efficiency of accumulation, all potentially varying systematically across different food-web architectures. However, these relationships require extensive validation through experimental approaches to establish definitive causal mechanisms rather than simple correlational associations.

5.2.2 Contamination Niches: Moving Beyond Trophic Magnification

These analytical approaches form an integrated framework examining contamination niches from complementary perspectives to address our three research objectives. The niche analysis identified discrete PFAS exposure clusters and characterised their ecological associations, establishing the existence of distinct contamination patterns beyond random variation. The conditional probability analysis quantified associations between isotopic foraging patterns and PFAS profiles, demonstrating that ecological strategies influence contamination outcomes. The structure analysis revealed consistent relationships between concentration magnitude and compound composition, indicating that these patterns follow organised ecological principles rather than stochastic processes. Together, these approaches provide multiple lines of evidence supporting the contamination niche concept, from establishing pattern existence to quantifying ecological drivers and revealing structural relationships.

First, integration of three complementary analyses—PFAS concentration clustering, compositional profiling, and isotopic foraging patterns—revealed three contamination niches: High-Exposure Atlantic Foragers, Intermediate-Exposure Mixed Foragers, and Low-Exposure Arctic Foragers. These niches emerged not from concentration data alone but from conditional probability relationships linking foraging strategies (isotopic clusters) to characteristic PFAS compositional profiles. This multidimensional approach demonstrates that contaminant accumulation forms discrete patterns shaped by integrated ecological strategies across spatial, temporal, and dietary dimensions, extending beyond simple concentration-based or trophic gradient frameworks. The

bivariate distribution of PFAS concentrations (Fig. 4-1) shows clear separation between clusters with limited overlap in exposure profiles. The Intermediate-Exposure cluster is characterised by a relatively higher proportion of PFCA, despite PFOS being the most abundant compound overall, a pattern that becomes apparent when PFAS are analysed cumulatively. This pattern resembles the discrete resource partitioning often observed in ecological communities [72,73].

Second, isotopic foraging patterns demonstrated significant but moderate associations with PFAS compositional profiles (Chapter 4, Table 4-2). Seabirds exhibiting consistent Atlantic-influenced foraging strategies (SI Cluster 2) showed strong association with PFOS-dominated compositional profiles (78.3% conditional probability), while Arctic-influenced foragers (SI Cluster 1) displayed more diverse profiles, including population-average (52.9%) and PFCA-dominated patterns (28.6%), with notable under-representation of PFOS-dominated patterns (18.6%, standardised residual = -2.00). Importantly, substantial isotopic overlap existed between PFAS-defined exposure clusters (Bhattacharyya coefficient > 0.50), indicating that mean isotopic values alone do not strongly differentiate contamination niches. These findings suggest that contamination niche occupancy reflects fine-scale foraging dimensions, such as temporal consistency in central-place foraging [48], individual prey specialisation [52], and depth-specific habitat utilisation [47], not fully captured by bulk isotopic measurements [133,137].

Third, the linkage between PFAS concentration and composition (Chapter 4, Fig. 4-2) indicates a structure to contaminant accumulation that parallels niche differentiation in ecological systems. The association between high exposures and PFOS-dominated profiles indicates that specific contaminant patterns represent ecological responses rather than random variation. This structured relationship between contaminant magnitude and composition suggests that chemical profiles serve as indicators of ecological processes in a manner similar to how stable isotope ratios reflect resource utilisation [39,40]. This finding further supports the contamination niche framework by demonstrating that contaminant patterns follow organised ecological principles.

5.2.3 Multidimensional Framework

The contamination niche framework integrates four ecological dimensions that structure foraging behaviour: spatial habitat utilisation, temporal foraging consistency, dietary specialisation, and taxonomic differentiation. Each dimension corresponds to established ecological theories and generates specific patterns in PFAS contamination, potentially providing a systematic approach to understanding chemical exposure in marine predators.

The spatial dimension aligns with habitat partitioning theories [164,165], manifested in our findings as threshold effects in PFAS variability patterns. A significant transition at $\delta^{13}C_{consist} = 0.19$ ($p < 0.01$) indicates distinct contamination regimes between Arctic and Atlantic water masses. Atlantic foragers demonstrated: (1) higher overall PFAS concentrations; (2) PFOS-dominated compositional profiles (78.3% probability); and (3) elevated PFOS variability patterns. Arctic foragers exhibited contrasting patterns with more diverse compositional profiles, including PFCA-dominated patterns (78.6% in the low-exposure cluster), and more constrained variability. These patterns are consistent with differences in food-web structure between oceanographic regimes [36,156]. The observed threshold effects suggest possible ecological transitions similar to ecotones described by Fagan *et al.* [166], where multiple environmental gradients intersect to create discrete ecological boundaries.

The temporal dimension connects with foraging consistency theories [167], revealed through associations between isotopic stability across tissues and exposure patterns. High-Exposure Atlantic Foragers exhibited stronger correlations between plasma and red blood cell isotope values ($r > 0.85$) with elevated PFOS-dominated profiles, indicating that temporal consistency in foraging behaviour is associated with more coherent contamination patterns. This relationship aligns with optimal foraging theory [80], where consistent resource use strategies generate predictable exposure patterns over time. The breeding season sampling captured this consistency effect within the constraints of central-place foraging behaviour.

The dietary dimension corresponds to food web theories [162,168,169], though our analysis revealed weaker associations than spatial patterns. While $\delta^{15}N_{consist}$ showed substantial effect size (55% of model influence) for PFCA patterns, the dietary

threshold was not statistically significant, indicating gradual rather than discrete transitions in PFCA accumulation across prey selection gradients. This contrasts with the spatial threshold observed for PFOS, suggesting that dietary effects on PFCA contamination may operate more subtly than spatial habitat effects on PFOS patterns, or may require different methodological approaches to detect.

The taxonomic dimension relates to resource partitioning theories [72,170,171], demonstrated through species-specific patterns that varied with ecological context. The two guillemot species showed both convergent and divergent PFAS profiles depending on foraging opportunities, indicating that ecological context influences contamination patterns beyond species identity alone. Cluster analyses revealed that both species were represented across multiple contamination clusters when ecological contexts varied, while showing convergent patterns when foraging opportunities aligned. Where species differences were detectable, these manifested as variation within rather than between contamination clusters, indicating that ecological context can be as influential as taxonomic identity in determining contamination niche occupancy. This finding supports the framework's emphasis on ecological context in shaping exposure patterns beyond taxonomic identity alone.

5.2.4 Theoretical Advances

This framework builds on existing bioaccumulation theory by demonstrating that variability in contaminant patterns represents meaningful ecological information reflecting specialised foraging strategies. This perspective could transform how we interpret heterogeneity in exposure data, suggesting that variability structures themselves might reveal ecological processes operating across food webs. However, the moderate explanatory power of ecological indicators in our study questions whether variability patterns consistently reflect ecological rather than analytical or physiological processes. This addresses an important limitation identified by Borgå *et al.* [31], who recognised that variability in bioaccumulation might reflect ecological processes, but primarily treated it as a confounding factor. Our work provides initial evidence supporting this perspective.

Despite the above-mentioned limitations, our findings demonstrate that chemical exposure represents a novel, exposure-mediated niche dimension arising from the

integrated effects of an organism's spatial habitat use and trophic interactions. This extends conventional niche theory by showing that exposure regimes emerge as a consequence of foraging decisions, analogous to how habitat selection shapes resource acquisition. The observed threshold effects (e.g. $\delta^{13}C_{consist} = 0.19$) provide empirical support for discrete contamination regimes structured by ecological processes. Our work complements established biomagnification frameworks by demonstrating PFAS patterns that arise from interactions between oceanographic gradients, trophic architecture, and individual behaviour. While Franklin [38] highlighted the limitations of linear models, our results demonstrate that discrete exposure clusters form where multiple ecological thresholds intersect, extending rather than rejecting biomagnification models.

5.3 Methodological and Conceptual Limitations

The contamination niche framework advances understanding of exposure dynamics in marine ecosystems while operating within inherent constraints of field-based ecological research. Three interconnected domains require consideration for interpreting findings and guiding future applications: (1) temporal and spatial sampling boundaries, (2) methodological trade-offs in integrating chemical and ecological data streams, and (3) analytical challenges in distinguishing biological signals from noise. Each domain carries specific implications for advancing contaminant ecology research.

5.3.1 Study Design and Temporal Constraints

The cross-sectional design during a single breeding season (June-July 2018) captures exposure patterns within the temporal window when seabirds exhibit central-place foraging behaviour, providing clear ecological context while limiting understanding of seasonal and interannual dynamics. This sampling approach effectively controls for breeding constraints while missing temporal variation that influences contamination patterns across broader time scales. Longitudinal studies tracking individual seabirds across multiple years would determine whether contamination niches remain stable or exhibit plasticity in response to changing environmental conditions, prey availability, or life-history stages.

The focus on breeding adults addresses the most ecologically constrained life stage while leaving demographic gaps in understanding contamination niches across age classes. Juveniles, non-breeders, and individuals of different age classes occupy different contamination niches due to ontogenetic shifts in foraging behaviour, physiological development, or habitat utilisation. Age-related changes in protein-binding capacity, metabolic rates, and detoxification efficiency could create contamination patterns that have no relationship to ecological niche partitioning. Future research should expand to include these demographic groups to test whether contamination niches show developmental plasticity or remain consistent throughout an individual's lifespan.

The temporal mismatch between stable isotope turnover rates and PFAS persistence in seabird tissues creates interpretative complexity. While dual-tissue isotope analysis captures foraging behaviour integrated over short periods (plasma: ~1 week; red blood cells: ~3-4 weeks), PFAS exhibit elimination half-lives ranging from months to years depending on compound and species [93,172]. This temporal disparity means that correlations between current isotopic patterns and PFAS profiles reflect historical exposure regimes from wintering areas, migration routes, or previous breeding seasons. Future applications require longitudinal tracking data or multi-tissue contaminant profiling to disentangle legacy exposures from current ecological drivers.

5.3.2 Methodological Limitations of Ecological Proxies

Bulk stable isotope analysis provides valuable but relatively coarse indicators of foraging ecology, potentially obscuring fine-scale dietary specialisation or foraging behaviour differences that influence contamination patterns. Compound-specific isotope analysis (CSIA) of nitrogen would improve resolution by distinguishing baseline isotopic shifts across oceanographic regions from actual changes in trophic position or prey selection [133,137]. Similarly, CSIA of carbon could establish niche partitioning and primary production source provenance with higher fidelity than bulk $\delta^{13}C$ analysis [136,173], and potentially inform about dietary stress [174].

The absence of direct baseline isotopic measurements across our study area limits attribution of isotopic differences to ecological factors versus regional baseline variation. This consideration affects all isotope-based inferences, particularly given the

distinct oceanographic regimes surrounding Iceland. Bulk isotope analysis cannot resolve potential influences of physiological factors such as nutritional stress, reproductive condition, or metabolic rate on isotopic incorporation, which vary systematically across breeding colonies or between species. These physiological effects can create apparent ecological signals in isotopic data that do not reflect actual foraging behaviour differences, potentially generating correlations with contamination patterns.

5.3.3 Analytical and Conceptual Constraints

The targeted analysis of 14 legacy PFAS (C5-C13) provides critical baseline data while inherently excluding thousands of emerging PFAS variants in commercial use [3,175]. Future studies incorporating non-targeted screening and multi-compartment physiochemical modelling could reveal compound-specific bioaccumulation pathways that refine niche dynamics. The absence of short-chain PFAS (C5-C6) in our samples, compounds with distinct environmental distributions and protein affinities [8,58], suggests additional niche axes operating at lower trophic levels or through alternative exposure routes. As industrial practices evolve and regulatory pressures shift production toward alternative PFAS, monitoring frameworks must adapt to capture changing contamination landscapes [105].

The distinct characteristics of Icelandic waters, including oceanographic transitions, specific prey assemblages, and particular contamination sources, created detectable contamination-ecology relationships that may not extend to other marine systems. Future validation requires testing across diverse geographic regions with different oceanographic characteristics, contamination sources, and prey assemblages to assess framework generalisability [19,20].

Moderate cluster differentiation (silhouette scores 0.35-0.46) reflects both biological realities, where niche boundaries are inherently fluid in marine systems, and analytical constraints associated with sample sizes for marine predator studies. While sample limitations constrain resolution of fine-scale ecological relationships, the overall patterning demonstrates statistical robustness across multiple analytical approaches. The exploratory analytical approach prioritised hypothesis generation over confirmatory testing, with findings requiring verification through replicated study designs across broader taxonomic and geographic scales.

The conceptual framework linking food-web structure to contamination patterns requires refinement through targeted observational and analytical advances. While manipulative experiments remain impractical for marine apex predators, future studies could strengthen causal inference by:

- leveraging natural environmental gradients (e.g. Arctic-Atlantic transitions) as quasi-experimental systems;
- integrating high-resolution dietary tracking (eDNA, fatty acid biomarkers);
- applying causal discovery algorithms to longitudinal exposure-ecology datasets.

The framework's theoretical robustness ultimately depends on demonstrating predictive capacity across multidimensional contamination landscapes while addressing scale dependencies from individual to ecosystem levels.

5.4 Conservation Considerations

The contamination niche framework offers new approaches for improving biomonitoring programme efficiency by tailoring sampling strategies to capture ecologically meaningful contamination patterns rather than simply maximising geographic coverage. By identifying 'sentinel niches' that integrate across particular contamination pathways, monitoring efforts can strategically target representative populations that provide the most informative contamination signals for specific environmental compartments. Building on these preliminary findings, validation across broader scales and systems would establish operational protocols. For example, High-Exposure Atlantic Foragers could serve as effective sentinels for monitoring PFOS contamination in offshore Atlantic food webs, while specialised Arctic foragers would better reflect changes in PFCA distribution in ice-associated ecosystems.

The multidimensional framework developed here demonstrates that conservation risk assessments should consider not only contamination exposure magnitude but also compositional profiles and variability structures, as these features reflect ecological vulnerabilities not captured by concentration data alone. Populations exhibiting specialised contamination niches with minimal variability may be particularly susceptible to sudden changes in their primary exposure pathways, while those occupying broader contamination niches would demonstrate greater resilience to changing contamination landscapes. Integrating these ecological considerations into regulatory frameworks would enhance protection for vulnerable populations beyond traditional toxicological thresholds alone.

This approach provides practical tools for environmental management by enabling optimisation of biomonitoring programmes through identification of sentinel niches and enhancing risk assessment protocols through integrated analysis of concentration, composition, and variability data. The framework complements existing biomagnification models by revealing how multidimensional ecological processes create discrete exposure clusters, thereby enabling more targeted conservation and management decisions in contaminated marine ecosystems.

5.5 Future Research Directions

Advancing the contamination niche framework requires targeted research to establish mechanistic foundations and validate broader applications across marine ecosystems. While our findings demonstrate that contamination patterns reflect distinct ecological niches, several important research directions would strengthen the framework's theoretical basis and expand its utility for contamination monitoring and ecological research.

The mechanistic links between foraging behaviours and contaminant exposure require direct investigation to advance beyond correlational associations. Several priority questions emerge from our proposed mechanistic framework:

- At what specific trophic position does trophic magnification overtake direct trophic transfer as the dominant process, and does this transition point differ across

oceanographic regimes? This question can be addressed through higher-resolution sampling across continuous trophic gradients within distinct oceanographic waters.

- Does competitive binding between PFOS and PFCAs explain the homogenisation of PFCA variability at higher trophic levels, or do other physiological or ecological processes contribute? Laboratory studies examining competitive binding kinetics in marine predator tissues could resolve this mechanism, though field validation would strengthen interpretations.

- How will climate-driven changes in Arctic sea ice distribution and associated food webs alter the balance between trophic transfer and magnification processes? Long-term monitoring of different water masses can track shifts in contamination niches as these ecosystems transform.

- Will extended food chains in warming Arctic waters enhance trophic magnification processes, potentially increasing PFOS dominance in previously PFCA-influenced regions? This question highlights the need to establish baseline contamination niche patterns before rapid Arctic transformation accelerates.

Climate-driven reorganisation of marine food webs adds urgency to understanding these trophic-dependent processes for developing predictive applications. Future studies should integrate direct behavioural observations, biologging technologies, and compound-specific isotope analysis to establish precise relationships between foraging tactics and contamination patterns. Miniaturised tracking technologies can address how individual movement decisions link with contamination profiles, improving understanding of how behavioural choices translate into exposure risk.

Advancing the contamination niche framework requires expansion to multiple contaminant classes and validation across ecological scales. While PFAS-specific findings demonstrate utility, broader applications must address fundamental challenges where distinct bioaccumulation mechanisms across contaminants create exposure trade-offs. Methodological innovation, particularly tissue-specific temporal alignment and non-targeted contaminant screening can disentangle these dynamics when paired with longitudinal studies across species and ecosystems. Validation must progress through natural gradient experiments and environmental baseline characterisation,

advancing from correlative patterns to mechanistic understanding. The framework's theoretical robustness depends on demonstrating predictive capacity across multidimensional contamination patterns while addressing scale dependencies from individual to ecosystem levels.

These research advances would enable conservation managers to use PFAS profiles for identifying populations with specialised foraging strategies that may be more vulnerable to environmental changes, while providing a mechanistic foundation for interpreting contamination data within ecological context and improving the efficiency and ecological relevance of marine contamination monitoring programmes.

Appendix A : Supplementary materials for Chapter 3

A.1 Methods and Materials

A.1.1 Target Compounds & Standards

Table A1. PFAS analytes. Chemical information of target per- and polyfluoroalkyl substances (PFAS) analysed in this study. The compounds are categorized into three major classes: carboxylic acids (C5-C13), sulfonic acids (C4, C6, C8, & C10), and ether (HFPO-DA). All analytical standards were obtained from Wellington Laboratories with certified purity >98%. The PFC-MXA mixture was prepared at 2.0 µg/mL ± 5%, while the HFPO-DA individual standard was prepared at 50 ± 2.5 µg/mL.

Class	Acronym	Chemical Name	CAS No.	Standard Information
Carboxylic Acids	PFPeA	perfluoro-*n*-pentanoic acid	2706-90-3	PFC-MXA mixture, Wellington Laboratories, 2.0 µg/mL ± 5%, >98%
	PFHxA	perfluoro-*n*-hexanoic acid	307-24-4	
	PFHpA	perfluoro-*n*-heptanoic acid	375-85-9	
	PFOA	perfluoro-*n*-octanoic acid	335-67-1	
	PFNA	perfluoro-*n*-nonanoic acid	375-95-1	
	PFDA	perfluoro-*n*-decanoic acid	335-76-2	
	PFUnDA	perfluoro-*n*-undecanoic acid	2058-94-8	
	PFDoDA	perfluoro-*n*-dodecanoic acid	307-55-1	
	PFTrDA	perfluoro-*n*-tridecanoic acid	72629-94-8	
Sulfonic Acids	PFBS	potassium perfluoro-*n*-butanesulfonate	375-73-5	
	PFHxS	sodium perfluoro-*n*-hexanesulfonate	355-46-4	
	PFOS	sodium perfluoro-*n*-octanesulfonate	1763-23-1	
	PFDS	sodium perfluoro-*n*-decanesulfonate	335-77-3	
Ether	HFPO-DA	2,3,3,3-tetrafluoro-2-(1,1,2,2,3,3,3-heptafluoropropoxy)-propanoic acid	13252-13-6	Individual standard, Wellington (50 ± 2.5) µg/mL, >98%

Table A2. List of solvents and reagents used in the analytical procedure. All chemicals were of high analytical grade suitable for LC-MS/MS analysis or equivalent high-purity grade. Ultrapure water was produced in-house using a Milli-Q water purification system. The reagent grade, purity specifications, and suppliers are provided to ensure reproducibility of the analytical method.

Chemical	Grade/Purity	Supplier
Methanol	LC-MS grade (LiChrosolv)	Merck
Ultrapure water	18.2 MΩ·cm at 25 °C	Milli-Q Integral 5, Merck
Acetic acid	≥99.8%, LC-MS grade	Honeywell Fluka
Ammonium acetate	LC-MS grade	Honeywell Fluka
Ammonia solution	25%, Suprapur	Merck

A.1.2 Sample Preparation

PFAS extraction from plasma samples was performed using a modified quaternary ammonium salt-based ion-pairing method.[123,124] Prior to extraction, plasma samples were fortified with mass-labelled internal standards and buffered with sodium carbonate (1 mL, 0.5 M, pH 10.0). Tetrabutylammonium hydrogen sulphate (2 mL, 0.5 M) was added as the ion-pairing agent.

The analytes were extracted three times with ethyl acetate (5 mL per extraction) using ultrasonication (20 min, room temperature) followed by centrifugation (3000 rpm, 15 min, 20°C). The combined organic extracts were concentrated under a gentle nitrogen stream at 40°C and reconstituted in methanol: water (1:1 v/v, 250 µL). Final extracts were filtered through a 0.2 µm polypropylene membrane filter prior to analysis.

A.1.3 Instrumental Analysis

Table A3. Detailed instrumental parameters for the LC-MS/MS analysis of PFAS. The chromatographic separation was performed using an Agilent 1100 HPLC system coupled to an AB Sciex API 4000 triple quadrupole mass spectrometer. The method utilised a reverse-phase C18 column with gradient elution using ammonium acetate buffer and methanol-based mobile phases. Mass spectrometric detection was performed using electrospray ionization in negative mode with multiple reaction monitoring (MRM).

System	Parameter	Specification
HPLC	System	HP 1100, Agilent Technologies
	Analytical Column	Synergi Fusion-RP C18, 150 × 2 mm, 4 μm, 80 Å (Phenomenex)
	Guard Column	SecurityGuard C18, 4 × 2 mm (Phenomenex)
	Mobile Phase A	2 mM ammonium acetate in water
	Mobile Phase B	0.05% acetic acid in methanol
	Flow Rate	0.2 mL/min
	Injection Volume	10 μL
	Column Temperature	30 °C
	Run Rime	30 min
MS/MS	System	API 4000 triple quadrupole, AB Sciex
	Source	Turbo V ESI, negative mode
	Ion Spray Voltage	-4500 V
	Source Temperature	400 °C
	Gases (N_2)	Nebulizer: 4.2 bar
		Heater: 2.8 bar
		Curtain: 1.0 bar
		Collision: 0.6 bar
	Scan Type	MRM

Table A4. LC-MS/MS parameters for the analysis of per- and polyfluoroalkyl substances (PFAS) and their corresponding internal standards. The table presents molecular formulas of detected ions, quantifier and qualifier transitions (m/z), and matched internal standards for each target analyte. The compounds are categorized into native PFCAs (C5-C13), PFSAs (C4, C6, C8 & C10), HFPO-DA, and isotope-labelled internal standards. Quantifier ion transitions (marked with asterisk) were used for quantitation, while qualifier transitions were monitored for confirmation where available.

Type	Compound	Molecular Formula	Quantifier Transition (m/z)	Qualifier Transition (m/z)	Internal Standard
Native PFCAs	PFPeA	[C5F9O2]-	263 > 219*	-	$^{13}C_2$-PFHxA
	PFHxA	[C6F11O2]-	313 > 269*	313 > 119	$^{13}C_2$-PFHxA
	PFHpA	[C7F13O2]-	363 > 169*	363 > 319	$^{13}C_4$-PFOA
	PFOA	[C8F15O2]-	413 > 369*	413 > 169	$^{13}C_4$-PFOA
	PFNA	[C9F17O2]-	463 > 419*	463 > 219	$^{13}C_5$-PFNA
	PFDA	[C10F19O2]-	513 > 469*	513 > 219	$^{13}C_2$-PFDA
	PFUnDA	[C11F21O2]-	563 > 519*	563 > 169	$^{13}C_2$-PFUnDA
	PFDoDA	[C12F23O2]-	613 > 569*	613 > 169	$^{13}C_2$-PFDoDA
	PFTrDA	[C13F25O2]-	663 > 619*	663 > 169	$^{13}C_2$-PFDoDA
Native PFSAs	PFBS	[C4F9O3S]-	299 > 80*	299 > 99	$^{18}O_2$-PFHxS
	PFHxS	[C6F13O3S]-	399 > 80*	399 > 99	$^{18}O_2$-PFHxS
	PFOS	[C8F17O3S]-	499 > 80*	499 > 99	$^{13}C_4$-PFOS
	PFDS	[C10F21O3S]-	599 > 80*	599 > 99	$^{13}C_4$-PFOS
Native Ether	HFPO-DA	[C6F11O3]-	329 > 285	-	$^{13}C_3$-HFPO-DA
Internal Standards	$^{13}C_2$-PFHxA	[13C2C4F11O2]-	315 > 270*	315 > 120	-
	$^{13}C_4$-PFOA	[13C4C4F15O2]-	417 > 372*	417 > 169	-
	$^{13}C_8$-PFOA	[13C8F15O2]-	421 > 376*	421 > 172	-
	$^{13}C_5$-PFNA	[13C5C4F17O2]-	468 > 423*	468 > 223	-
	$^{18}O_2$-PFHxS	[C6F13O2OS]-	403 > 84*	403 > 103	-
	$^{13}C_4$-PFOS	[13C4C4F17O3S]-	503 > 80*	503 > 99	-
	$^{13}C_3$-HFPO-DA	[13C3C3F11O3]-	332 > 287*	332 > 169	-

*Quantifier ion transition

A.1.4 Quality Assurance and Quality Control (QA/QC)

Background PFAS levels were evaluated through procedural blanks analysed with each batch of 10 samples. The Limit of Blank (LoB) was calculated as [176]:

$$LoB = mean(blank) + 1.645(SDblank)$$

Sample concentrations above LoB were considered detectable and were blank-corrected by subtracting the mean blank values. Values below LoB were reported as not detected. Recovery rates for all target compounds and their mass-labelled internal standards are summarized in Table A5.

Table A5. Mean percent recoveries and standard deviations (SD) for isotope-labelled per- and polyfluoroalkyl substances (PFAS) internal standards.

Standard	Mean	SD
$^{13}C_2$-PFHxA	78%	10%
$^{13}C_4$-PFOA	88%	11%
$^{13}C_5$-PFNA	87%	11%
$^{13}C_2$-PFDA	86%	17%
$^{13}C_2$-PFUnDA	87%	22%
$^{13}C_2$-PFDoDA	102%	17%
$^{18}O_2$-PFHxS	93%	12%
$^{13}C_4$-PFOS	102%	14%
$^{13}C_4$-PFDS	94%	13%
$^{13}C_3$-HFPO-DA	131%	80%

Calibration curves showed good linearity ($R^2 > 0.995$) over the concentration range of 0.0-100 pg/µL. Method detection limits (MDL) were determined based on signal-to-noise ratio calculations following the guidelines outlined in Agilent's technical report on mass spectrometry detection limits [177]. The calculated MDL, LoB and mean blank values for each target compound are detailed in Table A6.

Table A6. Method performance parameters for target PFAS.

Class	Acronym	MDL [ng/mL]	LoB [ng/mL]	Blanks [ng/mL]
Carboxylic	PFPeA	0.06	0.23	0.22
Acids	PFHxA	0.06	0.33	0.3
	PFHpA	0.06	< 0.06	< 0.06
	PFOA	0.06	0.11	0.13
	PFNA	0.06	< 0.06	< 0.06
	PFDA	0.07	< 0.07	< 0.07
	PFUnDA	0.05	< 0.05	< 0.05
	PFDoDA	0.05	< 0.05	< 0.05
	PFTrDA	0.06	< 0.06	< 0.06
Sulfonic	PFBS	0.06	< 0.06	< 0.06
Acids	PFHxS	0.06	< 0.06	< 0.06
	PFOS	0.05	0.34	0.28
	PFDS	0.06	< 0.06	< 0.06
Ether	HFPO-DA	0.06	< 0.06	< 0.06

A.2 Stats Results

A.2.1 PFAS Analysis

A.2.1.1 PCA

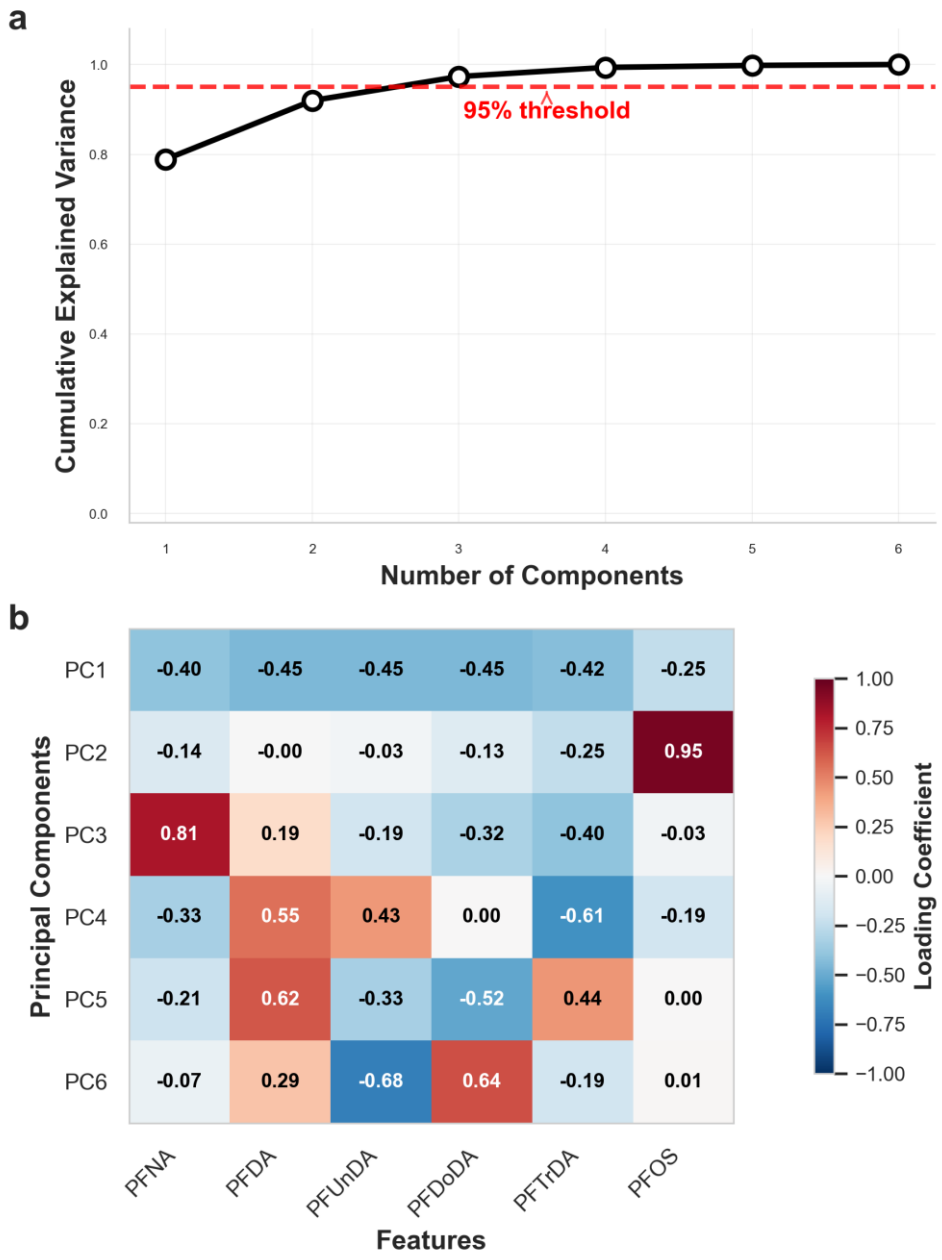

Figure A1. Principal Component Analysis (PCA) visualization of the PFAS dataset. (a) Explained variability ratio across principal components, showing the proportion of variability captured by each component. (b) Heatmap depicting feature contributions to the first six principal components, where colour intensity represents loading strength and direction.

A.2.2 Stable Isotope Analysis

A.2.2.1 Descriptives of SIR

Table A7. Statistical summary of stable isotope values ($\delta^{15}N$ and $\delta^{13}C$) in cell and plasma samples from UA (n = 67) and UL (n = 45) groups.

Species	Colony	$\delta^{15}N_{cell}$		$\delta^{13}C_{cell}$		$\delta^{15}N_{plasma}$		$\delta^{13}C_{plasma}$	
		Median	IQR	Median	IQR	Median	IQR	Median	IQR
UA	N	11.8	0.3	-20.3	0.1	11.9	0.2	-21.8	0.4
UA	NE	12.2	0.3	-20.0	0.2	11.9	0.4	-21.4	0.3
UA	NW	11.8	0.4	-20.4	0.2	12.0	0.6	-21.8	0.7
UA	SE	13.1	0.7	-19.2	0.4	13.1	0.4	-19.8	0.2
UA	SW	13.2	0.3	-19.3	0.2	13.2	0.4	-19.9	0.4
UL	N	11.8	0.2	-20.2	0.1	11.6	0.3	-21.3	0.4
UL	NE	12.1	0.2	-20.0	0.1	11.7	0.4	-21.3	0.5
UL	NW	12.8	0.8	-19.9	0.7	12.6	0.7	-21.6	0.8

A.2.2.2 Correlation Analysis

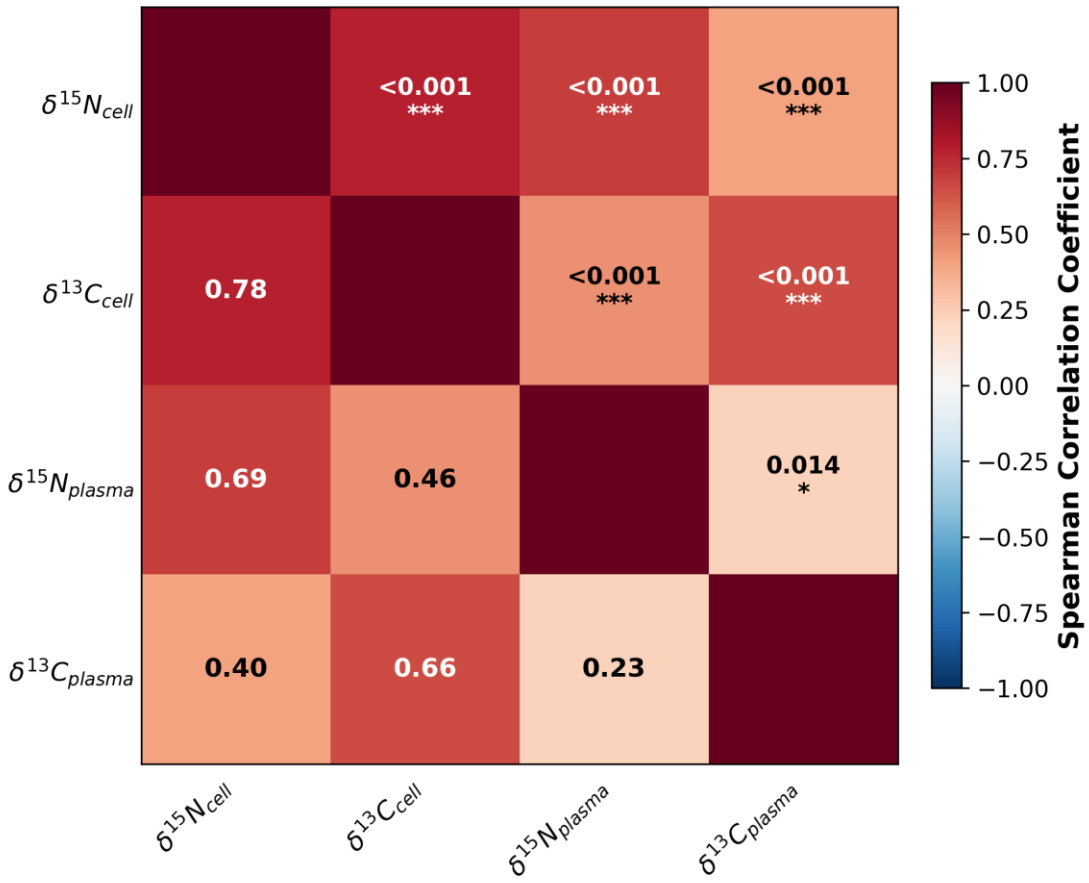

Figure A2. Spearman Correlation Heatmap of stable isotope values across tissue types. Correlation matrix illustrated the relationships between carbon ($\delta^{13}C$) and nitrogen ($\delta^{15}N$) isotope values in cell and plasma tissues. Colour intensity represents correlation strength, with red indicating positive correlations and blue indicating negative correlations. Asterisks denote statistical significance levels: *** $p < 0.001$, ** $p < 0.01$, * $p < 0.05$, ns $p \geq 0.05$. Values within each cell represent the Spearman correlation coefficient.

A.2.2.3 PCA

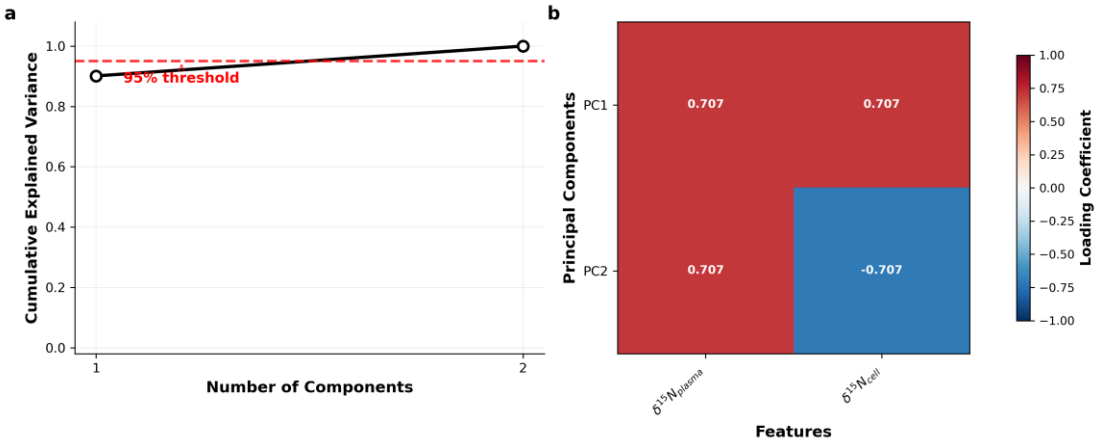

Figure A3. Principal Component Analysis of $\delta^{15}N$ in plasma and cells. (a) Scree plot showing cumulative explained variance by principal components. The red dashed line indicates the 95% variance threshold. (b) Feature contributions (loadings) to principal components PC1 and PC2. Loading coefficients range from -1 to +1, with red indicating positive loadings and blue indicating negative loadings. PC1 explains 90.1% of the total variance, while PC2 explains the remaining 9.9%.

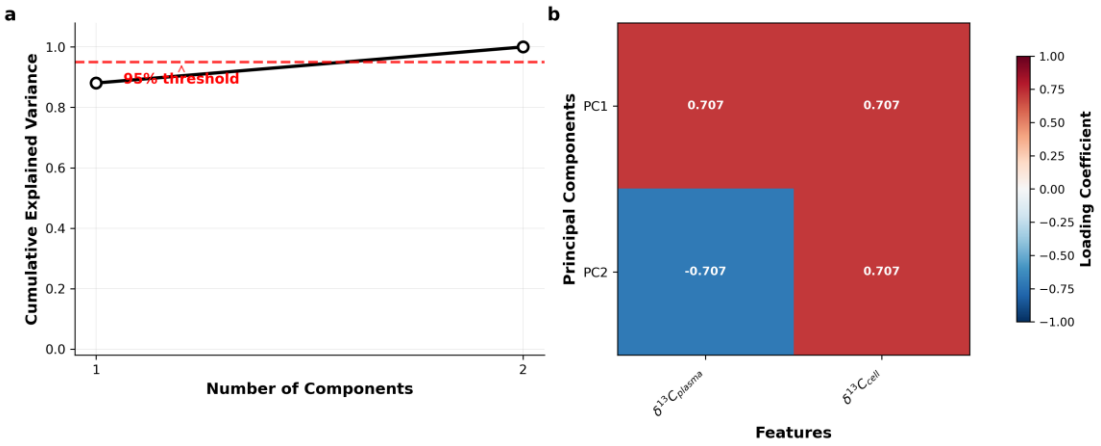

Figure A4. Principal Component Analysis of $\delta^{13}C$ in plasma and cells. (a) Scree plot showing cumulative explained variance by principal components. The red dashed line indicates the 95% variance threshold. (b) Feature contributions (loadings) to principal components PC1 and PC2. Loading coefficients range from -1 to +1, with red indicating positive loadings and blue indicating negative loadings. PC1 explains 88.1% of the total variance, while PC2 explains the remaining 11.9%.

A.2.3 Bivariate Segmented Regression Analysis

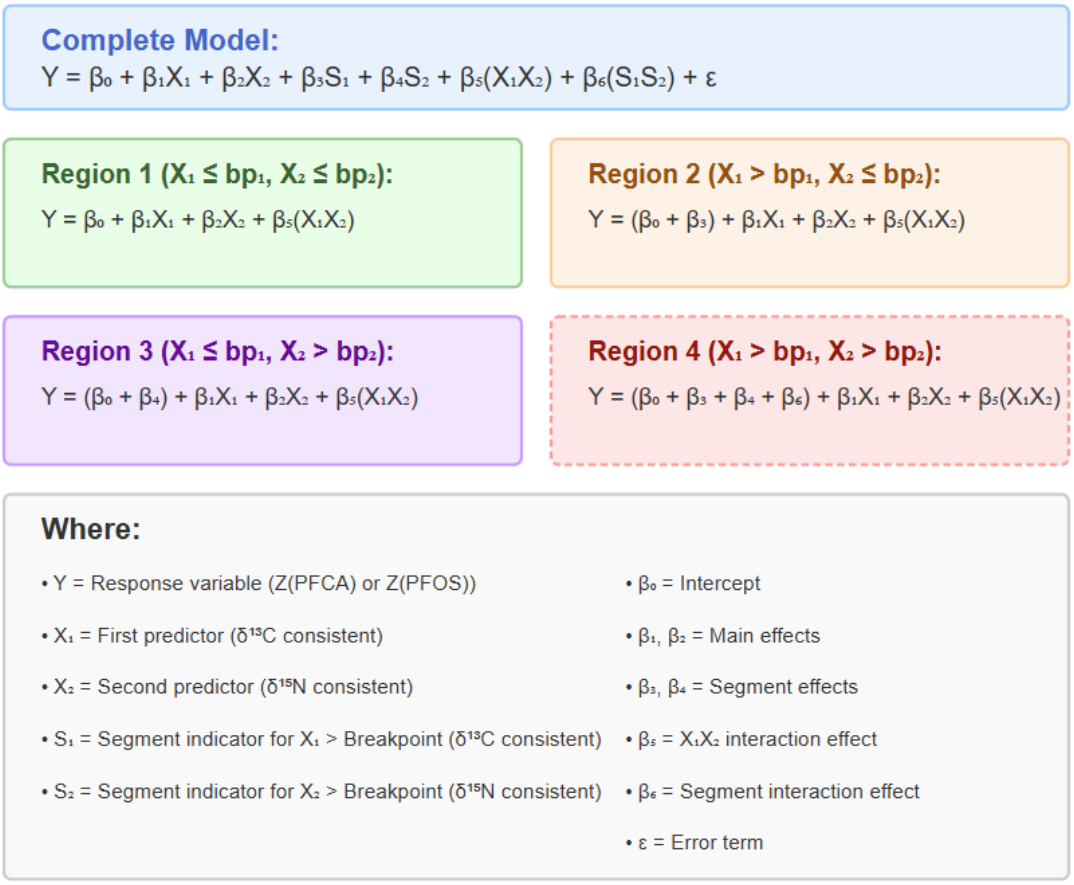

Figure A5. Segmented regression model with dual breakpoints for isotope values ($\delta^{13}C$ and $\delta^{15}N$). Due to small sample size, Region 4 was excluded from the analysis; the model was implemented using only Regions 1, 2, and 3 combined.

Table A8. Bivariate Segmented Regression Results (PFCA)

Component	Parameter	Value	SE	*t*	*p*	Training	Testing	% Effect	n	Mean	SD	Min	Max
Model Info	Response Variable	z_{PFCA}	-	-	-	-	-	-	-	-	-	-	-
	Predictor 1	$\delta^{13}C_{consist}$	-	-	-	-	-	-	-	-	-	-	-
	Predictor 2	$\delta^{15}N_{consist}$	-	-	-	-	-	-	-	-	-	-	-
	Training Observations	89	-	-	-	-	-	-	-	-	-	-	-
	Testing Observations	23	-	-	-	-	-	-	-	-	-	-	-
Performance	R^2	-	-	-	-	0.19	0.03	-	-	-	-	-	-
	MSE	-	-	-	-	0.78	1.12	-	-	-	-	-	-
	RMSE	-	-	-	-	0.88	1.06	-	-	-	-	-	-
Breakpoints	$\delta^{13}C_{consist}$	0.19	-	-	-	-	-	-	-	-	-	-	-
	$\delta^{13}C_{consist}$ Below	80 (71.4%)	-	-	-	-	-	-	-	-	-	-	-
	$\delta^{13}C_{consist}$ Above	32 (28.6%)	-	-	-	-	-	-	-	-	-	-	-
	$\delta^{15}N_{consist}$	0	-	-	-	-	-	-	-	-	-	-	-
	$\delta^{15}N_{consist}$ Below	71 (63.4%)	-	-	-	-	-	-	-	-	-	-	-
	$\delta^{15}N_{consist}$ Above	41 (36.6%)	-	-	-	-	-	-	-	-	-	-	-
Coefficients	Intercept	0.54	-	-	-	-	-	-	-	-	-	-	-
	$\delta^{13}C_{consist}$	0.34	0	1.96	0.05	-	-	13.18	-	-	-	-	-
	$\delta^{13}C_{consist}$ segment	0.27	1	0.5	0.62	-	-	10.5	-	-	-	-	-
	$\delta^{15}N_{consist}$	0.16	0	0.98	0.33	-	-	6.11	-	-	-	-	-
	$\delta^{15}N_{consist}$ segment	-0.74	0	-2.4	**0.02***	-	-	28.32	-	-	-	-	-
	$\delta^{13}C_{consist} \times \delta^{15}N_{consist}$ interaction	-0.22	0	-2.4	**0.02***	-	-	8.44	-	-	-	-	-
	Segment interaction	-0.87	1	-1.2	0.23	-	-	33.45	-	-	-	-	-
Segment Combinations	Low $\delta^{13}C_{consist}$, Low $\delta^{15}N_{consist}$	-	-	-	-	-	-	-	65	0.21	1	-1.5	2.9
	Low $\delta^{13}C_{consist}$, High $\delta^{15}N_{consist}$	-	-	-	-	-	-	-	15	-0.32	1	-2.3	1.5
	High $\delta^{13}C_{consist}$, Low $\delta^{15}N_{consist}$	-	-	-	-	-	-	-	6	0.78	1	-0.1	2.3
	High $\delta^{13}C_{consist}$, High $\delta^{15}N_{consist}$	-	-	-	-	-	-	-	26	-0.51	1	-2.1	0.9

Note: Bold *p*-values indicate statistical significance ($p < 0.05$). Asterisks (*) denote significant terms. The model shows poor predictive performance (Testing R^2 = 0.03). $\delta^{15}N_{consist}$ segment and the $\delta^{13}C_{consist} \times \delta^{15}N_{consist}$ interaction are the only significant predictors. Segment interaction accounts for the largest relative effect (33.45%). Training R^2 = 0.19 suggests potential overfitting. Dashes (-) indicate statistics not applicable for that parameter type.

Table A9. Bivariate Segmented Regression Results (PFOS)

Component	Parameter	Value	SE	*t*	*p*	Training	Testing	% Effect	*n*	Mean	SD	Min	Max
Model Info	Response Variable	z_{PFOS}	-	-	-	-	-	-	-	-	-	-	-
	Predictor 1	$\delta^{13}C_{consist}$	-	-	-	-	-	-	-	-	-	-	-
	Predictor 2	$\delta^{15}N_{consist}$	-	-	-	-	-	-	-	-	-	-	-
	Training Observations	89	-	-	-	-	-	-	-	-	-	-	-
	Testing Observations	23	-	-	-	-	-	-	-	-	-	-	-
Performance	R^2	-	-	-	-	0.35	-0.05	-	-	-	-	-	-
	MSE	-	-	-	-	0.63	1.09	-	-	-	-	-	-
	RMSE	-	-	-	-	0.79	1.04	-	-	-	-	-	-
Breakpoints	$\delta^{13}C_{consist}$	0.19	-	-	-	-	-	-	-	-	-	-	-
	$\delta^{13}C_{consist}$ Below	80 (71.4%)	-	-	-	-	-	-	-	-	-	-	-
	$\delta^{13}C_{consist}$ Above	32 (28.6%)	-	-	-	-	-	-	-	-	-	-	-
	$\delta^{15}N_{consist}$	0	-	-	-	-	-	-	-	-	-	-	-
	$\delta^{15}N_{consist}$ Below	71 (63.4%)	-	-	-	-	-	-	-	-	-	-	-
	$\delta^{15}N_{consist}$ Above	41 (36.6%)	-	-	-	-	-	-	-	-	-	-	-
Coefficients	Intercept	-0.61	-	-	-	-	-	-	-	-	-	-	-
	$\delta^{13}C_{consist}$	-0.45	0.2	-2.8	**0.01****	-	-	17.91	-	-	-	-	-
	$\delta^{13}C_{consist}$ segment	1.26	0.5	2.56	**0.01***	-	-	50.55	-	-	-	-	-
	$\delta^{15}N_{consist}$	0.03	0.2	0.19	0.85	-	-	1.1	-	-	-	-	-
	$\delta^{15}N_{consist}$ segment	-0.05	0.3	-0.2	0.86	-	-	1.93	-	-	-	-	-
	$\delta^{13}C_{consist} \times \delta^{15}N_{consist}$ interaction	0.16	0.1	1.96	0.05	-	-	6.44	-	-	-	-	-
	Segment interaction	0.55	0.7	0.85	0.4	-	-	22.06	-	-	-	-	-
Segment Combinations	Low $\delta^{13}C_{consist}$, Low $\delta^{15}N_{consist}$	-	-	-	-	-	-	-	65	-0.28	1	-2.3	2.9
	Low $\delta^{13}C_{consist}$, High $\delta^{15}N_{consist}$	-	-	-	-	-	-	-	15	-0.4	0.6	-1.8	0.5
	High $\delta^{13}C_{consist}$, Low $\delta^{15}N_{consist}$	-	-	-	-	-	-	-	6	0.54	0.7	-0.8	1.4
	High $\delta^{13}C_{consist}$, High $\delta^{15}N_{consist}$	-	-	-	-	-	-	-	26	0.8	0.9	-0.4	3.4

Note: Bold *p*-values indicate statistical significance ($p < 0.05$). Asterisks denote significance level (* $p < 0.05$, ** $p < 0.01$). The model shows better training performance than PFCA ($R^2 = 0.35$) but still poor testing performance ($R^2 = -0.05$). $\delta^{13}C_{consist}$ and its segment term are highly significant. $\delta^{13}C_{consist}$ segment accounts for the largest relative effect (50.55%). High $\delta^{13}C_{consist}$ segments show positive means regardless of $\delta^{15}N_{consist}$ levels. Dashes (-) indicate statistics not applicable for that parameter type.

Appendix B : Supplementary materials for Chapter 4

B.1 Methods and Materials

The sample size-corrected Standard Ellipse Area (SEAc) was calculated following Jackson *et al.* [138] to quantify isotopic niche width while accounting for small sample sizes. SEAc represents the core 40% of bivariate isotopic data and is calculated as:

$$SEAc = SEA \times \frac{n-1}{n-2}$$

where n is the sample size for the group, and SEA is the uncorrected standard ellipse area calculated as:

$$SEAc = \pi \times \sigma_1 \times \sigma_2$$

where σ_1 and σ_2 are the semi-major and semi-minor axes of the standard ellipse, derived from the eigenvalues (λ_1 and λ_2) of the covariance matrix $\mathbf{\Sigma}$ of the bivariate isotope data ($\delta^{13}C$ and $\delta^{15}N$):

$$\sigma_1 = \sqrt{\lambda_1}$$

$$\sigma_2 = \sqrt{\lambda_2}$$

B.2 Cluster Statistics

Table B1. Summary of clustering characteristics, composite score centroids, cluster quality metrics, and species and colony distributions across the three identified log-transformed PFAS concednetration clusters. Sample sizes, clustering quality indices (Silhouette Score, Calinski-Harabasz Index, Davies-Bouldin Index), centroid values (PFCA and PFOS), point density metrics, and Chi-square test results for species and colony distributions are provided for each cluster. Significance levels: * $p < 0.05$, ** $p < 0.01$, *** $p < 0.001$; † indicates statistically significant deviation from overall distribution ($p < 0.05$).

Parameter	Cluster 1	Cluster 2	Cluster 3	Overall
Clustering Characteristics				
Sample Size	62	36	14	112
Inertia	-	-	-	7.48
Silhouette Score	0.4	0.41	0.26	0.39
Calinski-Harabasz Index	-	-	-	85.02
Davies-Bouldin Index	-	-	-	0.95
Average Silhouette Score	0.4	0.41	0.26	0.39
Min Silhouette Score	0.11	0.12	-0.03	-
Max Silhouette Score	0.62	0.57	0.48	-
PFAS Concentration Metrics				
PFCA Centroid [ng/g DM]	1.53	1.87	1.02	-
PFOS Centroid [ng/g DM]	1.83	2.22	1.71	-
Cluster Quality Characteristics				
Point Density [points/unit area]	774.05	321.25	79	-
Convex Hull Area	0.31	0.39	0.39	-
Area Density [points/unit area]	200	92.31	36.36	-
Avg. Distance to Centroid	0.21	0.23	0.32	-
Max Distance to Centroid	0.44	0.68	0.63	-
Species Distribution				
UA	32	34†	1†	67
UL	30	2†	13†	45
Species distribution χ^2 (p-value)	1.74 ($p = 0.19$)	17.95***	16.16***	35.86***
Effect size (Cramér's V)	-	0.71	1.08	0.4
Colony Distribution				
N	16	5	9†	30
NE	24	3†	3	30
NW	18	10	2	30
SE	2	13†	0	15
SW	2	5	0	7
Colony distribution χ^2 (p-value)	9.12	24.06***	11.07**	44.25***
Effect size (Cramér's V)	-	0.41	0.45	0.36
χ^2 test				
Species-Colony interaction χ^2	5.08 ($p = 0.28$)	5.51 ($p = 0.24$)	0.60 ($p = 0.74$)	
Effect size (Cramér's V)	-	-	-	

Significance levels: * $p < 0.05$, ** $p < 0.01$, *** $p < 0.001$
†Indicates statistically significant deviation from overall distribution ($p < 0.05$)

Table B2. Summary of clustering characteristics, composite score centroids, cluster quality metrics, and species and colony distributions across the three identified PFAS profile clusters. Sample sizes, clustering quality indices (Silhouette Score, Calinski-Harabasz Index, Davies-Bouldin Index), centroid values (SCS_{PFCA} and SCS_{PFOS}), point density metrics, and Chi-square test results for species and colony distributions are provided for each cluster. Significance levels: * $p < 0.05$, ** $p < 0.01$, *** $p < 0.001$; † indicates statistically significant deviation from overall distribution ($p < 0.05$).

Parameter	Cluster 1	Cluster 2	Cluster 3	Overall
Clustering Characteristics				
Sample Size	52	36	24	112
Inertia	-	-	-	86.72
Silhouette Score	0.35	0.36	0.37	0.36
Calinski-Harabasz Index	-	-	-	86.27
Davies-Bouldin Index	-	-	-	0.97
Average Silhouette Score	0.35	0.36	0.37	0.36
Min Silhouette Score	0.05	0.01	-0.01	-
Max Silhouette Score	0.58	0.55	0.54	-
Composite Score Centroids				
SCS_{PFCA}	0.17	-0.91	1	-
SCS_{PFOS}	-0.1	1.03	-1.34	-
Cluster Quality Characteristics				
Point Density [points/unit area]	50.18	26.99	22.79	-
Convex Hull Area	3.81	4.73	3.58	-
Area Density [points/unit area]	13.65	7.61	6.7	-
Avg. Distance to Centroid	0.69	0.8	0.77	-
Max Distance to Centroid	2.6	2.28	2.06	-
Species Distribution				
UA	26	34†	7	67
UL	26	2†	17†	45
Species distribution χ^2 (p-value)	2.09 ($p = 0.15$)	17.95***	9.38**	29.43***
Effect size (Cramér's V)	-	0.71	0.63	0.36
Colony Distribution				
N	16	5	9	30
NE	17	3†	10	30
NW	15	10	5	30
SE	2	13†	0	15
SW	2	5	0	7
Colony distribution χ^2 (p-value)	5.09 ($p = 0.28$)	24.06***	8.04 ($p = 0.09$)	37.19***
Effect size (Cramér's V)	-	0.41	-	0.33
χ^2 test				
Species-Colony interaction χ^2	4.91 ($p = 0.30$)	5.51 ($p = 0.24$)	0.28 ($p = 0.87$)	-
Effect size (Cramér's V)	-	-	-	-

Significance levels: * $p < 0.05$, ** $p < 0.01$, *** $p < 0.001$
†Indicates statistically significant deviation from overall distribution ($p < 0.05$)

Table B3. Summary of clustering characteristics, isotopic composite score centroids, cluster quality metrics, and species and colony distributions across the three identified foraging pattern clusters. Sample sizes, clustering quality indices (Silhouette Score, Calinski-Harabasz Index, Davies-Bouldin Index), centroid values ($\delta^{13}C_{consist}$ and $\delta^{15}N_{consist}$), point density metrics, and Chi-square test results for species and colony distributions are provided for each cluster. Significance levels: * $p < 0.05$, ** $p < 0.01$, *** $p < 0.001$; † indicates statistically significant deviation from overall distribution ($p < 0.05$).

Parameter	Cluster 1	Cluster 2	Cluster 3	Overall
Clustering Characteristics				
Sample Size	70	23	19	112
Inertia	-	-	-	105.33
Silhouette Score	0.51	0.46	0.29	0.46
Calinski-Harabasz Index	-	-	-	151.89
Davies-Bouldin Index	-	-	-	0.86
Average Silhouette Score	0.51	0.46	0.29	0.46
Min Silhouette Score	0.12	-0.08	-0.06	-
Max Silhouette Score	0.66	0.64	0.54	-
Composite Score Centroids				
$\delta^{13}C$ Composite Score	-0.62	2.22	-0.41	-
$\delta^{15}N$ Composite Score	-0.86	1.92	0.85	-
Cluster Quality Characteristics				
Point Density [points/unit area]	80.89	9.62	12.1	-
Convex Hull Area	4.47	8.22	3.74	-
Area Density [points/unit area]	15.67	2.8	5.08	-
Avg. Distance to Centroid	0.69	1.05	0.93	-
Max Distance to Centroid	2.38	3.69	1.87	-
Species Distribution				
UA	40	22†	5	67
UL	30	1†	14†	45
Species distribution χ^2 (p-value)	0.21 ($p = 0.65$)	12.29***	8.87**	21.37***
Effect size (Cramér's V)	-	0.73	0.68	0.31
Colony Distribution				
N	30†	0†	0†	30
NE	24	0†	6	30
NW	16	1†	13†	30
SE	0†	15†	0	15
SW	0†	7†	0	7
Colony distribution χ^2 (p-value)	22.37***	84.29***	21.28***	127.95***
Effect size (Cramér's V)	0.28	0.96	0.53	0.62
χ^2 test				
Species-Colony interaction χ^2	4.92 ($p = 0.09$)	23.00***	1.07 ($p = 0.30$)	-
Effect size (Cramér's V)	-	0.72	-	-
Largest deviations	-	UL-NW: high, UA-NW: low	-	-

Significance levels: * $p < 0.05$, ** $p < 0.01$, *** $p < 0.001$
†Indicates statistically significant deviation from overall distribution ($p < 0.05$)

Reference

[1] Buck, R. C. *et al.* Perfluoroalkyl and polyfluoroalkyl substances in the environment: Terminology, classification, and origins. *Integr. Environ. Assess. Manag.* **7**, 513-541 (2011). https://doi.org:doi:10.1002/ieam.258

[2] Wang, Z., Cousins, I. T., Scheringer, M., Buck, R. C. & Hungerbühler, K. Global emission inventories for C4–C14 perfluoroalkyl carboxylic acid (PFCA) homologues from 1951 to 2030, Part I: production and emissions from quantifiable sources. *Environ. Int.* **70**, 62-75 (2014). https://doi.org:https://doi.org/10.1016/j.envint.2014.04.013

[3] Glüge, J. *et al.* An overview of the uses of per- and polyfluoroalkyl substances (PFAS). *Environ. Sci. Process. Impacts* **22**, 2345-2373 (2020). https://doi.org:10.1039/D0EM00291G

[4] Prevedouros, K., Cousins, I. T., Buck, R. C. & Korzeniowski, S. H. Sources, Fate and Transport of Perfluorocarboxylates. *Environ. Sci. Technol.* **40**, 32-44 (2006). https://doi.org:10.1021/es0512475

[5] Houde, M., De Silva, A. O., Muir, D. C. G. & Letcher, R. J. Monitoring of Perfluorinated Compounds in Aquatic Biota: An Updated Review. *Environ. Sci. Technol.* **45**, 7962-7973 (2011). https://doi.org:10.1021/es104326w

[6] Lohmann, R. *et al.* Are Fluoropolymers Really of Low Concern for Human and Environmental Health and Separate from Other PFAS? *Environ. Sci. Technol.* **54**, 12820-12828 (2020). https://doi.org:10.1021/acs.est.0c03244

[7] Ding, N., Harlow, S. D., Randolph Jr, J. F., Loch-Caruso, R. & Park, S. K. Perfluoroalkyl and polyfluoroalkyl substances (PFAS) and their effects on the ovary. *Hum. Reprod. Update.* **26**, 724-752 (2020). https://doi.org:10.1093/humupd/dmaa018

[8] Ng, C. A. & Hungerbühler, K. Bioaccumulation of Perfluorinated Alkyl Acids: Observations and Models. *Environ. Sci. Technol.* **48**, 4637-4648 (2014). https://doi.org:10.1021/es404008g

[9] Kelly, B. C. *et al.* Perfluoroalkyl Contaminants in an Arctic Marine Food Web: Trophic Magnification and Wildlife Exposure. *Environ. Sci. Technol.* **43**, 4037-4043 (2009). https://doi.org:10.1021/es9003894

[10] Aas, C. B., Fuglei, E., Herzke, D., Yoccoz, N. G. & Routti, H. Effect of Body Condition on Tissue Distribution of Perfluoroalkyl Substances (PFASs) in Arctic Fox (Vulpes lagopus). *Environ. Sci. Technol.* **48**, 11654-11661 (2014). https://doi.org:10.1021/es503147n

[11] Pérez, F. *et al.* Accumulation of perfluoroalkyl substances in human tissues. *Environ. Int.* **59**, 354-362 (2013). https://doi.org:https://doi.org/10.1016/j.envint.2013.06.004

[12] Dassuncao, C. *et al.* Phospholipid Levels Predict the Tissue Distribution of Poly- and Perfluoroalkyl Substances in a Marine Mammal. *Environ. Sci. Technol. Lett.* **6**, 119-125 (2019). https://doi.org:10.1021/acs.estlett.9b00031

[13] Jones, P. D., Hu, W., De Coen, W., Newsted, J. L. & Giesy, J. P. Binding of perfluorinated fatty acids to serum proteins. *Environ. Toxicol. Chem.* **22**, 2639-2649 (2003). https://doi.org:https://doi.org/10.1897/02-553

[14] Chen, Y.-M. & Guo, L.-H. Fluorescence study on site-specific binding of perfluoroalkyl acids to human serum albumin. *Arch. Toxicol.* **83**, 255 (2008). https://doi.org:10.1007/s00204-008-0359-x

[15] Alesio, J. L., Slitt, A. & Bothun, G. D. Critical new insights into the binding of poly- and perfluoroalkyl substances (PFAS) to albumin protein. *Chemosphere* **287**, 131979 (2022). https://doi.org:https://doi.org/10.1016/j.chemosphere.2021.131979

[16] Olsen, G. W. *et al.* Half-Life of Serum Elimination of Perfluorooctanesulfonate,Perfluorohexanesulfonate, and Perfluorooctanoate in Retired Fluorochemical Production Workers. *EHP* **115**, 1298-1305 (2007). https://doi.org:doi:10.1289/ehp.10009

[17] Zhang, Y., Beesoon, S., Zhu, L. & Martin, J. W. Biomonitoring of Perfluoroalkyl Acids in Human Urine and Estimates of Biological Half-Life. *Environ. Sci. Technol.* **47**, 10619-10627 (2013). https://doi.org:10.1021/es401905e

[18] Muir, D. & Miaz, L. T. Spatial and Temporal Trends of Perfluoroalkyl Substances in Global Ocean and Coastal Waters. *Environ. Sci. Technol.* **55**, 9527-9537 (2021). https://doi.org:10.1021/acs.est.0c08035

[19] Benskin, J. P. *et al.* Perfluoroalkyl Acids in the Atlantic and Canadian Arctic Oceans. *Environ. Sci. Technol.* **46**, 5815-5823 (2012). https://doi.org:10.1021/es300578x

[20] Zhao, Z. *et al.* Distribution and long-range transport of polyfluoroalkyl substances in the Arctic, Atlantic Ocean and Antarctic coast. *Environ. Pollut.* **170**, 71-77 (2012). https://doi.org:https://doi.org/10.1016/j.envpol.2012.06.004

[21] Cai, M. *et al.* Occurrence of Perfluoroalkyl Compounds in Surface Waters from the North Pacific to the Arctic Ocean. *Environ. Sci. Technol.* **46**, 661-668 (2012). https://doi.org:10.1021/es2026278

[22] Xie, Z. *et al.* Neutral Poly-/perfluoroalkyl Substances in Air and Snow from the Arctic. *Sci. Rep.* **5**, 8912 (2015). https://doi.org:10.1038/srep08912

https://www.nature.com/articles/srep08912#supplementary-information

[23] Casal, P. *et al.* Accumulation of Perfluoroalkylated Substances in Oceanic Plankton. *Environ. Sci. Technol.* **51**, 2766-2775 (2017). https://doi.org:10.1021/acs.est.6b05821

[24] Gobas, F. & Morrison, H. A. *Bioconcentration and biomagnification in the aquatic environment*. (2000).

[25] Borgå, K., Fisk, A. T., Hoekstra, P. F. & Muir, D. C. G. Biological and chemical factors of importance in the bioaccumulation and trophic transfer of persistent organochlorine contaminants in arctic marine food webs. *Environ. Toxicol. Chem.* **23**, 2367-2385 (2004). https://doi.org:https://doi.org/10.1897/03-518

[26] Fisk, A. T., Hobson, K. A. & Norstrom, R. J. Influence of Chemical and Biological Factors on Trophic Transfer of Persistent Organic Pollutants in the Northwater Polynya Marine Food Web. *Environ. Sci. Technol.* **35**, 732-738 (2001). https://doi.org:10.1021/es001459w

[27] Cabana, G. & Rasmussen, J. B. Modelling food chain structure and contaminant bioaccumulation using stable nitrogen isotopes. *Nature* **372**, 255-257 (1994). https://doi.org:10.1038/372255a0

[28] Tomy, G. T. *et al.* Fluorinated Organic Compounds in an Eastern Arctic Marine Food Web. *Environ. Sci. Technol.* **38**, 6475-6481 (2004). https://doi.org:10.1021/es049620g

[29] Hop, H., Borgä, K., Gabrielsen, G. W., Kleivane, L. & Skaare, J. U. Food web magnification of persistent organic pollutants in poikilotherms and homeotherms from

the Barents Sea. *Environ. Sci. Technol.* **36**, 2589-2597 (2002). https://doi.org:10.1021/es0102311

[30] Ruus, A., Ugland, K. I., Espeland, O. & Skaare, J. U. Organochlorine contaminants in a local marine food chain from Jarfjord, Northern Norway. *Mar. Environ. Res.* **48**, 131-146 (1999). https://doi.org:https://doi.org/10.1016/S0141-1136(99)00037-9

[31] Borgå, K. *et al.* Trophic magnification factors: Considerations of ecology, ecosystems, and study design. *Integr. Environ. Assess. Manag.* **8**, 64-84 (2012). https://doi.org:https://doi.org/10.1002/ieam.244

[32] Post, D. M. USING STABLE ISOTOPES TO ESTIMATE TROPHIC POSITION: MODELS, METHODS, AND ASSUMPTIONS. *Ecology* **83**, 703-718 (2002). https://doi.org:https://doi.org/10.1890/0012-9658(2002)083[0703:USITET]2.0.CO;2

[33] Layman, C. A., Arrington, D. A., Montaña, C. G. & Post, D. M. CAN STABLE ISOTOPE RATIOS PROVIDE FOR COMMUNITY-WIDE MEASURES OF TROPHIC STRUCTURE? *Ecology* **88**, 42-48 (2007). https://doi.org:https://doi.org/10.1890/0012-9658(2007)88[42:CSIRPF]2.0.CO;2

[34] Winder, M. & Schindler, D. E. CLIMATE CHANGE UNCOUPLES TROPHIC INTERACTIONS IN AN AQUATIC ECOSYSTEM. *Ecology* **85**, 2100-2106 (2004). https://doi.org:https://doi.org/10.1890/04-0151

[35] Giraldo, C. *et al.* Ontogenic changes in the feeding ecology of the early life stages of the Antarctic silverfish (Pleuragramma antarcticum) documented by stable isotopes and diet analysis in the Dumont d'Urville Sea (East Antarctica). *Polar Sci.* **5**, 252-263 (2011). https://doi.org:https://doi.org/10.1016/j.polar.2011.04.004

[36] Kortsch, S. *et al.* Food-web structure varies along environmental gradients in a high-latitude marine ecosystem. *Ecography* **42**, 295-308 (2019). https://doi.org:https://doi.org/10.1111/ecog.03443

[37] Wassmann, P. *et al.* The contiguous domains of Arctic Ocean advection: Trails of life and death. *Prog. Oceanogr.* **139**, 42-65 (2015). https://doi.org:https://doi.org/10.1016/j.pocean.2015.06.011

[38] Franklin, J. How reliable are field-derived biomagnification factors and trophic magnification factors as indicators of bioaccumulation potential? Conclusions from a case study on per- and polyfluoroalkyl substances. *IEAM* **12**, 6-20 (2016). https://doi.org:https://doi.org/10.1002/ieam.1642

[39] Bearhop, S., ADAMS, C. E., WALDRON, S., FULLER, R. A. & MACLEOD, H. Determining trophic niche width: a novel approach using stable isotope analysis. *J. Anim. Ecol.* **73**, 1007-1012 (2004). https://doi.org:https://doi.org/10.1111/j.0021-8790.2004.00861.x

[40] Newsome, S. D., Martinez del Rio, C., Bearhop, S. & Phillips, D. L. A niche for isotopic ecology. *Front. Ecol. Environ.* **5**, 429-436 (2007). https://doi.org:https://doi.org/10.1890/060150.1

[41] Frederiksen, M. *et al.* Multicolony tracking reveals the winter distribution of a pelagic seabird on an ocean basin scale. *Divers. Distrib.* **18**, 530-542 (2012). https://doi.org:https://doi.org/10.1111/j.1472-4642.2011.00864.x

[42] Hobson, K. A. & Clark, R. G. Assessing Avian Diets Using Stable Isotopes I: Turnover of 13C in Tissues. *The Condor* **94**, 181-188 (1992). https://doi.org:10.2307/1368807

[43] Elliott, J. E. & Elliott, K. H. Tracking Marine Pollution. *Science* **340**, 556-558 (2013). https://doi.org:doi:10.1126/science.1235197

[44] Furness, R. W. & Camphuysen, K. Seabirds as monitors of the marine environment. *ICES J. Mar. Sci.* **54**, 726-737 (1997). https://doi.org:10.1006/jmsc.1997.0243

[45] Burger, J. & Gochfeld, M. Marine Birds as Sentinels of Environmental Pollution. *EcoHealth* **1**, 263-274 (2004). https://doi.org:10.1007/s10393-004-0096-4

[46] Lavoie, R. A., Jardine, T. D., Chumchal, M. M., Kidd, K. A. & Campbell, L. M. Biomagnification of Mercury in Aquatic Food Webs: A Worldwide Meta-Analysis. *Environ. Sci. Technol.* **47**, 13385-13394 (2013). https://doi.org:10.1021/es403103t

[47] Elliott, K. H. *et al.* Central-Place Foraging in an Arctic Seabird Provides Evidence for Storer-Ashmole's Halo. *Auk* **126**, 613-625 (2009). https://doi.org:10.1525/auk.2009.08245

[48] Orians, G. H. & Pearson, N. E. in *Analysis of ecological systems* Vol. 155 177 (1979).

[49] Weimerskirch, H. Are seabirds foraging for unpredictable resources? *Deep Sea Res 2 Top Stud Oceanogr* **54**, 211-223 (2007). https://doi.org:https://doi.org/10.1016/j.dsr2.2006.11.013

[50] Woo, K. J., Elliott, K. H., Davidson, M., Gaston, A. J. & Davoren, G. K. Individual specialization in diet by a generalist marine predator reflects specialization in foraging behaviour. *J. Anim. Ecol.* **77**, 1082-1091 (2008). https://doi.org:https://doi.org/10.1111/j.1365-2656.2008.01429.x

[51] Ceia, F. R., Cherel, Y., Paiva, V. H. & Ramos, J. A. Stable Isotope Dynamics (δ13C and δ15N) in Neritic and Oceanic Waters of the North Atlantic Inferred From GPS-Tracked Cory's Shearwaters. *Front. Mar. Sci.* **5** (2018). https://doi.org:10.3389/fmars.2018.00377

[52] Bolnick, D. I. *et al.* The ecology of individuals:: Incidence and implications of individual specialization. *Am. Natur.* **161**, 1-28 (2003). https://doi.org:Doi 10.1086/343878

[53] Carneiro, A. P. B. *et al.* Consistency in migration strategies and habitat preferences of brown skuas over two winters, a decade apart. *Mar. Ecol. Prog. Ser.* **553**, 267-281 (2016). https://doi.org:10.3354/meps11781

[54] Karnovsky, N. J., Hobson, K. A., Iverson, S. & Hunt, G. L. Seasonal changes in diets of seabirds in the North Water Polynya: a multiple-indicator approach. *Mar. Ecol. Prog. Ser.* **357**, 291-299 (2008). https://doi.org:10.3354/meps07295

[55] Sun, J., Xing, L. & Chu, J. Global ocean contamination of per- and polyfluoroalkyl substances: A review of seabird exposure. *Chemosphere* **330**, 138721 (2023). https://doi.org:https://doi.org/10.1016/j.chemosphere.2023.138721

[56] Khan, B., Burgess, R. M. & Cantwell, M. G. Occurrence and Bioaccumulation Patterns of Per- and Polyfluoroalkyl Substances (PFAS) in the Marine Environment. *ACS ES&T Water* **3**, 1243-1259 (2023). https://doi.org:10.1021/acsestwater.2c00296

[57] Ahrens, L. Polyfluoroalkyl compounds in the aquatic environment: a review of their occurrence and fate. *J. Environ. Monit.* **13**, 20-31 (2011). https://doi.org:10.1039/C0EM00373E

[58] Conder, J. M., Hoke, R. A., Wolf, W. d., Russell, M. H. & Buck, R. C. Are PFCAs Bioaccumulative? A Critical Review and Comparison with Regulatory Criteria and Persistent Lipophilic Compounds. *Environ. Sci. Technol.* **42**, 995-1003 (2008). https://doi.org:10.1021/es070895g

[59] Braune, B. M. & Letcher, R. J. Perfluorinated Sulfonate and Carboxylate Compounds in Eggs of Seabirds Breeding in the Canadian Arctic: Temporal Trends (1975–2011)

and Interspecies Comparison. *Environ. Sci. Technol.* **47**, 616-624 (2013). https://doi.org:10.1021/es303733d

[60] Gebbink, W. A. *et al.* Target Tissue Selectivity and Burdens of Diverse Classes of Brominated and Chlorinated Contaminants in Polar Bears (Ursus maritimus) from East Greenland. *Environ. Sci. Technol.* **42**, 752-759 (2008). https://doi.org:10.1021/es071941f

[61] Miller, A., Elliott, J. E., Elliott, K. H., Lee, S. & Cyr, F. Temporal trends of perfluoroalkyl substances (PFAS) in eggs of coastal and offshore birds: Increasing PFAS levels associated with offshore bird species breeding on the Pacific coast of Canada and wintering near Asia. *Environ. Toxicol. Chem.* **34**, 1799-1808 (2015). https://doi.org:https://doi.org/10.1002/etc.2992

[62] Leat, E. H. K. *et al.* Effects of environmental exposure and diet on levels of persistent organic pollutants (POPs) in eggs of a top predator in the North Atlantic in 1980 and 2008. *Environ. Pollut.* **159**, 1222-1228 (2011). https://doi.org:https://doi.org/10.1016/j.envpol.2011.01.036

[63] Roscales, J. L., Vicente, A., Ryan, P. G., González-Solís, J. & Jiménez, B. Spatial and Interspecies Heterogeneity in Concentrations of Perfluoroalkyl Substances (PFASs) in Seabirds of the Southern Ocean. *Environ. Sci. Technol.* **53**, 9855-9865 (2019). https://doi.org:10.1021/acs.est.9b02677

[64] Munoz, G. *et al.* Evidence for the Trophic Transfer of Perfluoroalkylated Substances in a Temperate Macrotidal Estuary. *Environ. Sci. Technol.* **51**, 8450-8459 (2017). https://doi.org:10.1021/acs.est.7b02399

[65] Rubach, M. N., Crum, S. J. H. & Van den Brink, P. J. Variability in the Dynamics of Mortality and Immobility Responses of Freshwater Arthropods Exposed to Chlorpyrifos. *Arch. Environ. Contam. Toxicol.* **60**, 708-721 (2011). https://doi.org:10.1007/s00244-010-9582-6

[66] Segner, H. Moving beyond a descriptive aquatic toxicology: The value of biological process and trait information. *Aquat. Toxicol.* **105**, 50-55 (2011). https://doi.org:10.1016/j.aquatox.2011.06.016

[67] Ruan, T., Lin, Y., Wang, T., Jiang, G. & Wang, N. Methodology for studying biotransformation of polyfluoroalkyl precursors in the environment. *Trends Anal. Chem.* **67**, 167-178 (2015). https://doi.org:https://doi.org/10.1016/j.trac.2014.11.017

[68] Bustnes, J. O., Erikstad, K. E., Lorentsen, S. H. & Herzke, D. Perfluorinated and chlorinated pollutants as predictors of demographic parameters in an endangered seabird. *Environ. Pollut.* **156**, 417-424 (2008). https://doi.org:10.1016/j.envpol.2008.01.028

[69] Carravieri, A. *et al.* Wandering Albatrosses Document Latitudinal Variations in the Transfer of Persistent Organic Pollutants and Mercury to Southern Ocean Predators. *Environ. Sci. Technol.* **48**, 14746-14755 (2014). https://doi.org:10.1021/es504601m

[70] Yamashita, N. *et al.* Perfluorinated acids as novel chemical tracers of global circulation of ocean waters. *Chemosphere* **70**, 1247-1255 (2008). https://doi.org:https://doi.org/10.1016/j.chemosphere.2007.07.079

[71] Wei, S. *et al.* Distribution of perfluorinated compounds in surface seawaters between Asia and Antarctica. *Mar. Pollut. Bull.* **54**, 1813-1818 (2007). https://doi.org:10.1016/j.marpolbul.2007.08.002

[72] Schoener, T. W. Resource Partitioning in Ecological Communities. *Science* **185**, 27-39 (1974). https://doi.org:doi:10.1126/science.185.4145.27

[73] Huey, R. B. & Pianka, E. R. Ecological Consequences of Foraging Mode. *Ecology* **62**, 991-999 (1981). https://doi.org:Doi 10.2307/1936998

[74] Hutchinson, G. E. in *Cold Spring Harbor Symp. Quant. Biol.* 415-427.

[75] Chase, J. M. & Leibold, M. A. *Ecological niches: linking classical and contemporary approaches*. (University of Chicago Press, 2009).

[76] Holt, R. D. Bringing the Hutchinsonian niche into the 21st century: Ecological and evolutionary perspectives. *Proc. Natl. Acad. Sci. U.S.A* **106**, 19659-19665 (2009). https://doi.org:10.1073/pnas.0905137106

[77] Blonder, B., Lamanna, C., Violle, C. & Enquist, B. J. The n-dimensional hypervolume. *Global Ecol Biogeogr Glob. Ecol. Biogeogr* **23**, 595-609 (2014). https://doi.org:10.1111/geb.12146

[78] Ydenberg, R. C., Welham, C. V. J., Schmidhempel, R., Schmidhempel, P. & Beauchamp, G. Time and Energy Constraints and the Relationships between Currencies in Foraging Theory. *Behav. Ecol.* **5**, 28-34 (1994). https://doi.org:DOI 10.1093/beheco/5.1.28

[79] Stephens, D. W. & Krebs, J. R. *Foraging theory*. Vol. 6 (Princeton university press, 1986).

[80] Pyke, G. H., Pulliam, H. R. & Charnov, E. L. Optimal foraging: a selective review of theory and tests. *Q. Rev. Biol.* **52**, 137-154 (1977).

[81] Lyons, K., Kacev, D., Preti, A., Gillett, D. & Dewar, H. Organic contaminants as an ecological tool to explore niche partitioning: a case study using three pelagic shark species. *Sci. Rep.* **9**, 12080 (2019). https://doi.org:10.1038/s41598-019-48521-6

[82] Tartu, S. *et al.* To breed or not to breed: endocrine response to mercury contamination by an Arctic seabird. *Biol. Lett.* **9** (2013). https://doi.org:ARTN 20130317

10.1098/rsbl.2013.0317

[83] Sebastiano, M. *et al.* High levels of mercury and low levels of persistent organic pollutants in a tropical seabird in French Guiana, the Magnificent frigatebird, Fregata magnificens. *Environ. Pollut.* **214**, 384-393 (2016). https://doi.org:https://doi.org/10.1016/j.envpol.2016.03.070

[84] Astthorsson, O. S., Gislason, A. & Jonsson, S. Climate variability and the Icelandic marine ecosystem. *Deep Sea Res 2 Top Stud Oceanogr* **54**, 2456-2477 (2007). https://doi.org:https://doi.org/10.1016/j.dsr2.2007.07.030

[85] Wassmann, P. Arctic marine ecosystems in an era of rapid climate change. *Prog. Oceanogr.* **90**, 1-17 (2011). https://doi.org:https://doi.org/10.1016/j.pocean.2011.02.002

[86] Stefansson, U. & Olafsson, J. *Nutrients and fertility of Icelandic waters*. (Marine Research Inst., 1991).

[87] Bonnet-Lebrun, A.-S. *et al.* Cold comfort: Arctic seabirds find refugia from climate change and potential competition in marginal ice zones and fjords. *Ambio* (2021). https://doi.org:10.1007/s13280-021-01650-7

[88] Linnebjerg, J. F. *et al.* Sympatric Breeding Auks Shift between Dietary and Spatial Resource Partitioning across the Annual Cycle. *PLoS One* **8**, e72987 (2013). https://doi.org:10.1371/journal.pone.0072987

[89] Logemann, K., Ólafsson, J., Snorrason, Á., Valdimarsson, H. & Marteinsdóttir, G. The circulation of Icelandic waters – a modelling study. *Ocean Sci.* **9**, 931-955 (2013). https://doi.org:10.5194/os-9-931-2013

[90] Vander Zanden, H. B., Bjorndal, K. A., Reich, K. J. & Bolten, A. B. Individual specialists in a generalist population: results from a long-term stable isotope series. *Biol. Lett.* **6**, 711-714 (2010). https://doi.org:doi:10.1098/rsbl.2010.0124

[91] Hansen, J. H., Hedeholm, R. B., Sünksen, K., Tang Christensen, J. & Grønkjær, P. Spatial variability of carbon ($\delta^{13}C$) and nitrogen ($\delta^{15}N$) stable isotope ratios in an Arctic marine food web. *Mar. Ecol. Prog. Ser.* **467**, 47-59 (2012).

[92] Espinasse, B. *et al.* Temporal dynamics in zooplankton δ13C and δ15N isoscapes for the North Atlantic Ocean: Decadal cycles, seasonality, and implications for predator ecology. *Front. Ecol. Evol.* **10** (2022). https://doi.org:10.3389/fevo.2022.986082

[93] Kesic, R., Elliott, J. E., Elliott, K. H., Lee, S. L. & Maisonneuve, F. Perfluoroalkyl Substances in Seabird Eggs from Canada's Pacific Coast: Temporal Trends (1973–2019) and Interspecific Patterns. *Environ. Sci. Technol.* **57**, 10792-10803 (2023). https://doi.org:10.1021/acs.est.3c02965

[94] Palumbi, S. R. *et al.* Managing for ocean biodiversity to sustain marine ecosystem services. *Front. Ecol. Environ.* **7**, 204-211 (2009). https://doi.org:https://doi.org/10.1890/070135

[95] Duarte, C. M. *et al.* Rebuilding marine life. *Nature* **580**, 39-51 (2020). https://doi.org:10.1038/s41586-020-2146-7

[96] Butt, C. M., Berger, U., Bossi, R. & Tomy, G. T. Levels and trends of poly- and perfluorinated compounds in the arctic environment. *Sci. Total. Environ.* **408**, 2936-2965 (2010). https://doi.org:https://doi.org/10.1016/j.scitotenv.2010.03.015

[97] Zhang, X., Lohmann, R. & Sunderland, E. M. Poly- and Perfluoroalkyl Substances in Seawater and Plankton from the Northwestern Atlantic Margin. *Environmental Science & Technology* **53**, 12348-12356 (2019). https://doi.org:10.1021/acs.est.9b03230

[98] Chen, Y. *et al.* Occurrence, profiles, and ecotoxicity of poly- and perfluoroalkyl substances and their alternatives in global apex predators: A critical review. *J. Environ. Sci.* **109**, 219-236 (2021). https://doi.org:https://doi.org/10.1016/j.jes.2021.03.036

[99] Luebker, D. J., Hansen, K. J., Bass, N. M., Butenhoff, J. L. & Seacat, A. M. Interactions of flurochemicals with rat liver fatty acid-binding protein. *Toxicology* **176**, 175-185 (2002). https://doi.org:https://doi.org/10.1016/S0300-483X(02)00081-1

[100] Cheng, W. & Ng, C. A. Predicting Relative Protein Affinity of Novel Per- and Polyfluoroalkyl Substances (PFASs) by An Efficient Molecular Dynamics Approach. *Environ. Sci. Technol.* **52**, 7972-7980 (2018). https://doi.org:10.1021/acs.est.8b01268

[101] Haukås, M., Berger, U., Hop, H., Gulliksen, B. & Gabrielsen, G. W. Bioaccumulation of per- and polyfluorinated alkyl substances (PFAS) in selected species from the Barents Sea food web. *Environ. Pollut.* **148**, 360-371 (2007). https://doi.org:https://doi.org/10.1016/j.envpol.2006.09.021

[102] Loi, E. I. H. *et al.* Trophic Magnification of Poly- and Perfluorinated Compounds in a Subtropical Food Web. *Environ. Sci. Technol.* **45**, 5506-5513 (2011). https://doi.org:10.1021/es200432n

[103] Du, D. *et al.* Bioaccumulation, trophic transfer and biomagnification of perfluoroalkyl acids (PFAAs) in the marine food web of the South China Sea. *J. Hazard. Mater.* **405**, 124681 (2021). https://doi.org:https://doi.org/10.1016/j.jhazmat.2020.124681

[104] Elliott, K. H., Braune, B. M. & Elliott, J. E. Beyond bulk δ15N: Combining a suite of stable isotopic measures improves the resolution of the food webs mediating contaminant signals across space, time and communities. *Environ. Int.* **148**, 106370 (2021). https://doi.org:https://doi.org/10.1016/j.envint.2020.106370

[105] Munoz, G. *et al.* Bioaccumulation and trophic magnification of emerging and legacy per- and polyfluoroalkyl substances (PFAS) in a St. Lawrence River food web. *Environ. Pollut.* **309**, 119739 (2022). https://doi.org:https://doi.org/10.1016/j.envpol.2022.119739

[106] Borgå, K. *et al.* Why Do Organochlorine Differences between Arctic Regions Vary among Trophic Levels? *Environ. Sci. Technol.* **39**, 4343-4352 (2005). https://doi.org:10.1021/es0481124

[107] Armitage, J. *et al.* Modeling Global-Scale Fate and Transport of Perfluorooctanoate Emitted from Direct Sources. *Environ. Sci. Technol.* **40**, 6969-6975 (2006). https://doi.org:10.1021/es0614870

[108] Armitage, J. M., MacLeod, M. & Cousins, I. T. Comparative Assessment of the Global Fate and Transport Pathways of Long-Chain Perfluorocarboxylic Acids (PFCAs) and Perfluorocarboxylates (PFCs) Emitted from Direct Sources. *Environ. Sci. Technol.* **43**, 5830-5836 (2009). https://doi.org:10.1021/es900753y

[109] Clatterbuck, C. A. *et al.* Foraging in marine habitats increases mercury concentrations in a generalist seabird. *Chemosphere* **279**, 130470 (2021). https://doi.org:https://doi.org/10.1016/j.chemosphere.2021.130470

[110] Kortsch, S., Primicerio, R., Fossheim, M., Dolgov, A. V. & Aschan, M. Climate change alters the structure of arctic marine food webs due to poleward shifts of boreal generalists. *P Roy Soc B-Biol Sci* **282**, 31-39 (2015). https://doi.org:ARTN 20151546

10.1098/rspb.2015.1546

[111] Barrett, R. T. *et al.* Diet studies of seabirds: a review and recommendations. *ICES J. Mar. Sci.* **64**, 1675-1691 (2007). https://doi.org:10.1093/icesjms/fsm152

[112] Evans, T. J., Kadin, M., Olsson, O. & Åkesson, S. Foraging behaviour of common murres in the Baltic Sea, recorded by simultaneous attachment of GPS and time-depth recorder devices. *Mar. Ecol. Prog. Ser.* **475**, 277-289 (2013).

[113] Burke, C. M. & Montevecchi, W. A. Taking the Bite Out of Winter: Common Murres (Uria aalge) Push Their Dive Limits to Surmount Energy Constraints. *Front. Mar. Sci.* **5** (2018). https://doi.org:10.3389/fmars.2018.00063

[114] Jessopp, M., Arneill, G. E., Nykänen, M., Bennison, A. & Rogan, E. Central place foraging drives niche partitioning in seabirds. *Oikos Oikos* **129**, 1704-1713 (2020). https://doi.org:10.1111/oik.07509

[115] Rueffer, C. & Lehmann, L. Central place foragers, prey depletion halos, and how behavioral niche partitioning promotes consumer coexistence. *Proc. Natl. Acad. Sci. U.S.A* **121** (2024). https://doi.org:ARTN 2411780121

10.1073/pnas.2411780121

[116] Strøm, H., Descamps, S., Ekker, M., Fauchald, P. & Moe, B. Tracking the movements of North Atlantic seabirds: steps towards a better understanding of population dynamics and marine ecosystem conservation. *Mar. Ecol. Prog. Ser.* **676**, 97-116 (2021).

[117] Valdimarsson, H. & Malmberg, S.-A. Near-surface circulation in Icelandic waters derived from satellite tracked drifters. *Rit Fiskideild* **16**, 23-40 (1999).

[118] Símonarson, L. A., Eiríksson, J. & Knudsen, K. L. in *Pacific - Atlantic Mollusc Migration : Pliocene Inter-Ocean Gateway Archives on Tjörnes, North Iceland* (eds Jón Eiríksson & Leifur A. Símonarson) 13-35 (Springer International Publishing, 2021).

[119] Kędra, M. *et al.* Status and trends in the structure of Arctic benthic food webs. *Polar Research* **34**, 23775 (2015). https://doi.org:10.3402/polar.v34.23775

[120] Jason, L. Does food web theory work for marine ecosystems? *Marine Ecology Progress Series* **230**, 1-9 (2002).

[121] Frederiksen, M. *et al.* Migration and wintering of a declining seabird, the thick-billed murre Uria lomvia, on an ocean basin scale: Conservation implications. *Biol. Conserv.* **200**, 26-35 (2016). https://doi.org:https://doi.org/10.1016/j.biocon.2016.05.011

[122] Garðarsson, A., Guðmundsson, G. A. & Lilliendahl, K. Svartfugl í íslenskum fuglabjörgum 2006-2008. *Bliki*, 35-46 (2019).

[123] Hansen, K. J., Clemen, L. A., Ellefson, M. E. & Johnson, H. O. Compound-Specific, Quantitative Characterization of Organic Fluorochemicals in Biological Matrices. *Environ. Sci. Technol.* **35**, 766-770 (2001). https://doi.org:10.1021/es001489z

[124] Yeung, L. W. Y. *et al.* Perfluorooctanesulfonate and Related Fluorochemicals in Human Blood Samples from China. *Environ. Sci. Technol.* **40**, 715-720 (2006). https://doi.org:10.1021/es052067y

[125] Hansen, T. & Sommer, U. Increasing the sensitivity of $d^{13}C$ and $d^{15}N$ abundance measurements by a high sensitivity elemental analyzer connected to an isotope ratio mass spectrometer. *RCM* **21**, 314-318 (2007).

[126] Jardine, T. D., Kidd, K. A. & Fisk, A. T. Applications, Considerations, and Sources of Uncertainty When Using Stable Isotope Analysis in Ecotoxicology. *Environ. Sci. Technol.* **40**, 7501-7511 (2006). https://doi.org:10.1021/es061263h

[127] Bonnet-Lebrun, A.-S. *et al.* Effects of competitive pressure and habitat heterogeneity on niche partitioning between Arctic and boreal congeners. *Sci. Rep.* **11**, 22133 (2021). https://doi.org:10.1038/s41598-021-01506-w

[128] Neilson, J. D. & Perry, R. I. in *Encyclopedia of Ocean Sciences* (ed John H. Steele) 955-961 (Academic Press, 2001).

[129] Bandara, K., Varpe, Ø., Wijewardene, L., Tverberg, V. & Eiane, K. Two hundred years of zooplankton vertical migration research. *Biol. Rev.* **96**, 1547-1589 (2021). https://doi.org:https://doi.org/10.1111/brv.12715

[130] McMahon, K. W., Hamady, L. L. & Thorrold, S. R. A review of ecogeochemistry approaches to estimating movements of marine animals. *Limnology and Oceanography* **58**, 697-714 (2013). https://doi.org:https://doi.org/10.4319/lo.2013.58.2.0697

[131] Quillfeldt, P. *et al.* Variability of higher trophic level stable isotope data in space and time – a case study in a marine ecosystem. *Rapid Communications in Mass Spectrometry* **29**, 667-674 (2015). https://doi.org:https://doi.org/10.1002/rcm.7145

[132] Casey, M. M. & Post, D. M. The problem of isotopic baseline: Reconstructing the diet and trophic position of fossil animals. *Earth-Science Reviews* **106**, 131-148 (2011). https://doi.org:https://doi.org/10.1016/j.earscirev.2011.02.001

[133] Ohkouchi, N. *et al.* Advances in the application of amino acid nitrogen isotopic analysis in ecological and biogeochemical studies. *Org. Geochem.* **113**, 150-174 (2017). https://doi.org:https://doi.org/10.1016/j.orggeochem.2017.07.009

[134] Budge, S. M. *et al.* Tracing carbon flow in an arctic marine food web using fatty acid-stable isotope analysis. *Oecologia* **157**, 117-129 (2008). https://doi.org:10.1007/s00442-008-1053-7

[135] Larsen, T., Taylor, D. L., Leigh, M. B. & O'Brien, D. M. Stable isotope fingerprinting: a novel method for identifying plant, fungal, or bacterial origins of amino acids. *Ecology* **90**, 3526-3535 (2009). https://doi.org:https://doi.org/10.1890/08-1695.1

[136] Larsen, T. *et al.* Tracing Carbon Sources through Aquatic and Terrestrial Food Webs Using Amino Acid Stable Isotope Fingerprinting. *PLoS One* **8**, e73441 (2013). https://doi.org:10.1371/journal.pone.0073441

[137] McMahon, K. W. & McCarthy, M. D. Embracing variability in amino acid δ15N fractionation: mechanisms, implications, and applications for trophic ecology. *Ecosphere* **7**, e01511 (2016). https://doi.org:https://doi.org/10.1002/ecs2.1511

[138] Jackson, A. L., Inger, R., Parnell, A. C. & Bearhop, S. Comparing isotopic niche widths among and within communities: SIBER – Stable Isotope Bayesian Ellipses in R. *J. Anim. Ecol.* **80**, 595-602 (2011). https://doi.org:https://doi.org/10.1111/j.1365-2656.2011.01806.x

[139] Tartu, S. *et al.* Age-Related Mercury Contamination and Relationship with Luteinizing Hormone in a Long-Lived Antarctic Bird. *PLoS One* **9**, e103642 (2014). https://doi.org:10.1371/journal.pone.0103642

[140] Costantini, D. *et al.* Higher plasma oxidative damage and lower plasma antioxidant defences in an Arctic seabird exposed to longer perfluoroalkyl acids. *Environ. Res.* **168**, 278-285 (2019). https://doi.org:https://doi.org/10.1016/j.envres.2018.10.003

[141] Nøst, T. H. *et al.* Halogenated organic contaminants and their correlations with circulating thyroid hormones in developing Arctic seabirds. *Sci. Total. Environ.* **414**, 248-256 (2012). https://doi.org:https://doi.org/10.1016/j.scitotenv.2011.11.051

[142] Lewis, S., Sherratt, T. N., Hamer, K. C. & Wanless, S. Evidence of intra-specific competition for food in a pelagic seabird. *Nature* **412**, 816-819 (2001). https://doi.org:10.1038/35090566

[143] Masello, J. F. *et al.* Diving seabirds share foraging space and time within and among species. *Ecosphere* **1**, art19 (2010). https://doi.org:https://doi.org/10.1890/ES10-00103.1

[144] Graham, B. S., Koch, P. L., Newsome, S. D., McMahon, K. W. & Aurioles, D. in *Isoscapes: Understanding movement, pattern, and process on Earth through isotope mapping* (eds Jason B. West, Gabriel J. Bowen, Todd E. Dawson, & Kevin P. Tu) 299-318 (Springer Netherlands, 2010).

[145] Hussey, N. E. *et al.* Rescaling the trophic structure of marine food webs. *Ecol. Lett.* **17**, 239-250 (2014). https://doi.org:https://doi.org/10.1111/ele.12226

[146] Cummings, D. O., Buhl, C., Lee, R. W., Simpson, S. J. & Holmes, S. P. Estimating Niche Width Using Stable Isotopes in the Face of Habitat Variability: A Modelling Case Study in the Marine Environment. *PLoS One* **7**, e40539 (2012). https://doi.org:10.1371/journal.pone.0040539

[147] Víkingsson, G. A. *et al.* Distribution, abundance, and feeding ecology of baleen whales in Icelandic waters: have recent environmental changes had an effect? *Front. Ecol. Evol.* **Volume 3 - 2015** (2015). https://doi.org:10.3389/fevo.2015.00006

[148] Gaston, A. J. & Jones, I. L. *The Auks: Alcidae*. (Oxford University Press, 1998).

[149] Kelly, B. C. Food web-specific biomagnification of persistent organic pollutants (vol 317, pg 236, 2007). *Science* **318**, 44-44 (2007).

[150] Lescord, G. L. *et al.* Perfluorinated and Polyfluorinated Compounds in Lake Food Webs from the Canadian High Arctic. *Environ. Sci. Technol.* **49**, 2694-2702 (2015). https://doi.org:10.1021/es5048649

[151] Bustnes, J. O. *et al.* Influence of wintering area on persistent organic pollutants in a breeding migratory seabird. *Mar. Ecol. Prog. Ser.* **491**, 277-293 (2013).

[152] Renedo, M. *et al.* Contrasting Spatial and Seasonal Trends of Methylmercury Exposure Pathways of Arctic Seabirds: Combination of Large-Scale Tracking and Stable Isotopic Approaches. *Environ. Sci. Technol.* **54**, 13619-13629 (2020). https://doi.org:10.1021/acs.est.0c03285

[153] Kolanczyk, R. C., Saley, M. R., Serrano, J. A., Daley, S. M. & Tapper, M. A. PFAS Biotransformation Pathways: A Species Comparison Study. *Toxics* **11**, 74 (2023).

[154] Lo, J. C., Letinski, D. J., Parkerton, T. F., Campbell, D. A. & Gobas, F. A. P. C. In Vivo Biotransformation Rates of Organic Chemicals in Fish: Relationship with Bioconcentration and Biomagnification Factors. *Environ. Sci. Technol.* **50**, 13299-13308 (2016). https://doi.org:10.1021/acs.est.6b03602

[155] Sun, J. M., Kelly, B. C., Gobas, F. A. P. C. & Sunderland, E. M. A food web bioaccumulation model for the accumulation of per- and polyfluoroalkyl substances (PFAS) in fish: how important is renal elimination? *Environ. Sci. Process. Impacts* **24**, 1152-1164 (2022). https://doi.org:10.1039/d2em00047d

[156] Hobson, K. A. *et al.* A stable isotope (δ13C, δ15N) model for the North Water food web: implications for evaluating trophodynamics and the flow of energy and contaminants. *Deep Sea Res 2 Top Stud Oceanogr* **49**, 5131-5150 (2002). https://doi.org:https://doi.org/10.1016/S0967-0645(02)00182-0

[157] Walters, D. M. *et al.* Trophic Magnification of Organic Chemicals: A Global Synthesis. *Environ. Sci. Technol.* **50**, 4650-4658 (2016). https://doi.org:10.1021/acs.est.6b00201

[158] Muir, D. C. G. & de Wit, C. A. Trends of legacy and new persistent organic pollutants in the circumpolar arctic: Overview, conclusions, and recommendations. *Sci. Total. Environ.* **408**, 3044-3051 (2010). https://doi.org:https://doi.org/10.1016/j.scitotenv.2009.11.032

[159] Kraft, N. J. B. *et al.* Community assembly, coexistence and the environmental filtering metaphor. *Funct Ecol Funct. Ecol.* **29**, 592-599 (2015). https://doi.org:10.1111/1365-2435.12345

[160] HilleRisLambers, J., Adler, P. B., Harpole, W. S., Levine, J. M. & Mayfield, M. M. Rethinking Community Assembly through the Lens of Coexistence Theory. *Annu. Rev. Ecol. Evol. Syst.* **43**, 227-248 (2012). https://doi.org:10.1146/annurev-ecolsys-110411-160411

[161] Bizzarro, J. J., Field, J. C., Santora, J. A., Curtis, K. A. & Wells, B. K. Trophic guilds of marine predators in the California Current Large Marine Ecosystem. *Front. Mar. Sci.* **Volume 10 - 2023** (2023). https://doi.org:10.3389/fmars.2023.1195000

[162] Pimm, S. L., Lawton, J. H. & Cohen, J. E. Food Web Patterns and Their Consequences. *Nature Nature* **350**, 669-674 (1991). https://doi.org:DOI 10.1038/350669a0

[163] Ng, C. A. & Hungerbühler, K. Bioconcentration of Perfluorinated Alkyl Acids: How Important Is Specific Binding? *Environ. Sci. Technol.* **47**, 7214-7223 (2013). https://doi.org:10.1021/es400981a

[164] MacArthur, R. H. The theory of the niche. *J. Evol. Biol.*, 159-176 (1968).

[165] Levin, S. A. The Problem of Pattern and Scale in Ecology: The Robert H. MacArthur Award Lecture. *Ecology* **73**, 1943-1967 (1992). https://doi.org:https://doi.org/10.2307/1941447

[166] Fagan, W. F., Fortin, M.-J. & Soykan, C. Integrating edge detection and dynamic modeling in quantitative analyses of ecological boundaries. *Bioscience* **53**, 730-738 (2003).

[167] Mcnamara, J. M. & Houston, A. I. Partial Preferences and Foraging. *Anim. Behav.* **35**, 1084-1099 (1987). https://doi.org:Doi 10.1016/S0003-3472(87)80166-5

[168] Pimm, S. L. & Lawton, J. H. Number of Trophic Levels in Ecological Communities. *Nature Nature* **268**, 329-331 (1977). https://doi.org:DOI 10.1038/268329a0

[169] Pimm, S. L. & Lawton, J. H. Feeding on More Than One Trophic Level. *Nature Nature* **275**, 542-544 (1978). https://doi.org:DOI 10.1038/275542a0

[170] Macarthur, R. H. On the Relative Abundance of Bird Species. *Proc. Natl. Acad. Sci. U.S.A* **43**, 293-295 (1957). https://doi.org:DOI 10.1073/pnas.43.3.293

[171] MacArthur, R. On the relative abundance of species. *Am. Natur.* **94**, 25-36 (1960).

[172] Gebbink, W. A. *et al.* Perfluoroalkyl carboxylates and sulfonates and precursors in relation to dietary source tracers in the eggs of four species of gulls *(Larids)* from breeding sites spanning Atlantic to Pacific Canada. *Environ. Int.* **37**, 1175-1182 (2011). https://doi.org:10.1016/j.envint.2011.04.003

[173] Vane, K., Cobain, M. R. D. & Larsen, T. The power and pitfalls of amino acid carbon stable isotopes for tracing origin and use of basal resources in food webs. *Ecol. Monogr.* **95**, e1647 (2025). https://doi.org:https://doi.org/10.1002/ecm.1647

[174] Larsen, T., Wang, Y. V. & Wan, A. H. L. Tracing the Trophic Fate of Aquafeed Macronutrients With Carbon Isotope Ratios of Amino Acids. *Front. Mar. Sci.* **Volume 9 - 2022** (2022). https://doi.org:10.3389/fmars.2022.813961

[175] Wang, Z., DeWitt, J. C., Higgins, C. P. & Cousins, I. T. A Never-Ending Story of Per- and Polyfluoroalkyl Substances (PFASs)? *Environ. Sci. Technol.* **51**, 2508-2518 (2017). https://doi.org:10.1021/acs.est.6b04806

[176] Armbruster, D. A. & Pry, T. Limit of blank, limit of detection and limit of quantitation. *Clin. Biochem. Rev.* **29 Suppl 1**, S49-52 (2008).

[177] Wells, G., Prest, H., & Russ IV, C. W. Signal, Noise, and Detection Limits in Mass Spectrometry. (Santa Clara, CA, USA, 2011).

Publication list

Articles accepted

Shen, R., Ebinghaus, R., Vassão, D.G., Ratcliffe, N., & Larsen, T. (2025). Arctic-Atlantic gradient shapes PFAS exposure variability in sympatric guillemot species off Iceland. *Environmental Science & Ecotechnology,* (ESE-D-25-00426).

Articles in preparation

Shen, R., Vassão, D.G., Ratcliffe, N., & Larsen, T. (2025). Contamination Niche: Foraging Strategies Structure PFAS Exposure in Seabirds

Eidesstattliche Versicherung | Declaration on Oath

I hereby declare and affirm that this doctoral dissertation is my own work and that I have not used any aids and sources other than those indicated.

If electronic resources based on generative artificial intelligence (gAI) were used in the course of writing this dissertation, I confirm that my own work was the main and value-adding contribution and that complete documentation of all resources used is available in accordance with good scientific practice. I am responsible for any erroneous or distorted content, incorrect references, violations of data protection and copyright law or plagiarism that may have been generated by the gAI.

Ort,den | City,date	Unterschrift | Signature*
Hamburg, October 2025	Rui Shen